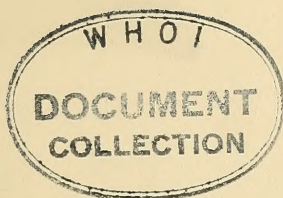


ocean - 1949 (25 Feb.)

Library

REPORT 91
PROBLEM 2A5
25 FEBRUARY 1949



RESTRICTED

interim report: **oceanographic measurements from the
USS NEREUS on a cruise to the bering and chukchi seas, 1947**

E. C. LAFOND, R. S. DIETZ, AND D. W. FRITCHARD, RESEARCH DIVISION

TK
7855
.45
nd 91

U. S. NAVY ELECTRONICS LABORATORY, SAN DIEGO, CALIFORNIA

RESTRICTED

This document contains information affecting the defense of the United States within the meaning of the Espionage Act, 30 U.S.C. 21 and 32, as amended. Transmission or the revelation of its contents in any manner to an unauthorized person is prohibited by law. Reproduction of this classified document in any form other than naval activities is not authorized without the specific approval of the Secretary of the Navy.

abstract

On the familiarization cruise to the Bering and Chukchi Seas during the summer of 1947, an oceanographic program was undertaken, designed to provide basic scientific information to determine the general navigational and operational conditions in these waters. For that purpose, measurements were made of the thermal conditions, salinity, depth, and transparency of the water. In addition, meteorological, sea, swell, ice, and slick observations were made. The sea floor was investigated from bottom samples obtained by means of coring and snapping devices and, in some instances, by bottom photographs. Ambient noise, scattering layers, and biological populations were also measured. Information regarding currents and harbor conditions was obtained wherever possible. These measurements are discussed, and explanations of the distribution of the physical, chemical, biological, and geological variables are proposed.

The data for this report were collected by members of the Marine Studies and Sonar Branches and the Photography Section of the U. S. Navy Electronics Laboratory, with assistance from members of the Scripps Institution of Oceanography.

The report was prepared by E. C. LaFond, R. S. Dietz, and D. W. Pritchard, with assistance from other members of the Oceanographic Studies Section. The analysis of diatoms was from the work of Mr. Brian Boden; the analysis of plankton from the work of Dr. Martin W. Johnson of the Scripps Institution of Oceanography.

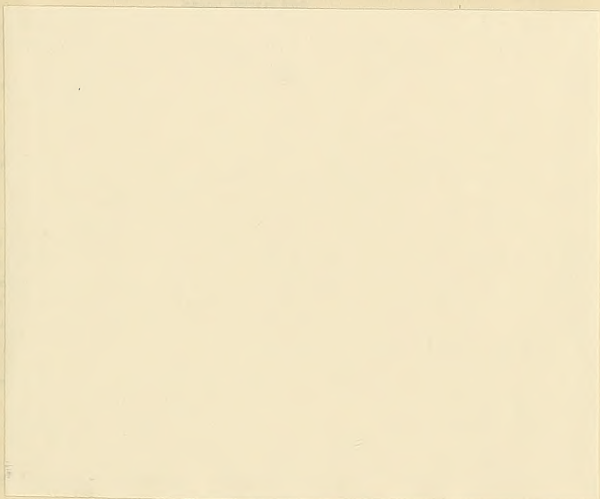


table of contents

	page
I. GENERAL	4
Synopsis of Results	4
Introduction	9
II. GEOLOGICAL OBSERVATIONS	13
Sea Floor Topography of the Bering Sea	13
Sea Floor Topography of the Chukchi Sea	17
Sediments of the Bering and Chukchi Seas	20
III. PHYSICAL OCEANOGRAPHIC OBSERVATIONS	38
Temperature and Salinity Structure	38
Internal Waves	68
Density	71
Dynamic Topography and Currents	74
Ice	76
Transparency Measurements	81
Ambient Noise	82
IV. BIOLOGICAL OBSERVATIONS	84
Deep Scattering Layer	84
Zooplankton	85
LIST OF REFERENCES	95

MBL/WHOI



0 0301 0072439 9

Hst of illustrations

figure	page
1. Track chart of USS NEREUS in the Bering and Chukchi Seas ..	8
2. Bottom sediment chart of the Bering Sea	12
3. Fathogram showing a profile of the continental slope and the shelf of the southern portion of the Bering Sea	14
4. Fathogram of the central and northern portions of the Bering Sea, Bering Strait, and the Chukchi Sea	15
5. Bottom sediment chart of the Chukchi Sea	18
6. Fathogram of the Chukchi Sea	19
7. Fathogram of the Chukchi Sea (Kotzebue Sound), Bering Strait, and Norton Sound	20
8. Bottom photograph taken in the Chukchi Sea	25
9. Bottom photograph taken in the Bering Strait	25
10. Glac on with surface laden with mud	35
11. Glac on heavily laden with well-sorted pebbles	35
12. Floeberg heavily laden with rafted detritus	35
13. Bathythermograph and hydrographic stations used for vertical sections	38
14. Bathythermograms taken in the southern Bering Sea	40
15. Vertical temperature section A	41
16. Vertical temperature section B	41
17. Horizontal distribution of temperature, at the surface	42
18. Horizontal distribution of temperature, at 25 meters	43
19. Horizontal distribution of temperature, at 40 meters	43
20. Horizontal distribution of salinity, at the surface	44
21. Horizontal distribution of salinity, at 25 meters	45
22. Horizontal distribution of salinity, at 40 meters	45
23. Vertical temperature section C	46
24. Vertical salinity section C	46
25. Bathythermograms and salinity traces taken in the Bering Sea between Pribilof Islands and Bering Strait	49
26. Temperature-salinity diagrams from stations in the Bering Sea	49
27. Vertical temperature section D	49
28. Vertical salinity section D	50
29. Bathythermograms and salinity traces taken across eastern side of Bering Strait	51
30. Temperature-salinity diagrams from stations across eastern side of Bering Strait	51
31. Vertical temperature section E	53
32. Vertical salinity section E	53
33. Bathythermograms taken in the ice pack region	54
34. Bathythermograms and salinity traces taken in the central Chukchi Sea	55
35. Bathythermograms and salinity traces taken in the eastern Chukchi Sea	55
36. Temperature-salinity diagrams from stations in the central Chukchi Sea	57
37. Temperature-salinity diagrams from stations in the northern Chukchi Sea	57
38. Temperature-salinity diagrams from stations in Kotzebue and Norton Sounds	59
39. Bathythermograms and salinity traces taken in Kotzebue and Norton Sounds	59
40. Continuous water temperature between Bering Strait and the ice pack	60
41. Continuous water temperature between the ice pack and Aleutian Islands	60
42. Fluctuations in vertical temperature structure in brash ice region (24 hours)	69

43. Fluctuations in vertical temperature structure in brash ice region (1 hour)	69
44. Fluctuations in vertical temperature structure in ice pack region (13 hours)	70
45. Horizontal distribution of σ_t at the surface	71
46. Horizontal distribution of σ_t at 25 meters	71
47. Horizontal distribution of σ_t at 40 meters	72
48. Vertical σ_t section C	73
49. Vertical σ_t section D	73
50. Vertical σ_t section E	73
51. Dynamic height contours	75
52. Composite chart of southern limit of arctic ice pack	76
53A. Brash and blocks making up the southern limit of drift ice	77
53B. Blocks and small floes found a few miles north of southern ice boundary	77
53C. Greater ice cover with increasing latitude	78
53D. Floe ice extending about 6 feet above water	78
53E. Glaçon showing relative amounts of ice submerged and above water	78
53F. Glaçon composed of rotten ice	79
53G. Flat glaçon about 50 feet in diameter	79
53H. Glaçon which appears to have tilted about 90 degrees	79
54. Transparency measurements made near the surface	82
55. Plankton stations of the USS NEREUS	86
56. Displacement volumes of total plankton	87
57. Locality records of certain copepods	89
58. Locality records of Echinopluteus	91
59. Locality records of Ophiopluteus	93
60. Locality records of Barnacle Nauplius and Cyprid Larva	94

list of tables

I. EMERY-GOULD CODE SYSTEM	21
II. ARCTIC SNAPPER SAMPLES	22
III. ARCTIC CORE SAMPLES	26
IV. MINERALS AND ORGANISMS IN ARCTIC BOTTOM SEDIMENTS	29
V. DIATOMS IN ARCTIC BOTTOM SEDIMENTS	31
VI. HYDROGRAPHIC DATA	61
VII. NUMBERS OF PRINCIPAL ORGANISMS TAKEN BY THE USS NEREUS IN THE BERING AND CHUKCHI SEAS, 1947 ..	90

I. general

SYNOPSIS OF RESULTS

In order to give the reader an over-all view of the findings of this cruise into the Bering and Chukchi Seas, the following synopsis is presented, necessarily in rather general terms. For a more detailed discussion of the subjects mentioned, it will be necessary to turn to the various sections of the report itself, listed in the Table of Contents under the general divisions: Geological Observations, Physical Oceanographic Observations, and Biological Observations.

The sea floor of the Bering Sea is divided into two physiographic provinces of approximately equal area by a precipitous continental slope which trends northwest-southeast. Depth profiles obtained by echo sounders show that a deep flat-bottomed basin with an average depth of about 2100 fathoms occupies the region between the continental slope and the Aleutian Islands arc. The northeastern portion of the Bering Sea and the Chukchi Sea are shoal continental shelf seas characterized by a remarkably smooth, flat, and featureless bottom; bottom gradients are typically less than one foot per mile. Although these shelves were almost certainly exposed to subaerial erosion during the lowered sea levels of the Pleistocene, recent sedimentation has apparently masked all physiographic features which were formed at that time so that the shelves are now devoid of even minor topographic irregularities. As it is unlikely that the profound erosive features associated with continental glaciation could have been masked by subsequent sedimentation, it appears that even the most northerly portions of these shelves escaped Pleistocene glaciation.

The shelf sediments of the Bering and Chukchi Seas were investigated by means of grab samplers, coring devices, and underwater photos. From these data and from existing information, a sediment chart was constructed showing the distribution of sediments of various grade sizes. This chart shows that uniform deposits exist over extensive areas. The sediments are largely clastic, consisting largely of sand, sand with mud, mud with sand, and mud. In the Chukchi Sea, ice-rafted detritus is quantitatively important. In addition to grade size determinations, the diatom, foraminiferal, bacterial, and mineralogical content of the sediments were investigated. The sediments are similar to other high latitude shelf sediments in that they have a low content of carbonate, organic matter, and authigenic minerals.

Several previous oceanographic cruises, notably those conducted by the U. S. Coast Guard in 1934¹⁵ (see list of references) and in 1937-1938,⁷ have made fairly complete investigations of the eastern Bering Sea and Norton Sound. The present cruise, however, was the first cruise on which extensive use was made of the bathythermograph, and hence much greater detail of the vertical temperature structure was obtained than on the previous cruises.

The same general distribution of physical variables was observed in the Bering Sea as on the previous cruises. The isolines of temperature and salinity run approximately parallel to the Alaskan coast. The bathythermograph sections taken in the southern Bering Sea tend to confirm the existence of clockwise eddy circulation at about 56°N, 165°W. Previous investigations⁷ have reported the existence of similar eddies in this region of the Bering Sea.

The nature of the circulation as indicated by previous current observations and by dynamic computations of the relative mass distribution is further confirmed by the study of the temperature-salinity relationships at the stations in the Bering Sea and their relation to the temperature-salinity diagram for the subarctic water found south of the Aleutians. This circulation (see fig. 51) carries water from the surface layers south of the Aleutians through the Aleutian chain and northward in the eastern Bering Sea towards, and thence through, the Bering Strait.

Though the previous investigators have taken several sections across Bering Strait, the greater detail of the temperature data from the bathythermograph makes the line of stations obtained by the USS NEREUS across the Strait of some additional importance. The vertical sections of temperature and salinity distinctly show the strong northward flow through the Bering Strait.

The data taken in the Chukchi Sea, especially, represents a considerable increase in physical oceanographic information concerning this area. The U. S. Coast Guard cruises in the summers of 1937 and 1938 occupied a number of stations along the Alaskan coast from Bering Strait nearly to Point Barrow, but these data are not sufficient to show the lateral distribution of the physical variables. Sverdrup in the MAUD obtained considerable data between Herald Shoal and Wrangell Island but occupied only two hydrographic stations east of 170°W in the Chukchi Sea. On the basis of these data, Sverdrup made several conclusions concerning the circulation in the Chukchi Sea. The data taken by the USS NEREUS confirm some of the conclusions but fail to confirm completely some

[REDACTED]

of the others.

The isolines of temperature and salinity continue to run approximately parallel to the Alaskan coast, with the warmer, less saline water near the coast. This distribution breaks down near the ice pack, where cold but low-salinity melt water complicates the picture.

Sverdrup had indicated that the northward flow of water through Bering Strait continued only at subsurface depths in the Chukchi Sea in summer, with a return current southward along the surface related to the prevailing northwest winds. A detailed study of the temperature-salinity relationships, and of the dynamic topography, observed on the NEREUS cruise, indicates, however, that in 1947 the flow in the central Chukchi Sea was northward at all depths as far as station N14, slightly north of 70°N . At this point there is evidence of cold, low-salinity melt water related to the melting of the ice. This water has apparently drifted southward from the ice region under the influence of the north-northwest wind prevailing at the time.

At the stations north of 70°N a very characteristic bottom water was found. This water was relatively cold and saline, and is apparently the result of the winter freezing. Between the cold, low-salinity melt water at the surface and the cold, high-salinity bottom water the relatively warm, moderately high-salinity water from the south enters as a wedge. The cold, high-salinity bottom water is probably formed both in the Chukchi and Bering Seas to the southern limit of the winter ice formation. Its appearance only north of 70°N on this cruise indicates that it has been displaced by the northward flowing water from the Bering Sea through Bering Strait. This is further substantiated by the fact that more recent observations, not yet reported on, show that this characteristic bottom water was not in evidence as far north as the edge of the ice pack in the summer of 1948. This finding indicates that this bottom water has been completely displaced from the shallow shelf region of the Chukchi Sea.

The presence of this peculiar layering of the various types of water in the northern Chukchi Sea during the cruise of the USS NEREUS caused very unusual vertical temperature structures. The cold surface layer is followed by a sharp positive temperature gradient below which occurs the negative gradient separating the bottom water from the intruding warmer water originating to the south. These positive gradients present important problems from the standpoint of underwater sound transmission.

The ice encountered during the period 1 to 6 August was in a state of melting, with rotten ice in all areas between 71°50' to 72°45' N and 161° to 160°W. The southern limits of ice in the summer of 1947 were farther north than usually observed, thus permitting navigation to about 72°N at these longitudes.

Transparency of the sea water was less than that observed in the open sea; however, it was greater than found in coastal regions, with an average Secchi disc reading of 30 feet observed in the Bering and Chukchi Seas. The regions of greatest transparency were found in the north central portion of the Bering Sea and north of 69°N in the Chukchi Sea.

Ambient noise throughout the areas was very low. Equipment limitations and ship noises prevented the establishment of exact levels. Near shore, surface noises were audible. In the melting ice, low sounds of rushing water were heard with an occasional splash. No biological noises were heard.

Two types of biological observations from the arctic region are reported here. One is the deep scattering layer (believed to be biological in nature); the other is the zooplankton obtained by net hauls. The observations of the deep scattering layer, the first ever reported in the Bering Sea, were picked up on the NEREUS' recording fathometer. It was first observed in the deep channel north of Adak, separating from the outgoing ping at 75 fathoms in the early hours of the morning daylight and reaching about 100 fathoms by early afternoon. It remained at this unusually shallow depth until the continental slope was reached. No scattering layer could be recorded on the continental slope.

The vertical zooplankton net hauls taken throughout the Bering Sea verified species and abundance of plankton found previously by the CHELAN in this area. Although this is the first extensive plankton sampling undertaken in the Chukchi Sea, practically all species found in the Bering Sea were also found near the southern limits of ice; however, many Chukchi Sea species were not found in the Bering Sea. This is significant since it shows that Bering Sea water flows through the Bering Strait to the ice pack.

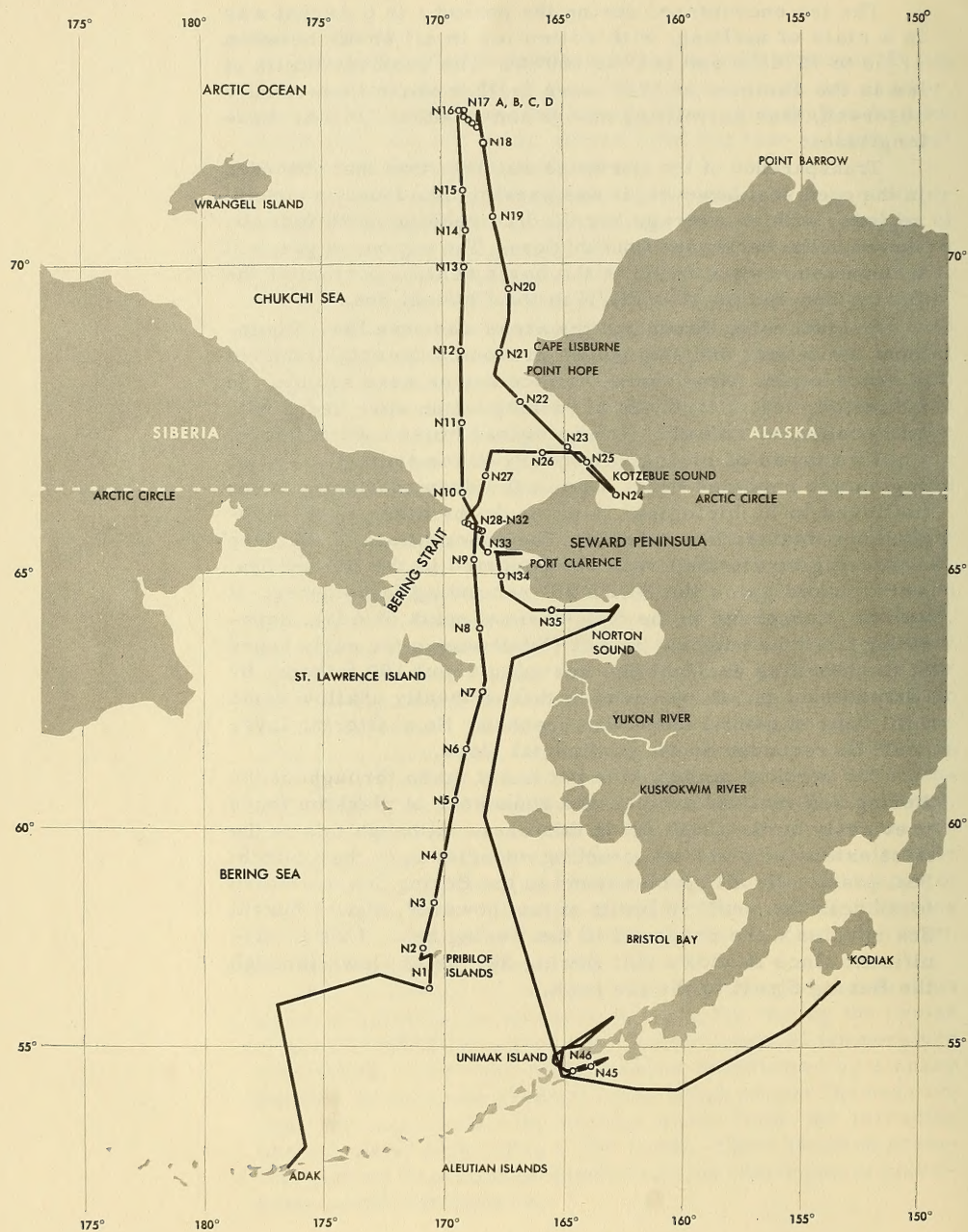


Figure 1. Track chart showing hydrographic stations of USS NEREUS in Bering and Chukchi Seas.

INTRODUCTION

The USS NEREUS (AS17) and four submarines of Submarine Squadron SEVEN, USS BOARFISH (SS327), USS CABEZON (SS334), USS CAIMAN (SS323), and USS CHUB (SS329), made a familiarization cruise to the Bering and Chukchi Seas during the summer of 1947. The main purpose of the cruise was to obtain operating experience in arctic waters. In addition to this operational purpose, an oceanographic program aboard the USS NEREUS was undertaken, designed to provide basic scientific information for determining the general navigational and operational conditions in these waters. For that purpose, measurements were made of the thermal conditions, salinity, depth, and transparency of the water. In addition, meteorological, sea, swell, ice, and slick observations were made. The bottom of the sea was investigated from bottom samples obtained by means of coring and snapping devices and, in some instances, by bottom photographs. Ambient noise, scattering layers, and biological populations were also measured. Information regarding currents and harbor conditions was obtained wherever possible. The USS BOARFISH obtained sea water temperatures and salinities in the Bering and Chukchi Seas and bathythermograms in the ice region; measurements of depth, sea, swell, and ice were made from all submarines.

Personnel and Itinerary. Aboard the USS NEREUS were: J. A. Knauss, E. C. LaFond, G. W. Marks, and D. E. Root of the Oceanographic Studies Section; R. E. McFarland of the Photography Section; and H. J. Mann and W. H. Munk of the Scripps Institution of Oceanography. Aboard the USS BOARFISH were: W. K. Lyon of the Marine Studies Branch, L. L. Morse of the Deep Submergence Section, and F. Baltzly, Jr. and A. H. Roshon of the FM Sonar Section.

The general track of the USS NEREUS in the Bering and Chukchi Seas is shown in figure 1; the dates of arrival and departure at the various points are listed below.

DEPARTED		ARRIVED	
San Diego	28 June	Mare Island	30 June
Mare Island	3 July	Pearl Harbor	9 July
Pearl Harbor	15 July	Adak	22 July
Adak	25 July	St. Paul Island	27 July
St. Paul Island	28 July	Chukchi Sea (Ice Pack)	1 August
Chukchi Sea	1 August	Kotzebue Sound	4 August
Kotzebue Sound	4 August	Port Clarence	5 August
Port Clarence	7 August	Norton Sound	8 August
Norton Sound	8 August	Kodiak	16 August
Kodiak	18 August	Seward	19 August
Seward	19 August	Juneau	21 August
Juneau	25 August	Vancouver, B. C.	28 August
Vancouver, B. C.	30 August	Mare Island	3 September

Observational Program. En route from San Francisco to Pearl Harbor several types of observations were made while the USS NEREUS was underway. These observations included bathythermograph lowerings made hourly throughout the entire passage; descriptions of sea surface characteristics made three times a day; and notations of the sea, swells, slicks, and all visible biological life.

En route from Pearl Harbor to Adak new types of observations were made in addition to the bathythermograph lowerings and surface characteristic descriptions. Complete weather data were taken. The fathometer was run continuously at high gain to detect the deep scattering layer. Once each morning the ship hove to in order to drop six SOFAR bombs to test the sound transmission. During these stops a plankton net haul was taken.

North from Adak the hourly bathythermograph and surface observations were continued until the 100-fathom contour was reached. At that time a more detailed program could be accomplished. In the shallow depths of the Bering and Chukchi Seas the USS NEREUS hove to four times a day at 0300, 0900, 1500 and 2100 LCT for a period of approximately one hour. During this time the following measurements were taken: (1) a bathythermograph lowering to the bottom, (2) a vertical series of simultaneous temperature and water samples, (3) a snapper sample of the sea bottom, (4) a core of sediment of the sea bottom, (5) a sea floor photograph, when possible, (6) a transparency measurement by means of a Secchi disc, (7) a plankton net haul through the water from bottom to surface, (8) an ambient noise measurement, and (9) surface observations including weather, waves, swell, ice, water color, phosphorescence, birds, whales, fish, etc. This program continued until the pack ice was reached.

In the pack ice the USS NEREUS hove to for 24 hours, during which time repeated bathythermograph observations were made every 30 minutes. Vertical series of water samples and temperature were taken every six hours. A small boat cruise was made eight miles farther into the pack ice to sample the bottom under more dense ice.

On the return cruise from the ice region to Norton Sound, four stops were made daily, and the same observational program was followed as on the northern passage. Five additional stations were occupied across the Alaskan side of Bering Strait.

From Norton Sound to Unimak Island only surface observations could be taken because search operations for a lost plane near Unimak prevented any stops. On the southern side of

SECRET

Unimak Island, however, two stations were occupied during the search. En route from Unimak Island to San Francisco only periodic bathythermograph lowerings and surface observations were made.

In harbors such as Village Cove (St. Paul Island), Fort Clarence, Womens Bay and Middle Bay (Kodiak), Resurrection Bay (Seward), and Gasteneau Channel and Taku Inlet (Juneau), motor launches were used to make additional measurements. Although insufficient time prevented making detailed surveys, it was possible at several locations in each of the above harbors to take bathythermograph lowerings and bottom samples and to make ambient noise measurements.

Oceanographic measurements were taken from the submarines as well as from the USS NEREUS. The USS BOARFISH dropped SOFAR bombs each day while en route from San Diego to Adak. In the Bering and Chukchi Seas observers on all four submarines took continuous soundings on recording fathometers, observations of sea and swell, and observations of ice limits and conditions. Observers on the USS BOARFISH made, in addition, bathythermograph lowerings from the surface in the ice region and obtained temperature and salinity readings en route through the Chukchi and Bering Seas by means of the ship's recording instruments.

The data collected by all ships are discussed in this report by subject and in some cases are combined with existing information of the area. The data on weather, depth, ice, sea, swell, discolored water, phosphorescence, birds, whales, and fish, as well as the bathythermograms taken south of the Bering Sea, were turned over to the U. S. Hydrographic Office. These data have thrown some new light on the subject of oceanographic conditions in the arctic and have served to corroborate the findings of previous investigations. It is expected that this report will serve as a basis for further analyses of arctic conditions.

II. geological observations

SEA FLOOR TOPOGRAPHY OF THE BERING SEA (fig. 2)

The Bering Sea is located in the northernmost portion of the Pacific Ocean. It lies inside the Aleutian Island arc and is bounded to the north by Siberia and Alaska. The narrow, shallow Bering Strait connects the Bering Sea to the Chukchi Sea (also known as the Chukotsk Sea), which is that portion of the Arctic Ocean lying immediately north of northeastern Siberia and northern Alaska.

The continental slope traverses the Bering Sea obliquely from southeast to northwest, cutting it into two approximately equal areas, (1) an abyssal ocean basin and (2) an extensive and shallow continental shelf. The recorded soundings on existing charts show that the abyssal ocean basin has a level floor at a depth of about 2100 fathoms, 100 fathoms deeper than could be recorded by the NMC-1 fathometer aboard the USS NEREUS. Along the track of the USS NEREUS from Adak to the Pribilof Islands, the abyssal floor of the central portion of the basin is everywhere deeper than 2000 fathoms and probably level because even minor seamounts rising from the basin to less than 2000 fathoms are absent (fig. 3A*). At the periphery of the basin near the continental slope, the floor rises to depths less than 2000 fathoms and has the form of a smooth, gentle, concave-upward slope suggestive of a depositional surface such as might have been formed by the sedimentation of large quantities of sediment transported into the basin from the continental shelf. In the immediate vicinity of the base of the continental slope, this gently rising plain is interrupted by a number of seamounts.

Beyond these deep seamounts toward the Pribilof Islands, the continental slope rises rapidly and straight. The mile-high portion of the slope between 1300 and 200 fathoms has an average declivity of 23 degrees, making it one of the steepest known

*The plotted geographic position of the strips in figures 3, 4, 6, and 7 can be determined by reference to figures 2 and 5.

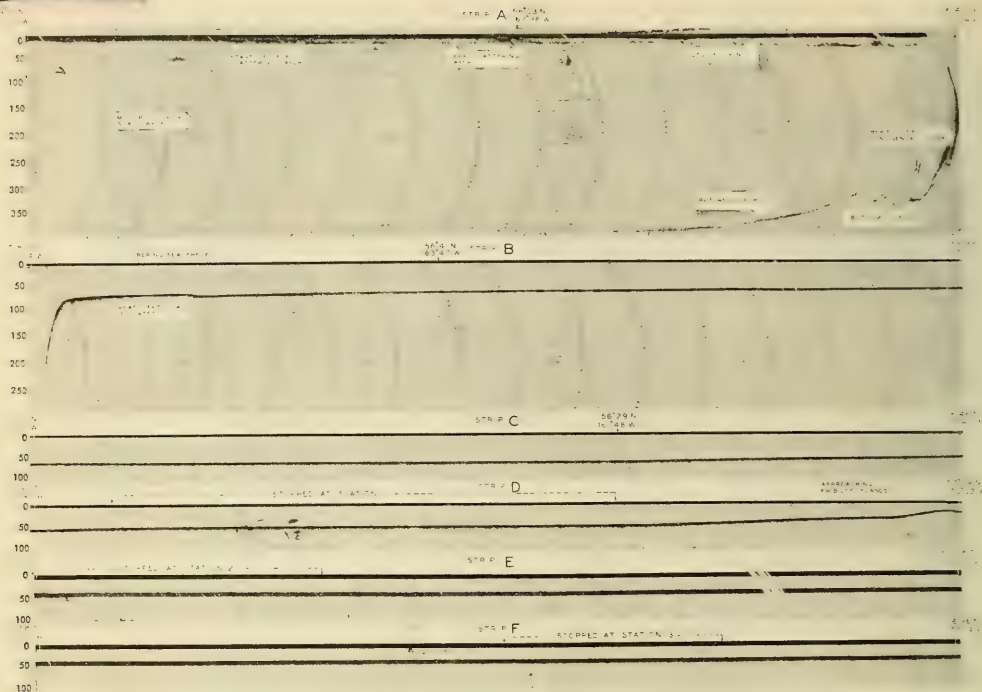


Figure 3. Fathogram showing a profile of the continental slope and the shelf of the southern portion of the Bering Sea (see fig. 1 for the geographic location of the strip). Add 3.7 fathoms to indicated depths for true depth of bottom since fathometer projector was 22 feet below surface.

continental slopes. * Although a thin veneer of sediment may cover this slope, it is too precipitous to be a depositional feature and is probably a fault scarp. This interpretation is strengthened by the presence, at the base of the slope, of the seamounts, which may be volcanic masses extruded along the fault line. It is likely that at least the deeper and more irregular portion of the continental slope is rocky.

*It is noteworthy that it has been previously estimated that this Bering Sea continental slope has a declivity of only 5 degrees. This estimated figure was obtained by computing the slope between soundings printed on published charts. This usual method is obviously inadequate as compared to using fathograms; it is likely that many continental slopes are steeper than is commonly believed, especially by those writers who have advocated a depositional origin of the continental slopes.

The break-in-slope between the continental slope and the shelf is at a depth of 89 fathoms,* but the slope does not level off until its depth is about 78 fathoms (fig. 3B). This break-in-slope depth of the shelf margin is not much deeper than the world average of approximately 72 fathoms for the depth of the greatest change in slope. The reason for the break-in-slope being at such a depth is controversial and not well understood; however, this depth appears to be related to a depth at which there is (or was at some time in the past) an equilibrium between erosive processes, such as wave cutting, and sedimentary processes. Eustatic changes in sea level, especially in the lower sea levels of the Ice Age, have probably played an important part in establishing the depth of the break-in-slope. However, it is evident that this area has not been glaciated, for the break-in-slope off glaciated shelves in both the arctic and the antarctic is characteristically much deeper.

*As the sound projector of the USS NEREUS was located 22 feet below the surface, 3.7 fathoms should be added to all the depth records of figures 3, 4, 6, and 7.

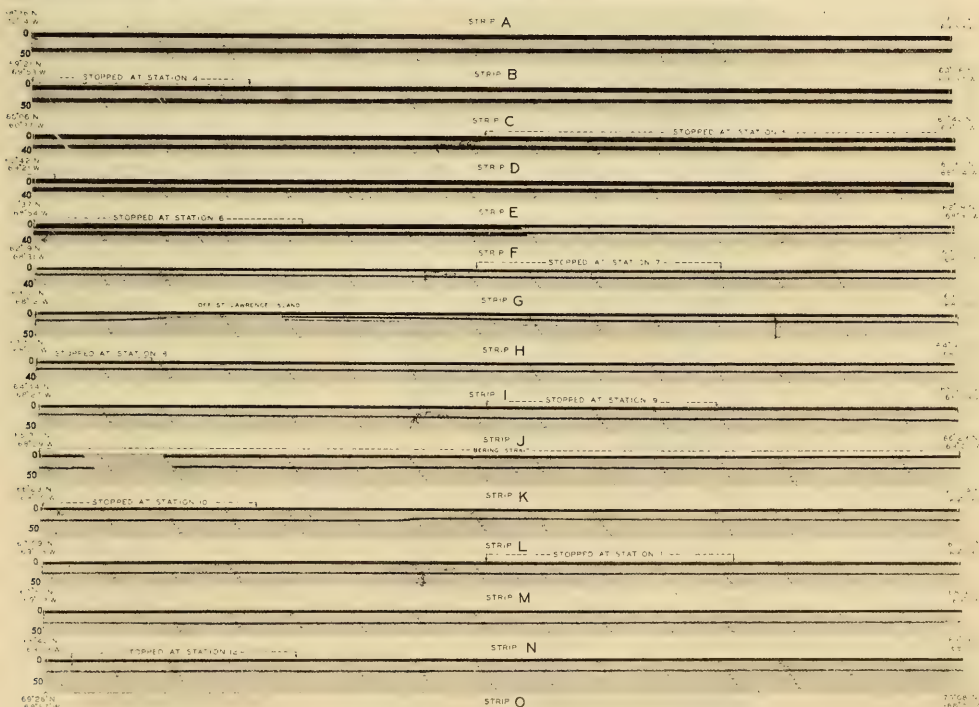


Figure 4. Bathogram of the central and northern portions of the Bering Sea, Bering Strait, and the Chukchi Sea (see fig. 1 for geographic location of the strips). The bottom profiles have a vertical exaggeration of about 26 times. The sea floor is remarkably smooth. Add 3.7 fathoms to indicated depths.

For example, on Operation HIGHJUMP during seven crossings from the antarctic slope to the shelf, Dietz noted that the break-in-slope depth varied from 230 to 280 fathoms.²

Extension of the bottom echo (fig. 3B), on both sides of the break-in-slope, may show that steep slopes lie near to and parallel with the ship's track and suggests that the outer margin of the shelf may be furrowed. However, the passage parallel with and close to the outer edge of the shelf (figs. 3B and 3C) shows a smooth bottom between 60 and 70 fathoms in depth so that even if canyons or furrows are present near the break-in-slope, they do not deeply indent this shelf.

After leaving the Pribilof Islands, the USS NEREUS proceeded northward to Bering Strait (figs. 3E, 3F, and 4A through 4I). Except when stopped to occupy a station, the USS NEREUS was continuously underway at about 13 knots, so that the bottom profiles of figures 3, 4, 6, and 7 generally have a vertical exaggeration of about 26 times. Considering such a vertical exaggeration, the shelf along this track is remarkably smooth, being completely devoid of even minor irregularities. For example, the gradient between stations 2 and 3 (figs. 3E and 3F) is 3 fathoms (18 feet) in 65 nautical miles, or 0.28 feet per mile (1 in 17,000). Such an extremely low gradient is of a magnitude more similar to that of a slow flowing river than to that of even the flattest of land surfaces. Thus, the Bering Sea has a surprisingly level bottom, which is probably flatter than any other land surface of comparable extent in the world.

Along the track of the USS NEREUS, the bottom rises gently and regularly to the north with an extremely low gradient, reaching a minimum depth of about 21 fathoms, with the exception of the track abeam of St. Lawrence Island, where the depth is somewhat shallower. The smoothness of the bottom makes it quite evident that this portion of the Bering Sea was not glaciated during the Pleistocene. However, even the conservative estimate of from 57 to 66 fathoms as the maximum Pleistocene sea level lowering⁶ indicates that a large portion of the Bering Sea must have been dry land. Yet, there are no minor irregularities on the shelf that might be interpreted as wave-cut terraces, stream valleys, or ancient strand lines. It is, therefore, quite probable that there has been sufficient recent sedimentation, plus some wave-cutting on the shelf, to cover and mask any minor topographical irregularities produced during the Pleistocene lower stands of sea level. The relatively shoal depth of the Bering Sea shelf, as compared to shelves in other parts of the world,

also suggests a large amount of sedimentation. During the summer floods, many large rivers, such as the Yukon and Kuskokwim, carry great volumes of sediment, which is presumably deposited in large part on the shelf. However, the possibility that the shoal depth of the Bering Sea is due to post-glacial upwarping, such as has taken place in the arctic, must not be overlooked, although such upwarping has been largely confined to areas which were glaciated and plastically deformed by the weight of a thick ice sheet.

In the Bering Strait (fig. 4J) the bottom is slightly deeper, presumably because of strong north-setting currents which scour the bottom and prevent deposition of fine-grained sediment. The bottom is also slightly irregular or hummocky. Bottom samples and bottom photographs obtained there showed that a stony bottom is associated with this irregularity. Examination of fathograms from other shelves of the world has likewise shown that a rocky, hard, stony, or other coarse-grained bottom invariably shows an irregular bottom trace, while the trace of a sand or mud bottom is characteristically smooth.

SEA FLOOR TOPOGRAPHY OF THE CHUKCHI SEA (fig. 5)

The floor of that section of the Chukchi Sea traversed by the USS NEREUS (figs. 4K to 4O, 6, and 7A to 7G) is in most respects similar to the Bering Sea shelf but is even flatter and more featureless. Whereas the Bering Sea tended to shoal toward the north with a minimum depth abeam St. Lawrence Island and had an average depth of about 30 fathoms, the depth of the Chukchi Sea is between 15 and 30 fathoms and averages about 25 fathoms in the area traversed.

The floor of the Chukchi Sea is a portion of a broad and shallow nonglaciated continental shelf which extends out into the Arctic Ocean from Siberia to Alaska. The findings of the MAUD expedition¹² show that, as to both topography and sediments, the shelf off Siberia is probably similar in character to the Chukchi shelf. The arctic shelf east of Alaska (off northern Canada) has been severely glaciated and is strikingly different in nature. The hummocky bottom trace from the

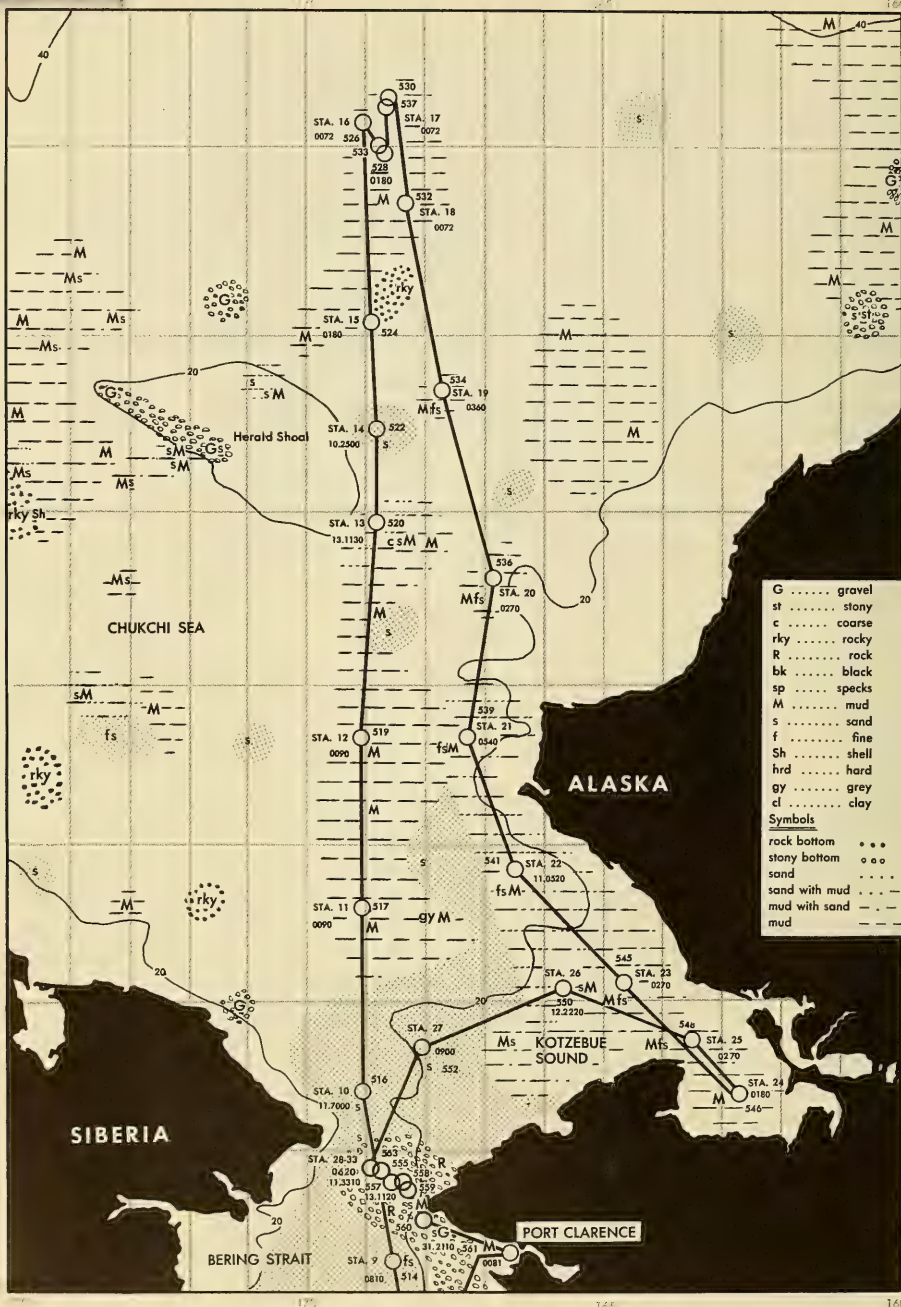


Figure 5. Bottom sediment chart of the Chukchi Sea showing stations and bottom sample numbers.

vicinity of Kotzebue Sound (figs. 6L and 6M) indicates the presence of stony bottom. Elsewhere, the bottom is smooth and probably fine-grained. (The irregular appearance of the bottom trace in other parts of figure 6 is due to irregularity of the outgoing sound signal.)

A notable feature of the Chukchi shelf is the shallow basin lying between Bering Strait and Herald Shoal; the deepest part of this basin is about 34 fathoms, or about 7 fathoms below the surrounding shelf. Herald Shoal rises to 7 fathoms and is the shoalest part of a large swell rising from about 20 fathoms.

The position of the margin of the shelf in the Chukchi Sea is not known, as the polar ice pack has prevented penetration and the obtaining of soundings much further north than about 73°N. North of Point Barrow the shelf narrows to 30 miles, and the deep Arctic Basin, where soundings up to 1333 fathoms have been recorded, lies near shore.

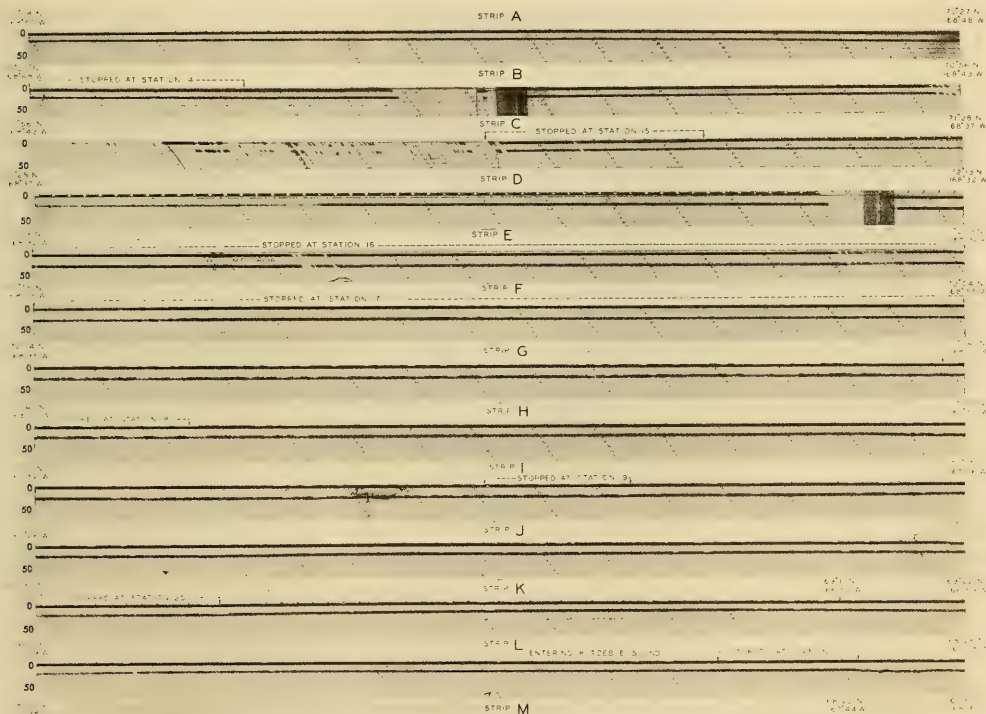


Figure 6. Fathogram of the Chukchi Sea showing the remarkably level and shoal bottom (see fig. 1 for geographic location of the strips). Add 3.7 fathoms to indicated depths.

٤٠

fr



Figure 7. Fathogram of the Chukchi Sea (Kotzebue Sound), Bering Strait, and Norton Sound (see fig. 1 for geographic locations of the strips). Add 3.7 fathoms to indicated depths.

and sieving. Sand-sized material was further separated according to specific gravity. The lightest material, consisting of diatom frustules, foraminiferal tests, ostracode tests, and certain other organic remains, was floated off with carbon tetrachloride (specific gravity 1.595). Then, the light minerals were separated from the heavy minerals by flotation using bromoform (specific gravity 2.89).

Grade-Size Determinations and Sediment Chart. Ninety-five snapper samples were collected by lowering a new type of snapper⁹ to the bottom from a small winch. Grade-size determinations were made on most of the samples using the code system of Emery and Gould⁴ and, for greater accuracy, pipette analyses were made on eight of the samples. In the Emery-Gould code system (table I), the mechanical analysis is determined by microscopic inspection of the sample placed on a millimeter grid. The size distribution is expressed by the percentage of each size grade in the order of decreasing diameter of size grades from left to right. Each digit between 0 and 9 expresses the percentage of material by weight in that grade. For example, the digit 3 means 30.0 to 39.9 per cent, or 35.0 plus or minus 5.0 per cent. To differentiate between medium and coarse sand, a reference point further simplifies the system. For instance, the notation 12.3210 denotes a sediment containing 10 to 19 per cent gravel (greater than 4 mm.), 20 to 29 per cent coarse sand (1 to 4 mm.), 30 to 39 per cent medium sand (0.25 to 1 mm.), 20 to 29 per cent fine sand (0.062 to 0.25 mm.), 10 to 19 per cent silt (0.004 to 0.062 mm.), and less than 10 per cent clay (less than 0.004 mm.). If no gravel or coarse sand is present, the reference point is dropped. For instance, 0630 denotes a silty fine sand. It is desirable to indicate genesis of a sediment as well as grade size, so that if shells make up 25 per cent or more of the sample, the letters Sh follow the bottom notation, 5400 Sh. The letter F is used in this connection if Foraminifera make up 25 per cent or more of the sample, and R is used if the sample is predominately rock, cobbles, or pebbles. The results of these analyses, together with sediment color, consistency and grain shape, are shown in table II.

TABLE I
EMERY-GOULD
CODE SYSTEM

	Coarse Material Present	Coarse Material Not Present	Grain Size (Diameter in mm)	Sediment Name	
			4-64	Pebbles	
			1-4	Coarse Sand	} Sand
		1	0.25-1	Medium Sand	
		2	0.062-0.25	Fine Sand	
		3	0.004-0.062	Silt	} Mud
		4	0.004	Clay	

Digit in Code

TABLE II ARCTIC SNAPPER SAMPLES

NEL Sample No.	Date (1947)	Latitude North	Longitude West	Depth (fathoms)	Grade Size*	Color	Consistency	Grain Shape†
501	27 July	56° 54'	170° 36'	56	0360	Grey	Fine Granular	SA to SR
503	28 July	57° 21'	170° 44'	46	0540	Grey	Fine Granular	SA to SR
505	29 July	58° 23'	170° 20'	43½	0630	Grey	Fine Granular	SA to SR
507	29 July	59° 21'	169° 53'	34½	0630	Grey	Fine Granular	SA to SR
509	30 July	60° 32'	169° 25'	25½	0810	Grey	Granular	SA to SR
510	30 July	61° 37'	168° 54'	23	0810	Grey	Granular	SA to SR
511	30 July	62° 46'	168° 15'	21½	0810	Grey	Granular	SA to SR
512	30 July	63° 57'	168° 20'	21	0810	Grey	Granular	SA to SR
514	31 July	65° 12'	168° 31'	29	0810	Grey	Granular	SA to SR
515	31 July	65° 12'	168° 31'	29	1710	Brownish Grey	Granular	SA to SR
516	31 July	66° 24'	169° 03'	32	11.7000	Grey	Coarse Granular	SA to SR
517	31 July	67° 35'	169° 03'	30	0090	Light Grey	Slightly Plastic	SA to SR
519	31 July	68° 31'	169° 03'	29	0090	Light Grey	Slightly Plastic	SA to SR
520	1 Aug.	69° 55'	168° 51'	30	13.1130	Light Grey	Slightly Plastic	SA to SR
521	1 Aug.	69° 55'	168° 51'	30	12.1120	Light Grey	Slightly Plastic	SA to SR
522	1 Aug.	70° 27'	168° 48'	23	10.2500	Grey	Granular	SA to SR
523	1 Aug.	70° 27'	168° 48'	23	10.1500	Grey	Granular	SA to SR
524	1 Aug.	71° 02'	168° 51'	24	0180	Light Grey	Slightly Plastic	SA to SR
526	1 Aug.	72° 07'	169° 00'	31	0072	Light Grey	Slightly Plastic	SA to SR
528	1 Aug.	71° 54'	168° 40'	29	0180	Light Grey	Slightly Plastic	SA to SR
530	2 Aug.	72° 14'	168° 35'	29	0072	Light Grey	Slightly Plastic	A to SR
532	3 Aug.	71° 41'	168° 20'	28	0072	Light Grey	Slightly Plastic	SA to SR
534	3 Aug.	70° 39'	167° 39'	29	0360	Light Grey	Fine Granular	SA to SR
536	3 Aug.	69° 37'	166° 53'	26	0270	Light Grey	Slightly Plastic	SR
537	2 Aug.	72° 10'	168° 40'		36.0000	Buff	Coarse Granular	SA to R
538	1 Aug.	72° 00'	168° 49'		0090	Light Grey	Slightly Plastic	A to SA
539	4 Aug.	68° 39'	167° 25'	25	0540	Grey	Fine Granular	SA to SR
540	4 Aug.	68° 39'	167° 25'	25	0540	Grey	Fine Granular	A to SR
541	4 Aug.	67° 50'	166° 32'	28	11.0520	Grey	Granular	A to SR
545	4 Aug.	67° 07'	164° 40'	17½	0270	Grey	Fine Granular	SA to SR
546	4 Aug.	66° 21'	162° 43'	6½	0180	Grey	Slightly Plastic	SA to SR
546A	4 Aug.	66° 21'	162° 43'	6½	0180	Grey	Slightly Plastic	SA to SR
548	5 Aug.	66° 43'	163° 35'	14	0270	Grey	Fine Granular	SA to SR
550	5 Aug.	67° 03'	165° 40'	15	12.2220	Grey	Granular	SA to SR
552	5 Aug.	66° 40'	168° 03'	16½	0900	Grey	Granular	A to SR
553	5 Aug.	65° 52'	168° 54'	27	11.3310	Grey	Granular	A to SR
554	5 Aug.	65° 52'	168° 54'	27	90.0000R	Buff	Gravelly & Rocky	A to SA
555	5 Aug.	65° 50'	168° 44'	30½	1620	Buff	Granular	SA to SR
556	5 Aug.	65° 50'	168° 44'	30½	71.0000R	Buff	Rocky	A to SA
557	5 Aug.	65° 46'	168° 33'	31	90.0000R	Buff	Rocky	A to SA
558	5 Aug.	65° 45'	168° 20'	30	90.0000RSh	Buff	Rocky	A to SA
559	5 Aug.	65° 43'	168° 15'	25	13.1120	Buff	Coarse Granular	A to R
560	6 Aug.	65° 23'	167° 59'	24½	31.1210	Buff	Coarse Granular	SA to SR
561		65° 17'	166° 28'	7	0081	Light Grey	Slightly Plastic	SA to SR
563	8 Aug.	64° 58'	167° 28'	18	42.2000	Grey	Granular to Gravelly	SA to SR
564	8 Aug.	64° 17'	165° 19'	12	0450	Grey	Fine Granular	SA to SR
567	11 Aug.	54° 37'	163° 59'	12	1800	Black	Granular	SA to SR
568	12 Aug.	54° 23'	164° 33'	21	90.0000R	Grey	Gravelly	SR

* Emery-Gould Code (see Table I).

† A — Angular; SA — Subangular; R — Rounded; SR — Subrounded.

HARBOR BOTTOMS TABLE II (continued)

NEL Sample No.	Date (1947)	Latitude North	Longitude West	Depth (fathoms)	Grade Size*
569	27 July	57° 08'	170° 18'	7½	0900
570	27 July	57° 08'	170° 18'	7	1800
571	27 July	57° 09'	170° 19'	4½	71.0000Sh
572	27 July	57° 08'	170° 20'	12	0900R
573	27 July	57° 08'	170° 20'	9	1800Sh
574	28 July	57° 08'	170° 17'	4½	1800Sh
575	28 July	57° 08'	170° 17'	2½	3600
576	28 July	57° 08'	170° 17'	3	0900
577	28 July	57° 08'	170° 17'	3	2700
578	28 July	57° 08'	170° 17'	3	2700
579	28 July	57° 08'	170° 17'	4	0900
580	28 July	57° 07'	170° 17'	4½	2700
581	28 July	57° 08'	170° 17'	6½	0900
582	28 July	57° 08'	170° 17'	5	0900
583	28 July	57° 08'	170° 18'	8	0900
584	28 July	57° 08'	170° 17'	7	0900
585	28 July	57° 08'	170° 17'	7	0900
586	28 July	57° 07'	170° 17'	6½	0900
587	28 July	57° 07'	170° 17'	5	0900
588	28 July	57° 07'	170° 16'	1	3600
589	7 Aug.	65° 19'	166° 30'	6	21.0140
590	7 Aug.	65° 18'	166° 40'	7	0090
591	7 Aug.	65° 17'	166° 37'	6½	0090
592	7 Aug.	65° 17'	166° 33'	6½	0090
593	8 Aug.	65° 16'	166° 29'	5	2520
594	8 Aug.	65° 16'	166° 26'	4½	2330
595	8 Aug.	65° 17'	166° 25'	5	1350
596	17 Aug.	57° 43'	152° 32'	10	0090
597	17 Aug.	57° 43'	152° 33'	11	0090
598	17 Aug.	57° 49'	152° 32'	6½	0090
599	17 Aug.	57° 43'	152° 30'	10	1160
600	18 Aug.	57° 40'	152° 28'	2	1700
601	18 Aug.	57° 40'	152° 28'	6½	1800
602	18 Aug.	57° 41'	152° 29'	6	1530
603	18 Aug.	57° 42'	152° 25'	18	1710
604	18 Aug.	57° 44'	152° 26'	11	2700
605	18 Aug.	57° 43'	152° 32'	10½	0090
606	18 Aug.	57° 43'	152° 29'	4½	31.1310
607	18 Aug.	57° 44'	152° 28'	5	90.0000R
608	18 Aug.	57° 44'	152° 26'	10½	2700Sh
609	22 Aug.	58° 26'	133° 04'	2	0530
610	23 Aug.	58° 17'	134° 24'	18	0360
611	23 Aug.	58° 17'	134° 24'	18	0360
612	23 Aug.	58° 17'	134° 24'	6	11.1230
613	23 Aug.	58° 18'	134° 25'	18	90.0000
614	23 Aug.	58° 18'	134° 26'	12	60.1200
615	23 Aug.	58° 19'	134° 27'	6	90.0000

* Emery-Gould Code (see Table I).

The sediment charts (figs. 2 and 5) utilize the data obtained from the USS NEREUS samples, from the bottom notations on the U. S. Navy Hydrographic Office charts Nos. 0068, 10639-1, and 10639-15, and from a few ALBATROSS samples as noted by Trask.¹⁴ For the purpose of the chart, the sediments were classified as rocky, stony (includes bottoms marked as gravel, pebbles, and hard on H. O. chart No. 0068), sand, sand with mud, mud with sand, and mud. As the charts are based on only a relatively few bottom samples, the accuracy is not great; however it is believed that the sediment distribution indicated on the charts is correct in a general way.

By comparing the bottom samples with the fathometer bottom traces at the various stations, it was found that gravel or rock bottom is invariably irregular and hummocky and that soft bottoms are flat and featureless. Thus, the nature of the bottom sediments along the entire track of the USS NEREUS was determined with some certainty by correlating the fathometer trace with the bottom samples obtained at intervals of many miles. An attempt was also made to obtain bottom sediment information by studying the nature of the bottom echo itself, but this was not successful.

Bottom Cores. Twenty cores were obtained by plunging into the bottom a device similar to that described by Emery and Dietz³ and consisting of a $2\frac{1}{2}$ -inch core tube weighted with lead. Because the small size (0.25 inch) of the wire used to lower the coring device necessitated limiting the weight of the sampler to less than 150 pounds, only short cores were obtained (minimum length = 8.5 inches, maximum length = 70 inches, average length = 30 inches).

Since most of the cores taken in the Bering Sea were very short, sandy cores, the nature of the sediment is known for only an unfortunately short distance below the sea bottom. These Bering Sea cores suggest a change in sedimentation in comparatively recent times. The appearance of the upper 1 to 3 inches of the core is usually higher in color and more loosely packed. Other texture changes from silty sand to silt take place at varying distances below the bottom in a number of cores. In core NEL 502 (54 fathoms), the change occurs at about 30 inches below the bottom; in core NEL 508 (32 fathoms), the change takes place gradually at about 7 inches; and in core NEL 513 (19 fathoms), a sharp change occurs at 10 inches. Core NEL 504 is probably too short to show any change, and core NEL 506 shows very little change. The cores taken at the entrance to Norton Sound show changes to coarser sediment at about 10 to 12 inches below the bottom, then to finer sediment below $14\frac{1}{2}$ inches.

In the Chukchi Sea, three of the six cores display changes to coarser sediment from 10 to 46 inches below the sea floor. The core taken in Kotzebue Sound shows a change to coarser material taking place about 6 inches below the bottom. A description of the core samples is given in table III.

Bottom Photography. An attempt was made to obtain a number of bottom photographs with the underwater camera at almost every station occupied by the USS NEREUS. However, at only two stations were photographs obtained in which the bottom was clearly discernible. In the Chukchi Sea near snapper sample NEL 520, a photograph (fig. 8) showed the bottom to be composed of sand, gravel, and minor amounts of silt. In the Bering Strait near snapper sample NEL 557, a photograph (fig. 9) showed the bottom to be composed of shells, gravel, and rock. Abundant bottom-living organisms are present. It is noteworthy that both of these photographs, and the sediment samples obtained close by, showed a coarse bottom in these localities. At all other stations, the bottom water was too turbid for the camera to penetrate even when placed only three feet from the sea floor.

Constant checking of the equipment showed that improper functioning did not contribute to the inability to obtain good bottom photographs. The fact that this inability was caused by the turbid nature of the bottom water was further substantiated by lowering the equipment with the camera focused



Figure 8. Bottom photograph taken in the Chukchi Sea at station N13 (latitude 70° N, longitude 169° W), showing coarse and poorly sorted bottom material. Note abundant bottom-living organisms including crab in lower center portion of the photo.



Figure 9. Bottom photograph taken in the Bering Strait, showing stony bottom with abundant bottom-living organisms. Shell fragments are abundant, and the large pelecypod valve in center of the photo has a sponge growing in it.

TABLE III
ARCTIC CORE SAMPLES

NEL Sample No.	Location	Latitude North	Longitude West	Depth (fathoms)	Length of Dry Core (inches)	Description
502	South of Pribilof Island	56° 54'	170° 36'	54	32	Grey-green, well-sorted sandy silt, becoming a little finer toward base. Molluscan fragments scattered throughout.
504	North of Pribilof Island	57° 21'	170° 44'	43	15	Grey-green, moderately well-sorted sandy silty sand. Molluscan fragments scattered throughout.
506	North of Pribilof Island	58° 23'	170° 20'	37	32	Grey-green, moderately well-sorted, silty sand. Molluscan fragments common in top 8 to 9 inches, but rarer toward bottom.
508	East Bering Sea	59° 21'	169° 53'	32	31	Grey-green silty sand in top 7 inches, grading into finer grained sandy silt. Occasional molluscan fragments near top of core.
513	North Bering Sea	63° 57'	168° 20'	19	13	Grey-green slightly silty fine sand containing molluscan fragments in top 10 inches; changes abruptly to dark sandy silt in basal 3 inches of core.
518	North of Bering Strait	67° 35'	169° 03'	31	20	Coarse greenish-grey silt containing little clay and a few scattered molluscan fragments.
525	North Chukchi Sea	71° 02'	168° 51'	24	24	Slightly sandy coarse greenish-grey silt containing minor amounts of clay.
527	North Chukchi Sea	72° 07'	169° 00'	31	70	Grey-green clayey fine-grained silt containing a few scattered Foraminifera and molluscan fragments.
529	North Chukchi Sea	71° 54'	168° 40'	29	49	Grey-green clayey fine-grained silt, containing a small amount of fine sand which increases in basal 3 inches of core.
531	North Chukchi Sea	72° 14'	168° 35'	30	20	Greenish-grey clayey silt, containing several small and several irregular fine-to-medium sand partings near base; occasional small mollusks, Foraminifera, and fragments of unidentifiable organic material.
533	North Chukchi Sea	71° 41'	168° 20'	29	40	Greenish-grey clayey silt, occasional rounded to subrounded pebbles, and sand grains scattered throughout; organic remains common, including fragments of wood and shells, fish scales, and occasional foraminiferal tests.
535	East Chukchi Sea	70° 39'	167° 39'	29	25	Greenish-grey sandy silt, separated 5 inches from top by somewhat sandier parting, then grading again to sandy silt 9½ inches from top, where it grades into silty sand becoming coarser toward bottom; medium sand and pebbles common in basal 15 inches.
543	Kotzebue Sound	67° 50'	166° 32'	29	8½	Greenish-grey, poorly sorted silty sand, containing minor amounts of gravel, becoming coarser toward the base; wood fragments at bottom.
544	Kotzebue Sound	67° 07'	164° 40'	17	8½	Greenish-grey, poorly sorted silty sand, containing minor amounts of gravel, becoming coarser toward base.
547	Kotzebue Sound	66° 21'	162° 43'	6½	14	Greenish-grey, fine sandy silt containing occasional foraminiferal tests and molluscan fragments.

TABLE III (continued)
ARCTIC CORE SAMPLES

NEL Sample No.	Location	Latitude North	Longitude West	Depth (fathoms)	Length of Dry Core (inches)	Description
549	Kotzebue Sound	66° 43'	163° 35'	13	12	Grey sandy silt, grading 6 inches from the top into fine to medium sand; molluscan shells common at base of core.
551	Entrance to Kotzebue Sound	67° 03'	165° 40'	16	20	Poorly sorted sand, with sizable silt and gravel fractions grading 8 inches below top into finer, better-sorted sand, then rapidly into silty sand, and finally to sandy silt near the bottom of the core; 4 inches from the top a pebble 20 mm. in diameter occurs.
562	Port Clarence	65° 18'	166° 28'	25	67	Clayey fine silt, containing occasional rounded pebbles including one more than 6 mm. in diameter at 2¾ inches from top; organisms include mollusks, shallow water forams, and ophiurids (6 inches and 10 inches from top).
565	Entrance to Norton Sound	64° 17'	165° 19'	11	12	Sandy silt, with occasionally siltier or sandier partings in upper part, becoming progressively sandier 10 inches from top; includes occasional scattered molluscan fragments and foraminiferal tests.
566	Entrance to Norton Sound	64° 25'	166° 30'	14	20	Fine sandy silt, with prominent medium-to-coarse sand partings at 5 inches and 11 inches from top, with less prominent partings between 11 inches and 14½ inches; laminations resemble faint bedding below 11 inches; below 14½ inches sediment becomes finer and clay fraction becomes noticeable.

on an object at the lower portion of the camera support and making exposures at various levels from the surface to the bottom. This experiment clearly showed that the transparency of the water decreased with depth and that a highly turbid layer was present along the bottom.

Surface-water transparency readings were obtained at each station by recording the depth to which a white disc 30 centimeters in diameter (Secchi disc) could be seen (see Transparency Measurements, below). Readings obtained varied from 9 to 50 feet, average depths for coastal water. There appeared to be no correlation between the surface water transparency and bottom water transparency but, wherever the snapper samples showed the bottom to consist of fine sand or mud, a turbid layer was present near the bottom. Thus, although phytoplankton may largely account for the opacity of the surface water, the turbidity of the bottom water must be due to sediment in suspension.

Mineralogy and Petrology. The mineral grains and rock fragments were identified in a general way, using only a binocular microscope. For this reason no attempt was made to distinguish between the ferromagnesian minerals or, in most instances, between the feldspars. The minerals and rocks identified are listed in table IV.

Of the minerals identified, quartz and feldspar are almost ubiquitous. However, they are most abundant in the north Bering Sea and the Chukchi Sea. Pyriboles (pyroxenes and amphiboles) and olivine are most common in the south Bering Sea near the volcanic rock source in the Pribilof and Aleutian Islands, but they were noted also in most of the other samples. Of the micas, biotite is the most common, especially in the north Bering Sea and the Chukchi Sea and near Juneau, Alaska. A white amphibole common in the Juneau area has been identified as tremolite. Noteworthy is the abundance of magnetite in the snapper sample NEL 567 taken just south of Unimak Island in the Aleutians. At this location, magnetite is the most abundant constituent of the sand comprising the bottom.

As might be expected, basalt grains are common in the south Bering Sea, becoming less common toward the north where they are mixed with grains of granite and quartzite. Volcanic glass is a common constituent in the Chukchi Sea, into which it has possibly been carried by north-setting currents from the more volcanic areas of the Bering Sea. In many of the samples taken from the Kodiak area, pumice is the most prominent constituent. In the Juneau area metamorphic rock fragments and pebbles are common, including slate, schist, and gneiss.

Authigenic minerals such as glauconite and phosphorite are practically absent from these sediments. This finding suggests that rapid deposition is taking place on the shelves of the Bering and Chukchi Seas, since such authigenic minerals tend to form under conditions of very slow or no deposition. Unweathered mineral grains of species which are subaerially unstable, such as olivine, biotite, and the pyriboles, are abundant.

Diatoms. Diatom frustules are not abundant either as to numbers or species in the bottom sediments. In all cases they represent less than one per cent of the sample. The identifications of the diatoms (see table V) were made by Mr. Brian Boden of the Scripps Institution of Oceanography.

Diatoms are most abundant in the sediments of the south Bering Sea and to a lesser extent in Kotzebue Sound. Coscinodiscus centralis Ehrenberg is the dominant species, being found in nearly all the samples; Coscinodiscus curvatus

TABLE IV
MINERALS AND ORGANISMS IN ARCTIC BOTTOM SEDIMENTS

NEL Sample	LIGHT MINERALS			HEAVY MINERALS		ROCKS	ORGANISMS			
	No.	Quartz	Feldspar	Mica	Pyriboles	Others	Siliceous	Calcareous	Chitinous	
501	A	C	b; m	?		ol	qtzte; bas; sl	Di(A)	F	Cr
503	C	C	m(R)	hyp		ol(C)	qtzte; bas	Di(A)	F	
505	C	C	m; b	hyp; hbl; aug		ol	bas	Di	F	
507	C	C	m; b	(P)		ol(?)	sl; bas	Di	F	
509	C	C	m; b	(P)		ol	bas	Di	F	wm; Cr
510	C	C	m; b	hyp; hbl		ol	bas	Di	F	
511	A	C	m; b	hbl		ol	bas; qtzte	Di(R)	F	
512	A	C	m; b(R)	hbl; aug(?)		ol	sl; qtzte		F; Ostr; Moll	
514	A	C	m; b	hbl(?); aug		ol	bas; qtzte		F; Moll; Ostr	Cr
515	A	C	m; b	hbl		ol	bas; v. gl	Di	F	
516	A	C		hbl(R)		ol	bas	Di	F; Moll; Ech	
517	A	C	m(C); b	(P)		ol(R)	bas	Di	F; Ostr	
519	C	C	m; b	(P)			bas	Di	F; Ostr	
520	C	C	m(R)	(P)		ol	qtzte; v. gl; bas	Di	F	Alg
521	C	C	m(R); b(R)	(P)		ol	qtzte; v. gl; bas	Di	F	
522	P	A	m(R)	(P)		ol	v. gl; sl; bas	Di	F	
523	P	A	m(R)	(P)		ol	v. gl; sl; bas	Di	F	
524	C	C	m; b	(P)			v. gl; bas; qtzte	Di	F	
526	A	C	m; b	(P)		ol	bas		F	
528	A	C	m; b	(P)			v. gl; bas(R)	Di	F; Moll frags	Alg
530	A	C	m; b	(P)			qtzte; v. gl; bas	Di(R)	F	
532	A	C	m; b	(P)			qtzte; v. gl; bas	Di	F; Ostr; Moll	Alg
534	A	C	m; b	(P)			qtzte; v. gl; bas	Di	F; Moll frags	
536	C	C	m; b(R)	(P)				Di	F	
537	C	C	in rocks	in rocks			gr; gn; sch; sl		Moll frags	
538	P	P	m(C); b	(R)			pum	Di	F	Alg
539	C	C	m(C); b	(P)			v. gl; bas		F	Alg
540	C	C	m(C); b	(P)			v. gl; bas	Di	F; Moll frags	Alg
541	C	C	m; b	(P)			qtzte; bas	Di	F; Moll frags	
545	C	C	m(C); b	(P)			v. gl; bas; qtzte	Di(R)	F	Alg
546	C	C	m(C); b	(P)			bas		F	Alg; f. sc
546A	C	C	m(C); b	(P)			bas		F	Alg; f. sc
548	C	C	m; b	(P)			qtzte; bas; sch	Di(R)	F; Moll frags; Ostr	Alg
550	A	C	m; b(R)	(P)			bas; qtzte	Di; sp spic	F; Bra; Ech sp; Moll frags	Alg
552	A	C	m; b	(P)			bas; sch; sl		F; Ostr; Moll frags; Ech sp	Alg
553	C	C	m & b(R)	(P)			qtzte; v. gl(R); bas		Ostr; Bra; Moll	Alg
555	A	C	m & b(R)	(P)			qtzte; bas	Di(R); sp spic	F; Ostr; Moll frags	Alg
556	R						qtzte		F; Bry	Alg
557							qtzte		Moll; Bry	sp; Cr
558							gab		Alg; Bry	
559	C	C	m; b	(P)			qtzte; gab; bas	Di(R)	F; Ostr; Moll frags	Alg
560	C	C	m; b	(P)			qtzte; bas; sl; sch; gab		F	Alg
561	A	C	m; b(C)	(P)			gr; qtzte; bas		F; Ostr; Moll frags	Alg
563	C	C	m(C); b	(P)			bas		F; Ostr; Moll	Alg; Cr
564	A	C	m(C); b	(P)			bas		F; Ostr; Moll frags	Alg
567	R	A		(C)		mag; ol	bas		F; Ostr	Cr
569	P	A	m(R); b	(C)		mag; ol	v. gl	sp spic	F; Ech sp; Ostr Moll frags	Cr

TABLE IV (continued)
MINERALS AND ORGANISMS IN ARCTIC BOTTOM SEDIMENTS

NEL Sample	LIGHT MINERALS			HEAVY MINERALS		ROCKS	ORGANISMS			
	No.	Quartz	Feldspar	Mica	Pyriboles		Others	Siliceous	Calcareous	Chitinous
571	R	R		b(R)					F; Ech sp; Moll frags	
589	C	C		m(R); b	(R)	v. gl	qtzte; gr; bas; sch		F; Bra	Alg
590	P	P		m; b	(R)	ol(?)	qtzte; sch; bas; v. gl		F; Ostr; Moll	Alg
594	C	C		m(R); b(C)	(P)		qtzte; gn; sch; bas		F	Alg
596	R	VR		B(R)	(R)		sch; pum; bas	Di(R)	F	Alg
600							sch; v. gl; pum		F(R)	
601							sch; v. gl; pum(A)		Moll	Cr(R); Alg(R)
605	P						qtzte; sch; bas; v. gl		F; Ostr	Alg(R)
607							sch		Moll frags	
608							sch; v. gl; pum		F(R); Moll	Alg(R)
609	A	C		m; b(C)	hbl; etc(P)	tr; mag			F(R)	Alg
610	C	C		m; b(C)	(P)	tr; mag	pum	Di(C)	F; Moll	Alg; wm; wood
612	P	R		b	(R)	tr; mag	sch(C)	Di	F; Ostr	Alg
615							sl; sch; gn		Moll; Alg; Bry	

ABBREVIATIONS:

Alg	Algae	hyp	hypersthene
aug	augite	m	muscotite
b	biotite	mag	magnetite
bas	basalt	Moll	Mollusca
Bra	Brachiopoda	ol	olivine
Bry	Bryozoa	Ostr	Ostracoda
Cr	Crustacea	pum	pumice
Di	Diatoms	qtzte	quartzite
Ech	Echinoids	sch	schist
F	Foraminifera	sl	slate
frag	fragment	sp	sponge
f.sc	fish scales	spic	spicule
gab	gabbro	spin	spine
gn	gneiss	tr	tremolite
gr	granite	v.gl	volcanic glass
hbl	hornblende	wm	worm trails or tubes

FREQUENCY SYMBOLS: A....Abundant C....Common P....Present
R....Rare If no frequency symbol is used, item is considered as present

Grünow is present in most of the Bering Sea samples; and Melosira sulcata (Ehrenberg) was identified in all the Kotzebue Sound samples.

There is little correlation between the abundance and type of living diatoms obtained from the overlying water in net hauls by Phifer¹⁰ and the number and species present in the bottom sediment. For example, Coscinodiscus centralis, although widely distributed, is found in net hauls in only relatively small numbers. Many diatoms which are abundant in the water are completely absent from the sediments. These are generally the filamentous forms whose frustules are

TABLE V
DIATOMS IN ARCTIC BOTTOM SEDIMENTS

NBS Sample No.	General Locality	Coscinodiscus Centralis	C. Curvatus	C. Radiatus	C. Lineatus	C. Marginatus	C. Concinus	C. Oculusiridis	Actinocyclus Ehrenbergii	Actinoprychnus Senarius	Melosira Sulcata	Biadulphia Aurita
501	Bering Sea	A	R		R							
507		A				R		R				
505		R										
507		C	R			R					R	
505		A	R	R		R	R		R	R	R	R
510		R	R									
516	Chukchi Sea	no diatoms										
517		R										
519		R										
520		R			R							
521		no diatoms										
522		R										
523		R										
524		R										
525		R										
530		no diatoms										
532		R										
538		R	R								R	
540		no diatoms										
541	Kotzebue Sound	C									R	
545		C					R				R	
550		C				R			R		R	

readily comminuted and dissolved. Also these frustules are probably transported off the shelf and into the oceanic basins by even the weakest of currents.

Foraminifera. Foraminifera are not abundant in the bottom sediments of the Bering and Chukchi Seas. However, a few were separated from most of the samples by floating them off with carbon tetrachloride. The fauna was quite uniform from sample to sample so that there was little to be gained from considering each sample separately. The great abundance of arenaceous tests as compared with calcareous forms is noteworthy. Some of the species are probably new species.

The following is a composite list of species identified from 30 bottom samples by M. L. Natland of the Richfield Oil Corporation.

Cassidulina sp.
Elphidium cf. *articulatum* (d'Orbigny)
Elphidium cf. *bughesi* Cushman and Grant
Eponides frigida Cushman
Haplophragmoides sp.
Lagena gracilis Williamson
Lagena striata var. *strumosa* Reuss
Martinotiella sp.
Nonion labradoricum (Dawson)
Nonion cf. *scapha* (Fichtel and Moll)
Nonionella turgida var.?
Reophax excentricus Cushman
Textularia sp.
Verneuilina advena Cushman
Virgulina cf. *bramletti* Galloway and Morrey
Trochammina sp.
Uvigerina juncea Cushman and Todd

Although the assemblage is boreal, many of the species are commonly found off southern California at depths similar to the depth at which they are found in the Bering and Chukchi Seas. The arenaceous species Verneuilina advena is noted by Natland as being very abundant. This is especially significant because he has found this species abundant in the Gulf of Panama. Apparently some factor other than temperature, such as depth or character of the sea floor, controls the distribution of this species.

Bacteria. Aseptic mud samples from various portions of the core samples from the Bering and Chukchi Seas were extracted by Fred Sisler of the Scripps Institution of Oceanography in order to study the bacterial flora. The detailed results of this study are being reported separately by ZoBell and Sisler. Among other things, this study showed the usual presence of anaerobic hydrogen-consuming heterotrophes (bacteria which utilize organic matter as a source of energy) and the complete absence of anaerobic hydrogen-consuming autotrophes (bacteria which utilize inorganic matter as a source of energy).

Distribution of Shelf Sediments. At first view, the sediment distribution in the Bering and Chukchi Seas, as shown in figures 2 and 5, requires some explanation. There is no support for the often-stated belief that sediments are coarse near shore and become progressively finer with depth and distance from shore; such a belief is based upon wind wave action alone and grossly fails to consider the many other processes at work. However, the grade-size distribution of

[REDACTED]

sediments is largely explainable when the following factors are considered: (1) the depth; (2) the topography of the bottom; (3) the distance from a source of sediments such as the shore or a river mouth; (4) the exposure of the bottom to currents related to internal waves, the tide, semipermanent currents, or surface waves. Tidal currents are an especially important cause of bottom erosion because both theory and actual measurement show that they extend to the sea floor with little loss of velocity except that caused by frictional drag against the bottom. Currents in general reach maximum velocities wherever the flow is constricted, either horizontally or vertically, such as in narrow bay entrances, over submarine hills, in straits, over sills, or at breaks-in-slope.

On the shelves of the Bering and Chukchi Seas, rocky, stony, and coarse sandy areas appear to be largely confined to topographic highs on the bottom, to the vicinity of the break-in-slope between the shelf and the continental slope of the Bering Sea, and to bottoms swept by strong semipermanent currents. A zone of coarse sand appears to lie along the margin of the shelf of the Bering Sea near the break-in-slope. According to Trask,¹⁴ coarse sediment is also found down to a depth of 1,080 fathoms (2,000 meters) on this continental slope. The presence of coarse sediment near the break-in-slope appears to be a characteristic of most continental shelves. Stetson¹¹ recorded coarse sediment at the edge of the shelf off the eastern United States. He ascribed this finding to vigorous wave action during lower Pleistocene sea levels which washed out the mud, and suggested that since that time fine material from shore has been deposited before reaching the break-in-slope. The authors of this report, however, are inclined to ascribe the coarse sediment along the margin of the shelf to the stronger currents, especially tidal currents, which winnow out the mud. Fleming and Revelle⁵ have shown theoretically that such a concentration of currents must take place. Currents moving onto the shelf from the open ocean are greatly speeded up because the vertical cross-sectional area of the ocean is reduced.

The stony and rocky bottom present in the Bering Strait is undoubtedly related to the strong scouring action of the north-setting current which funnels through this strait. The USS NEREUS measured a surface velocity of 2 knots at the time of her passage (see Dynamic Topography and Currents, below). This strong current continues northward along the Alaskan coast toward Point Barrow and probably accounts for the coarse sediments found at stations 22 and 26 outside of Kotzebue Sound (fig. 5).

No topographic highs were encountered on the track of the USS NEREUS, but it is likely that any which exist are rocky or stony areas. This is especially true of topographic highs which are also shoals, but such highs, regardless of depth, are invariably covered with at least coarse sand. For this reason, it is likely that the bottom in the vicinity of Herald Shoal is coarse grained.

The bottom of the Bering Sea is largely covered by fine sand, whereas the somewhat shoaler Chukchi Sea has typically a mud bottom. This condition is probably related to stronger bottom currents which oceanographic conditions show must exist in the Bering Sea. In the Chukchi Sea, moreover, the tides are smaller than in the Bering Sea; the small tide that does exist (at Point Barrow the mean tide change is only $1/2$ foot) is caused by the Atlantic tidal wave traversing the Arctic Ocean. Throughout most of the year the Chukchi Sea is ice-covered, promoting quiet bottom conditions. Surface waves of more than a short period are almost entirely absent, and these have little effect on the bottom because waves only generate appreciable bottom currents to a depth equal to one-half their wave length. There is also a large amount of fine sediment carried into the Chukchi Sea by rivers, ice rafting, and currents through the Bering Strait. All these factors probably account for the muddy character of the Chukchi Sea floor.

Ice Rafting. The most striking method of transportation of sediments in the arctic is ice rafting. Ice is capable of rafting large amounts of detritus of all sizes, from clay up to large boulders, for long distances. The quantitative importance of this process is demonstrated by the bottom sediments which, in the Chukchi Sea, are generally poorly sorted. In the mud, pebbles are frequently found which can have reached their present position only by ice rafting (figs. 10 and 11). However, some sediments are fairly well sorted, suggesting that there has been some reworking of the bottom sediments. A large percentage of the floebergs observed from the USS NEREUS in the vicinity of the ice pack contained detritus although this ice was 150 miles from the nearest land. Some of the floebergs had the appearance of floating rock piles (fig. 12).

For geographic reasons, icebergs are only rarely present in this part of the arctic, and the ice rafting is accomplished by river ice washed out to sea and, especially, by fast ice (sea ice which has frozen to the bottom). Sverdrup¹² writes that extensive floes become grounded every winter in water depths up to 20 meters. In shallow areas near shore, sediment

Figure 10. Glaçon with surface laden with mud. The shell in the center is about one centimeter in diameter.

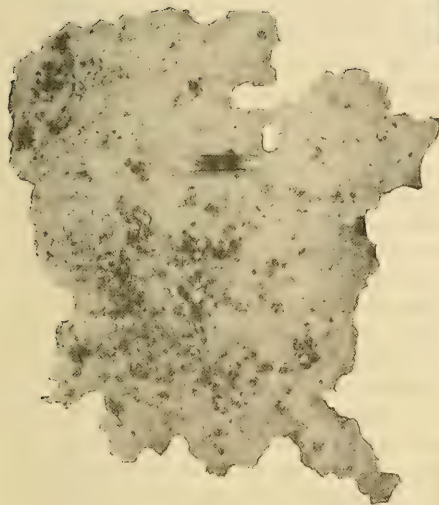
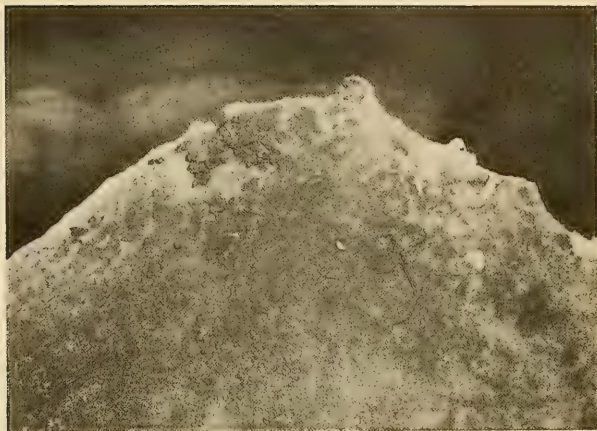


Figure 11. Glaçon heavily laden with well-sorted pebbles (latitude 72° N, longitude 169° W).

Figure 12. Floesberg heavily laden with rafted detritus, located near the ice pack almost 200 miles from the nearest land (latitude 72° N, longitude 169° W).



becomes frozen fast to the bottom of ice. By surface melting in summer and bottom freezing in winter, sediment tends to work its way toward the top of the floe in a few years. Such grounded floes may be turned over by the pressure of large floes carried against them by currents. The charts of the shoal shelves of northern Siberia and Canada show that there are extensive areas where the water is less than 11 fathoms deep (20 meters), shoal enough for the grounding of ice.

It would seem that the catastrophic outflow of water with the advent of the summer thaw must also carry great quantities of detritus by rafting in river ice. However, the finding of shell fragments in a sample (NEL 537) collected from the ice by the USS NEREUS shows that this ice picked up its load from the sea floor. Two samples were collected from the ice at the periphery of the polar pack; one sample (NEL 538) consisted of silt and clay, and the other (NEL 537) consisted entirely of rounded to angular gravels 2 to 10 mm. in diameter.

Observation of drifting ice has shown that when the large blocks of landfast ice break loose from the Canadian Archipelago, they move west toward the Chukchi Sea and then north toward the pole. Although the circulation in the central part of the arctic basin is clockwise (from east to west), currents along the shore are largely affected by the wind. Since these wind-induced currents are commonly east-setting, the debris-laden ice from the shoal and extensive shelf off North Siberia can also be transported into the Chukchi Sea.

An undoubtedly significant relationship exists between the shelves of the Bering and Chukchi Seas and the position of seasonal ice cover. According to the U. S. Navy Hydrographic Office Ice Atlas of the Northern Hemisphere,¹⁶ the deep arctic basin is almost everywhere covered by a permanent ice pack. The shelves of the Bering and Chukchi Seas are almost entirely covered by seasonal ice, and the position of the Bering Sea continental slope agrees fairly well with the maximum extent of the ice. Although the seasonal ice cover on the shelves is an important factor controlling the type and amount of deposition, the position of these shelves is a cause of the ice cover rather than a result of it because of the fact that shoal shelf waters undergo marked seasonal changes. In this connection, associated physical oceanographic factors are important; these are: (1) low salinity, (2) the partial restriction imposed by the continental slope of the intrusion of warmer southern water, and especially, (3) the rapid cooling owing to the shoal depth. In contrast to fresh water, where a positive temperature gradient becomes stable near the freezing point, the entire volume of

sea water must approach the freezing point before the surface freezes.

Little is known of the character of the continental slope in the Chukchi Sea. However, because of the oceanographic factors involved, one can predict that its geographic position coincides closely with the limits of the permanent polar ice-pack.

Transport of Sediment by Currents. Although bottom currents in the Bering Sea and especially in the Chukchi Sea are presumably weak, the grade size and sorting of the bottom sediments show that current action has effectively sorted and transported large amounts of bottom material. The Bering Sea is largely covered by fine sand, indicating that the silt and clay carried in from shore must bypass the shelf. Judging from the surface currents, it is likely that the silt and clay, when carried out to the open shelf, are largely transported to the north into the Chukchi Sea. The quieter water of the Chukchi Sea permits the settling out of finer material, but even there the sediments are low in clay and diatom frustules, showing that the finest sediment must also bypass this shelf and move into the arctic basin.

The sediment-laden and turbid bottom water layer detected by photography is direct evidence of detritus being transported in suspension. It was not possible to determine if this turbid layer assumes the properties of a suspension current, but the general absence of an appreciable grade for such a current to move down makes this unlikely. It is probable that the suspended material is carried along by the north-setting, semipermanent currents.

Most of the samples, when fresh, had a watery layer of brownish (oxidized) sediment about 1 to 3 inches thick at the top resting on a stiffer and darker (reduced) substratum. It is possible that this water layer is material which goes into suspension under conditions of maximum bottom agitation and that it is thus being actively transported.

III. physical oceanographic observations

TEMPERATURE AND SALINITY STRUCTURE

The USS NEREUS hove to four times each day in the shallow areas of the Bering and Chukchi Seas for vertical series of temperature, salinity, and other oceanographic observations. The locations of these hydrographic stations are shown in figure 13. Thirty-nine hydrographic stations were obtained north of the Aleutian Islands, twenty-two of these being located north of Bering Strait in the Chukchi Sea.

Several previous oceanographic cruises, notably those conducted by the U. S. Coast Guard in 1934,¹⁵ and in 1937-1938,⁷ have made fairly complete investigations of the eastern Bering Sea and Norton Sound. However, relatively little data have previously been obtained in the central Chukchi Sea area. The U. S. Coast Guard cruises in the summers of 1937 and 1938 occupied a number of stations along the Alaskan coast from Bering Strait nearly to Point Barrow, but these data are not sufficient to show the lateral distribution of the physical variables. Sverdrup in the MAUD¹² obtained considerable data between Herald Shoal and Wrangell Island but occupied only two hydrographic stations east of 170°W in the Chukchi Sea. Thus, the data taken during this cruise of the USS NEREUS

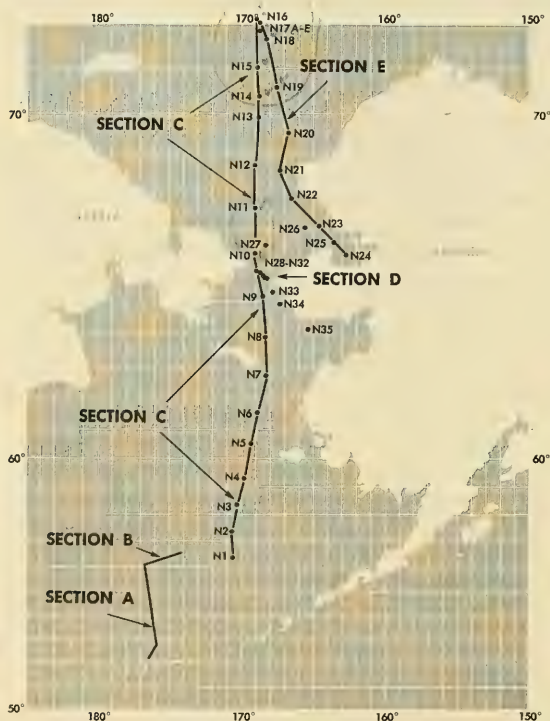


Figure 13. Bathythermograph and hydrographic stations used for vertical sections.

in the Chukchi Sea represent a considerable increase in the oceanographic information available concerning this area.

Also shown on figure 13 is the location of the line of bathythermograms obtained in the run from Adak north to the southern edge of the extensive shallow water area of the Bering Sea. It was in this shallow water region, north from the area of the Pribilof Islands, that all the hydrographic stations in the Bering Sea were obtained. At each hydrographic station vertical water temperatures were obtained from both bathythermograms and reversing thermometers. The bathythermograph observations are extremely valuable from the standpoint of description of the thermal structure, since a continuous temperature trace with depth is obtained. Because of this greater detail given by the bathythermograph observations, all vertical cross sections are based on bathythermograms and the isotherms are in degrees F.

The accuracy of the temperatures from bathythermograms varies with the calibration and construction of the instrument. Instruments which have developed a temperature set are compensated for, in printing of bathythermograms, by adjusting all temperatures by the amount of the average set, based on the average difference between the surface trace and the surface bucket temperatures. The accuracy of temperatures from bathythermograms is thought to be within 0.2 to 0.3 degree F by compensating for sets. The bathythermograph depth recordings, aside from adjustments in setting the top of the trace on the zero depth line, were not calibrated while in use. All depths are based on the previous calibrations of the individual instruments.

Temperatures taken by means of reversing thermometers were more accurate than those taken by means of bathythermographs. Both German- and American-made thermometers were used. Because of the low temperature water encountered, the thermometers were allowed in all cases to come to equilibrium for 15 minutes before tripping. By comparing duplicate readings and from previous experience with similar thermometers, it is believed that the accuracy of the German thermometers is within 0.02 degree C and that the accuracy of the American thermometers is within 0.05 degree C. Whenever readings were taken using only American thermometers, these readings are noted in the tabulation of temperature data with an asterisk. The greater accuracy of the temperatures obtained by the use of reversing thermometers simultaneously with the taking of water samples is needed for computations of density and dynamic topography.

Adak to the Pribilof Islands. Bathythermograph observations were made every hour along a section from Adak northward to $56^{\circ}03'N$, $176^{\circ}38'W$ and then along a section east northeastward to $56^{\circ}36'N$, $173^{\circ}39'W$. These sections (sections A and B, fig. 13) are over the eastern end of the deep Bering Sea basin, with the depth running at about 2100 fathoms at most stations. The bathythermograph, therefore, suffices in obtaining only a relatively small portion (300 to 400 feet) of the vertical thermal structure of this region. It has been shown, however, that the temperature and salinity structures of the Bering Sea basin below 100 meters are very similar to those in the subarctic region of the North Pacific.* The mean flow is northward through the channels of the Aleutian chain, and the bathythermograph traces characteristic of most of these observations in the southern Bering Sea are not unlike those found in the subarctic water south of the Aleutians.

A group of bathythermograph observations typical of this region are shown in figure 14. The locations of the observation stations move northward from left to right. The thermocline is more intense on observations taken farther north (fig. 14c), but the mean temperatures do not change greatly.

Two vertical cross sections of the temperature structure have been constructed from these data. Temperature sections A and B are shown in figures 15 and 16, respectively. In the first five stations in section A, the slope of the isotherms

*Sverdrup, Johnson, and Fleming, The Oceans (ref. 13), pp. 732-733.

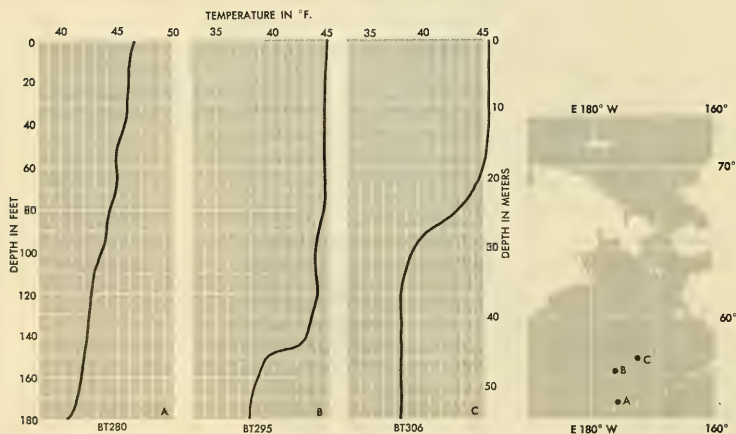


Figure 14. Bathythermograms taken in the southern Bering Sea.

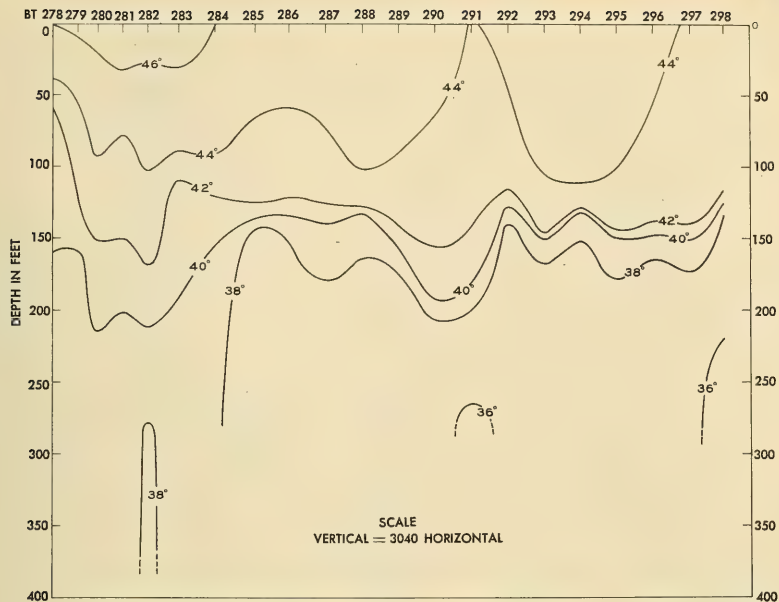


Figure 15. Vertical temperature section A (degrees F) near the Aleutian Islands (see fig. 13 for location of section).

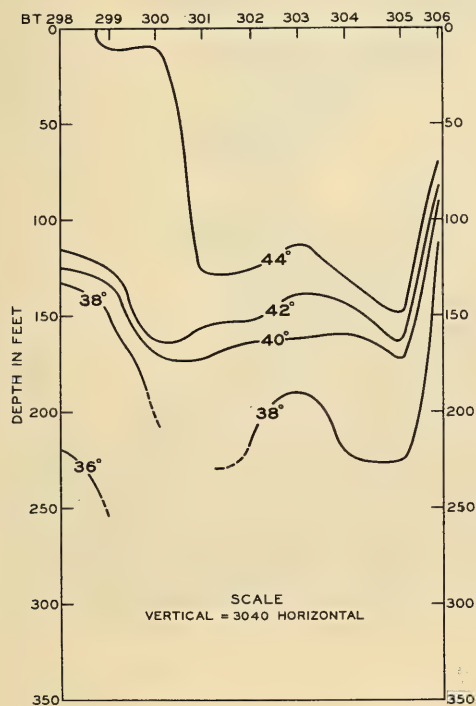


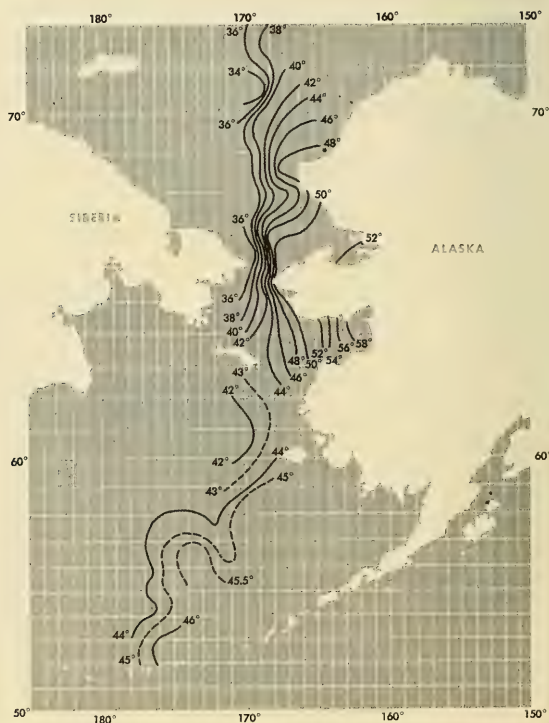
Figure 16. Vertical temperature section B (degrees F) near the Aleutian Islands (see fig. 13 for location of section).

extending on a line running southwest to northeast, is downward from southwest to northeast and is, therefore, indicative of a current with a northerly component.* The remainder of section A runs just west of north, and the slight slope of the isotherms upward to the north is indicative of a weak east component of the current across the section.

Section B runs mainly in a west-east direction, and the slope of the isotherms, downward from west to east, indicates a northerly current. At the eastern edge of the section the slope is reversed, indicating a southerly flow. Such a temperature structure is evidence of a large eddy circulation. The horizontal temperature structure at the surface, at 25 meters (82 feet), and at 40 meters (131 feet), is shown in figures 17, 18, and 19 and further emphasizes the existence of a clockwise eddy at about 55°N, 175°W. These features will be discussed further in a later section.

*A discussion of the relationship between thermal structure and currents is given in The Oceans (ref. 13), p. 394.

Figure 17. Horizontal distribution of temperature (degrees F) in Bering and Chukchi Seas, at the surface.



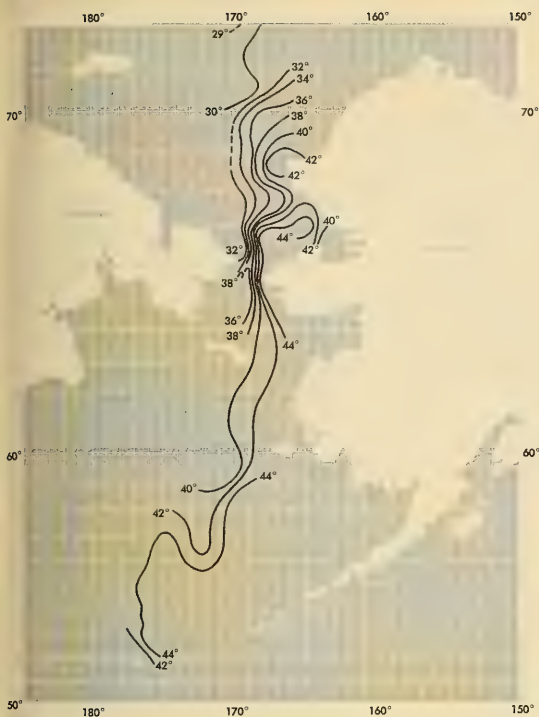


Figure 18. Horizontal distribution of temperature (degrees F) in the Bering and Chukchi Seas, at a depth of 25 meters.

Figure 19. Horizontal distribution of temperature (degrees F) in the Bering and Chukchi Seas, at a depth of 40 meters.



The Bering Sea from the Pribilof Islands to Bering Strait.

Nine hydrographic stations were occupied along a line running from a point just south of the Pribilof Islands to the eastern side of St. Lawrence Island and then north to Bering Strait; three more stations were occupied on a line southeast from Cape Prince of Wales toward Norton Sound. See figure 13 for the location of these stations.

The temperatures taken at all hydrographic and bathythermograph stations were scaled off at the surface, at 25 meters (82 feet), and at 40 meters (131 feet) for the construction of charts showing the horizontal temperature structure. Two-degree F isotherm intervals were used. In areas of weak horizontal gradients, additional isotherms could be included. Where only a single line of stations was taken, extrapolation of isotherms was made.

Similar charts have been constructed to show the horizontal distribution of salinity at the surface, at 25 meters, and at 40 meters (figs. 20, 21, and 22). Here only the hydrographic station data could be used.

As shown by the horizontal distribution of temperature and salinity at various depths (figs. 17 through 22), the major change in these variables occurs in an east-west direction



Figure 20. Horizontal distribution of salinity in parts per thousand (‰) in the Bering and Chukchi Seas, at the surface.

Figure 21. Horizontal distribution of salinity in parts per thousand (‰) in the Bering and Chukchi Seas, at a depth of 25 meters.

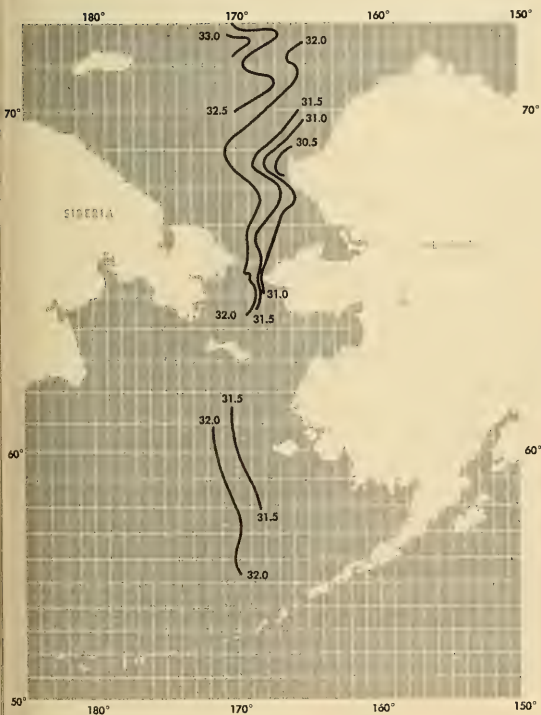


Figure 22. Horizontal distribution of salinity in parts per thousand (‰) in the Bering and Chukchi Seas, at a depth of 40 meters.

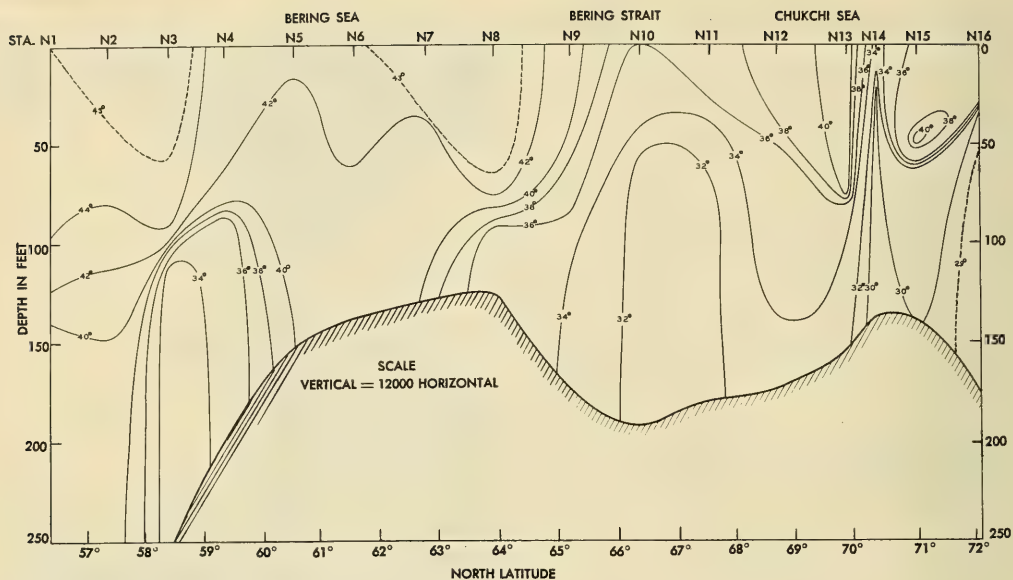


Figure 23. Vertical temperature section C (degrees F) from Pribilof Islands through Bering Strait to 72° N latitude (see fig. 13 for location of section).

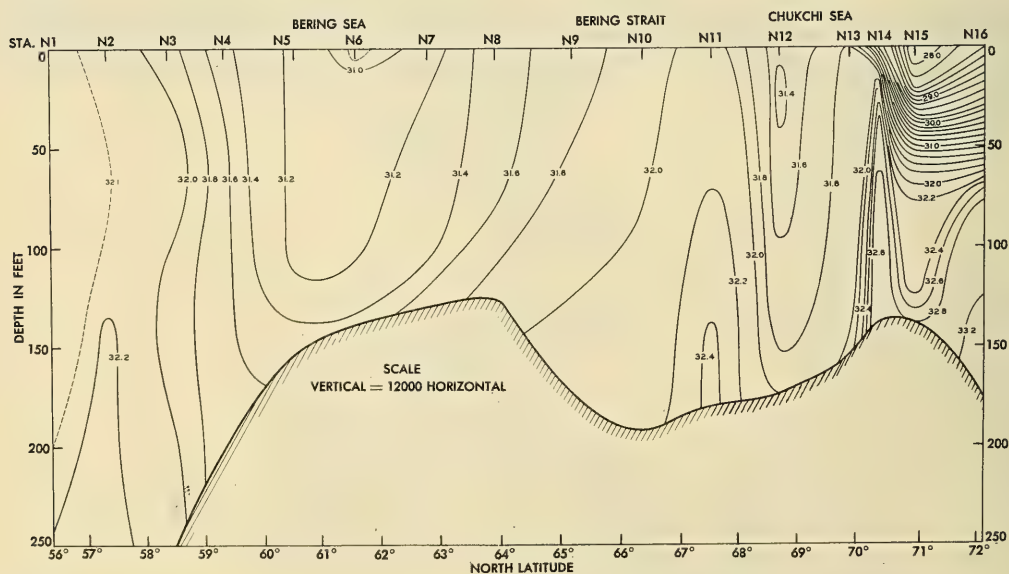


Figure 24. Vertical salinity section C in parts per thousand (‰) from Pribilof Islands through Bering Strait to 72° N latitudes (see fig. 13 for location of section).

rather than along the line of stations running from the Pribilof Islands to the Bering Strait. In general, the warmer and less saline water is found toward the Alaskan coast. The isotherms tend to run southwest-northeast in the region of the four southernmost stations; however, the ridge extending out from Cape Romanzof appears to deflect the warm coastal water west, so that the isotherms run southeast-northwest in the region south of St. Lawrence Island.

The isotherms and isohalines for the southernmost four stations are not parallel; the isohalines run from southeast to northwest, while the isotherms run approximately southwest-northeast, as mentioned above. The protrusion of the isohalines to the west in the region of Cape Romanzof occurs somewhat south of the same protrusion of the isotherms. North of St. Lawrence Island the isotherms and isohalines run approximately parallel, converging toward Bering Strait.

The highest surface temperatures encountered occurred in Norton Bay, where temperatures of 58 degrees F were observed. Although the lowest surface temperature obtained south of Bering Strait was 41 degrees F, the trend of the isotherms indicates that much lower temperatures exist off the Siberian coast opposite Seward Peninsula.

Vertical cross sections of the temperature and salinity along a line running from just south of the Pribilof Islands up through Bering Strait and thence north along the 169°W meridian to 72°N latitude are plotted in figures 23 and 24. The left-hand portions of these sections, from stations N1 through N9, apply to the Bering Sea. The temperature structure for figure 23 shows the protrusion of a cold tongue near the bottom at stations N3 and N4 (58° to 59°N), but the water over the ridge between Cape Romanzof and St. Lawrence Island (60° to 63°N) is uniformly warm from top to bottom. The temperature decreases again at subsurface depths north of St. Lawrence Island (63°N).

The salinity cross section (fig. 24) also shows the extension of a low salinity tongue off Cape Romanzof (60° to 63°N). The major features of the salinity section occur farther south than corresponding features in the temperature section.

Typical temperature-depth and salinity-depth traces for this section of the Bering Sea are shown in figure 25. The salinity-depth traces show only slight variation of salinity with depth in the central Bering Sea. To the south, in the region of the Pribilof Islands, and to the north of St. Lawrence Island, cold bottom water is found (traces A and C). Off Cape Romanzof, however, the temperature structure remains relatively warm to the bottom (trace B).

The study of temperature-salinity relationships provides a convenient method for determining water mass characteristics and origin. Temperature-salinity diagrams, therefore, were plotted for all stations in the Bering Sea except those in Norton Sound (see fig. 26). These stations in Norton Sound, together with those in Kotzebue Sound, are dealt with later. Also in figure 26 is the T-S relationship for the upper layers of the subarctic water found to the south of the Aleutians, as given by the upper 100 meters of Carnegie Station 120 ($47^{\circ}02'N$, $166^{\circ}20'E$). The T-S relationships at NEREUS stations N1, N2, and N3 are similar to those at the Carnegie station but with lower salinity. The shape of the T-S relationship remains about the same, but the average salinity decreases to the north (stations N4, N5, N6, N7) until the region between St. Lawrence Island and Bering Strait is reached. Here the water has a higher salinity because of the mixing with the more saline water which apparently flows northward along a line to the west of the line of the NEREUS stations.⁷

Bering Strait. Five hydrographic stations were occupied across the eastern half of the Bering Strait. Very large horizontal gradients of the physical variables were encountered here, the most extreme gradients occurring along the Alaskan side of the strait. In this location, a surface temperature drop of 10 degrees F in 30 miles was observed; 8 degrees of this change occurred in the 10 miles between the two stations nearest the Alaskan coast. The corresponding salinity change is 2.5 parts per thousand.

Vertical cross sections of temperature and salinity have been constructed for the line of five stations across the eastern part of the Bering Strait (section D, fig. 13). The temperature section (fig. 27) shows the change from cold water on the western side of the section to relatively warm water near the Alaskan coast at all depths. The warm water overruns the cold water in the middle of the section, producing fairly large vertical variations in the temperature. The salinity section (fig. 28) shows the decrease in salinity from west to east. The greatest horizontal change at all depths occurs between the two stations nearest the Alaskan coast. This low-salinity water is apparently related to runoff from Alaskan rivers. This distribution of mass must be associated with a relatively strong current running northward through Bering Strait.

Typical temperature-depth and salinity-depth traces in the Bering Strait are plotted in figure 29. The locations of the observations A, B, and C progress from west to east across the strait and are shown on the inset chart.

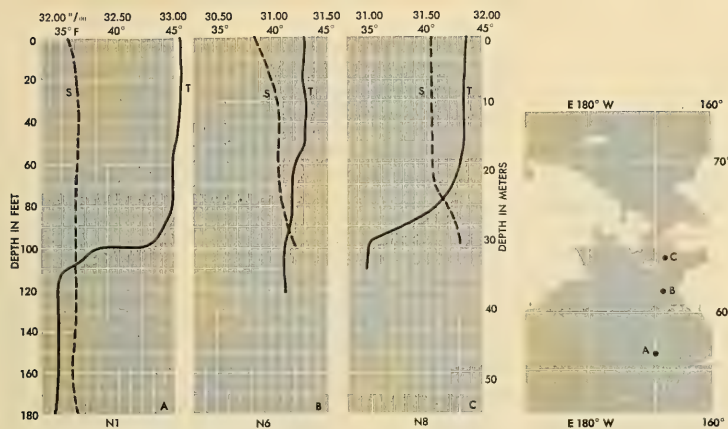


Figure 25. Bathythermograms (T) and salinity traces (S) taken in the Bering Sea between Pribilof Islands and Bering Strait.

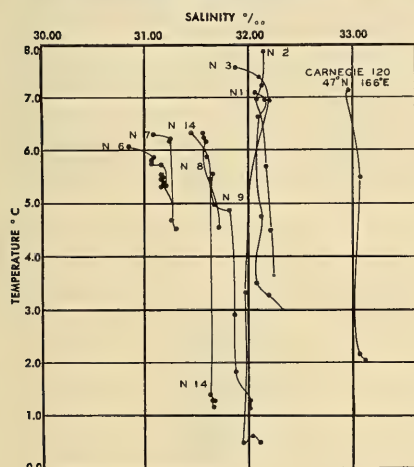


Figure 26. Temperature-salinity diagrams from stations in the Bering Sea (see fig. 1 for location of stations).

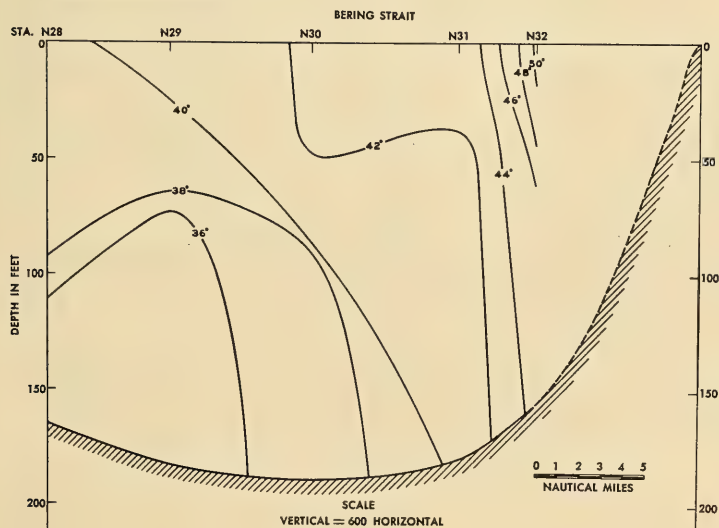


Figure 27. Vertical temperature section D (degrees F) across the eastern side of Bering Strait (see fig. 13 for location of section).

The depth of the thermocline decreases from west to east, with the greatest gradients in the thermocline occurring at the central station. The vertical temperature gradients below the thermocline are small. The vertical salinity gradients increase from west to east. The layer of maximum vertical salinity gradient occurs just below the thermocline in figure 29 C (station N32).

The temperature-salinity diagrams for this area are shown in figure 30. The stations on the western and middle portions of the section show the same T-S characteristics shown by the stations in the central Bering Sea (stations N28 to N30). However, station N32, on the far eastern side of the strait, shows water of different character. This water is warmer and less saline with a considerable salinity gradient. Station N31 is apparently a mixture of the western and eastern waters in the strait. As will be seen later, the T-S relation at station N32 is very similar to that of the Alaskan coastal stations N33, N34, and N35 extending into Norton Sound, and to stations N26 and N27 in the Chukchi Sea, northeast of Bering Strait.

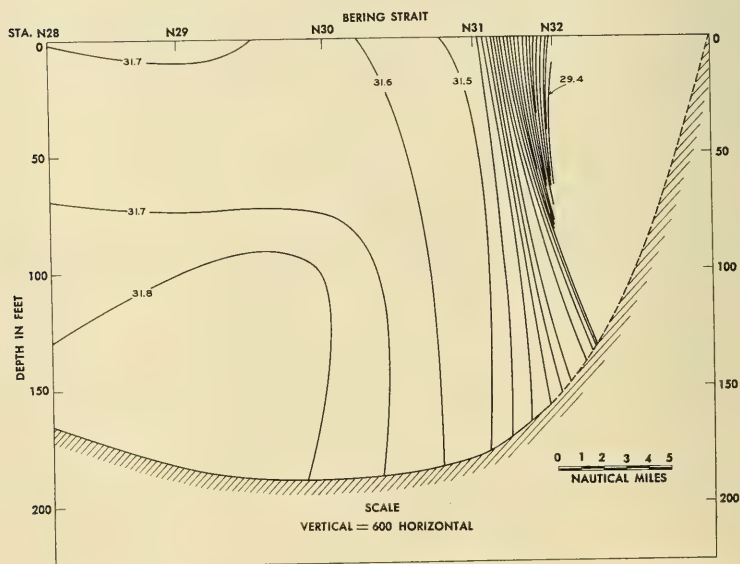


Figure 28. Vertical salinity section D in parts per thousand (‰) across the eastern side of Bering Strait (see fig. 13 for location of section).

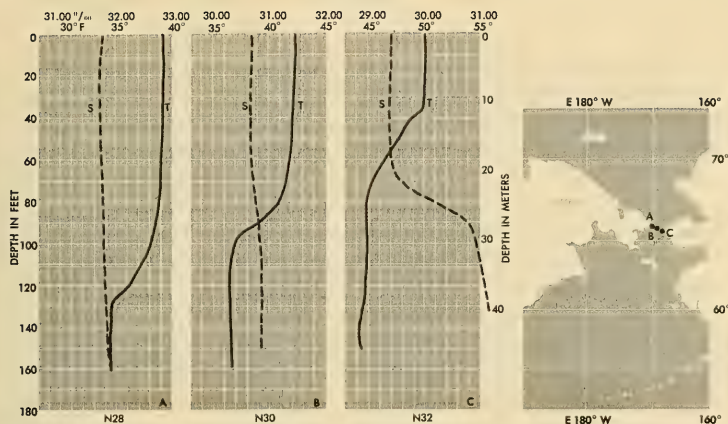


Figure 29. Bathythermograms (T) and salinity traces (S) taken across the eastern side of Bering Strait (see fig. 1 for location of stations).

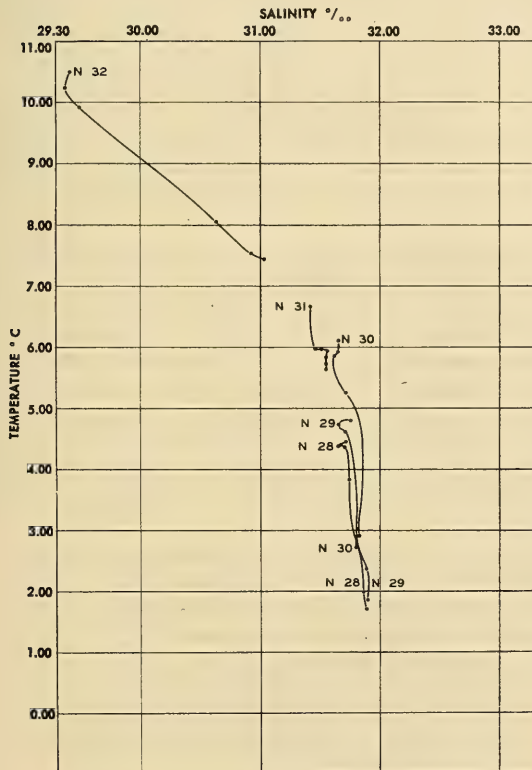


Figure 30. Temperature-salinity diagrams from stations across the eastern side of Bering Strait (see fig. 1 for location of stations).

Chukchi Sea. Twenty-two hydrographic stations were occupied north of Bering Strait in the Chukchi Sea. Seven stations were taken in a north-south line from Bering Strait to the edge of the pack ice found just north of 72°N . Five stations were occupied over a 24-hour period while the ship was drifting southeastward in the immediate vicinity of the ice pack. Another eight stations along the line from the ice pack into Kotzebue Sound, together with the two stations between the sound and Bering Straits, complete the list of stations occupied in this area. This collection of stations provides the most extensive data yet obtained in this section of the Chukchi Sea and provides a good network for the study of the distribution of the physical properties of the sea water.

As was the case in the Bering Sea, the over-all distribution of temperature and salinity in the Chukchi Sea leads to horizontal contour charts which are remarkably similar for the various depths and for both temperature and salinity. The warm, low-salinity water is found at all depths on the Alaskan side of the Chukchi Sea. The isopleths of both temperature and salinity (figs. 17 through 22) run at first in a north-south direction out of Bering Strait and then bend into Kotzebue Sound. The projection of Alaska at Cape Hope leads to a westward trend of the isolines, followed by an eastward trend north of this land projection. Thus, the isolines of both temperature and salinity tend to follow the contours of the coast.

The only marked departure from the similarity between the trend of the isopleths of temperature and salinity occurs at station N15, where low-salinity surface water occurs in conjunction with the low-temperature water found on the westward side of the area. This region of cold, low-salinity surface water may be explained as a pocket of melt water, blown down from the ice area by the characteristic northwest winds which prevailed during the period the NEREUS was in the region. The similarity of station N15 to the stations occupied in the ice area will be noted further in the discussion of the T-S relationship.

The vertical cross sections of the temperature and salinity for the Chukchi Sea are shown in figures 23, 24, 31, and 32. The right side of section C (figs. 23 and 24) gives the conditions from Bering Strait to the ice pack, while section E (figs. 31 and 32) gives the conditions along a line from the ice pack southeastward into Kotzebue Sound. An intrusion of cold water occurs between stations N10 and N11 (fig. 23), just north of Bering Strait. A similar tongue of high-salinity water, well-marked at all depths, appears in figure 24. Just

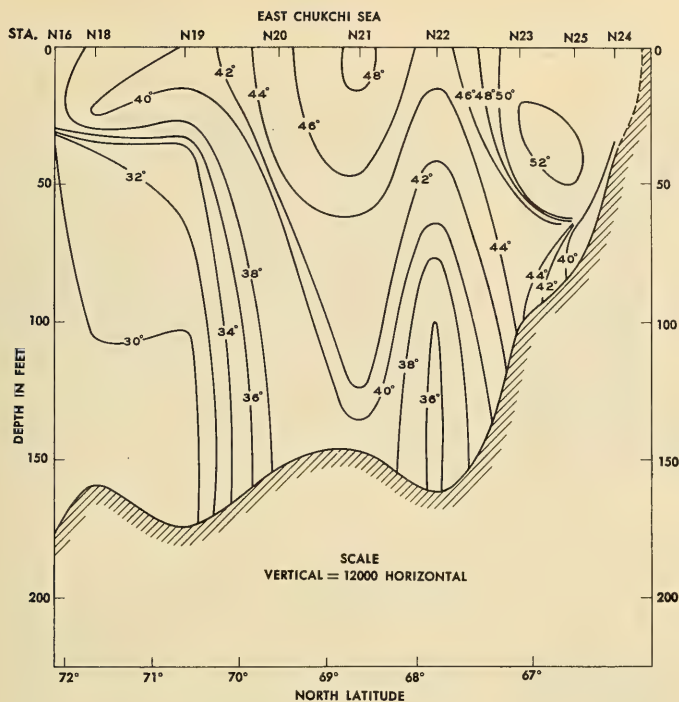


Figure 31. Vertical temperature section E (degrees F) from ice pack to Kotzebue Sound (see fig. 13 for location of section).

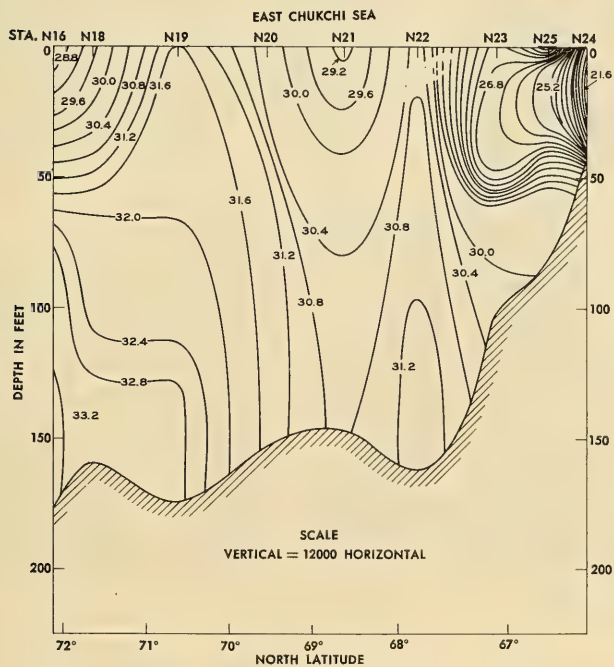


Figure 32. Vertical salinity section E in parts per thousand (‰) from ice pack to Kotzebue Sound (see fig. 13 for location of section).

north of this cold, high-salinity tongue, a protrusion of relatively warm, low-salinity water was found. At station N14 (70°N) the water was found to be colder at all depths, with a subsurface tongue of less than 30 degrees F. The salinity at this station shows low values at the surface overlying relatively high-salinity water at subsurface depths. North of 70°N, the section is characterized by warmer waters in the surface layers, with a subsurface temperature maximum and sharp gradients in the thermocline. At the station farthest to the north, water with temperatures less than 29 degrees F was encountered at depths below 50 feet. The salinity section north of 70°N is characterized by low salinity at the surface and large vertical gradients. The low salinities in the surface layers are characteristic of melt water.

Similar characteristics of temperature and salinity were encountered on the northern part of the return run from the ice pack into Kotzebue Sound (compare figs. 31 and 32 with figs. 23 and 24). The temperature increases at all depths along the section from the ice pack to station N21 off Point Hope. The low salinity in the surface layers north of station N19 is due to the presence of melt water. Between stations N19 and N21 the salinity decreases as the Alaskan coast is approached. The increase in depth at station N22 is associated with a decrease in temperature and an increase in salinity. This tongue of low-temperature, high-salinity water is due to the tendency of the isotherms and isohalines to follow the depth contours. Higher temperatures and very low salinities were encountered in Kotzebue Sound.

Examples of the temperature-depth and salinity-depth plots for the Chukchi Sea are given in figures 33, 34, and 35.

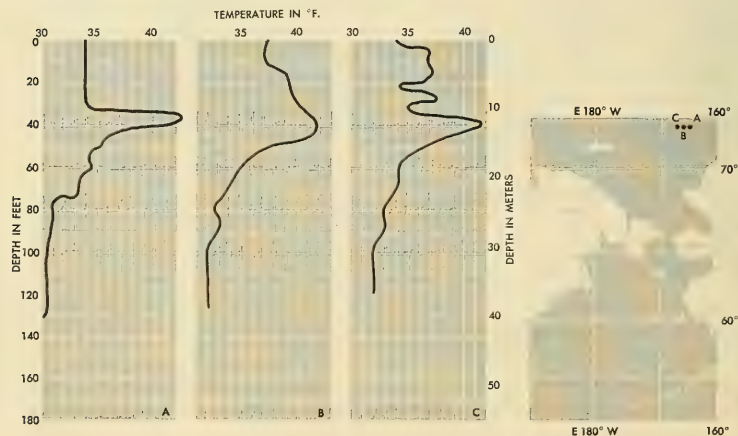


Figure 33. Bathythermograms taken in the ice pack region.

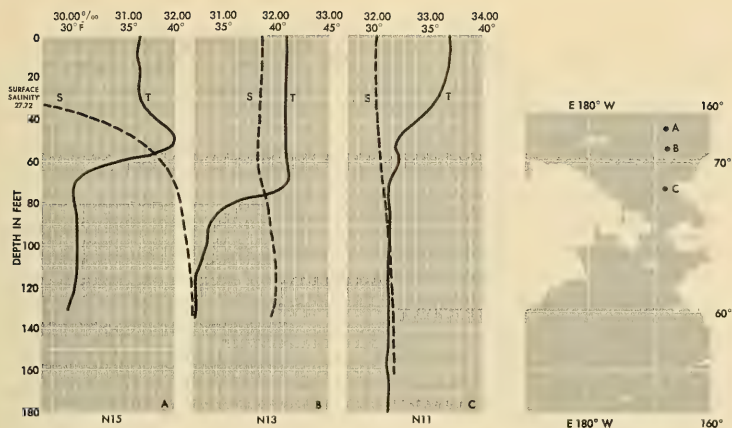


Figure 34. Bathythermograms (T) and salinity traces (S) taken in the central Chukchi Sea.

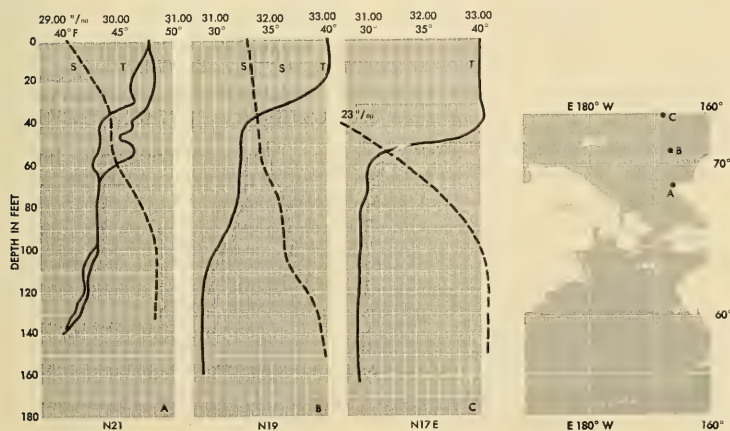


Figure 35. Bathythermograms (T) and salinity traces (S) taken in the eastern Chukchi Sea. Double trace in A represents the observed temperature when lowering and retrieving the bathythermograph.

Several unusual features of these structures appear from the bathythermograph observations. At several stations, a subsurface maximum in temperature was observed. These subsurface temperature maximums, or positive gradients, were frequently observed north of 70°N near the boundary of the ice. In the region of the ice pack, observations showing pronounced positive gradients (fig. 33) were made from the USS BOARFISH. The temperature in the warm subsurface layer was 9 degrees F higher than the overlying isothermal layer (fig. 33A). Repeated observations show that the layer may take on different characteristics. For example, the isothermal layer may be completely lacking, and a positive gradient may extend almost to the surface (fig. 33B). In some cases

multiple layers of positive temperature gradients were observed (fig. 33C). The subsurface maximum occurs most usually at a depth of between 30 and 50 feet, in all cases less than 50 feet. In most cases the salinity gradient is large enough to counteract the temperature gradient, and the vertical stability is maintained (fig. 34A). At some stations, however, the increase in salinity in the layer of positive temperature gradients was not sufficient to compensate for the decreasing density caused by the temperature, and thus resulted in apparent instability. In some cases apparent instability was observed to result from vertical salinity gradients alone. At station N13 (fig. 34B), for example, the surface layers are isothermal, but the salinity decreases slightly with the depth in the upper 20 meters. Such a combination of vertical temperature and salinity structure leads to apparent instability in the upper layers. The fact that instability is present is further substantiated by the bathythermogram at station N21 (fig. 35A). One of the traces shown is the trace made by the instrument while it was sinking through the water; the other trace was made by the instrument while it was being hauled in. If only one such bathythermogram had been obtained, it could be supposed that there was something wrong with the instrument; however, two bathythermographs were lashed together at most of these stations, and nearly identical traces were obtained from both instruments. The rapid change in the thermal structure indicated here (the difference in time between the two traces is but 1 or 2 minutes) may well be explained as the result of vertical convection set up by recently established instability. Typical examples of vertical temperature and salinity plots (fig. 35) indicate that the vertical gradients increase with increasing latitude. The layers near the bottom, especially at the northern stations, show low temperatures of approximately 29 degrees F, and high salinities of about 33 o/oo (fig. 35, B and C). A possible explanation of the formation of this bottom water is given in the discussion of the temperature-salinity relationships below.

The temperature-salinity relationships for stations N10 through N15 are shown in figure 36. The T-S diagrams for N10, N11, N12, and N13 show characteristics similar to those found at the central Bering Sea stations, though the temperatures at the Chukchi Sea stations are somewhat colder. It would seem apparent from this similarity in T-S relationship that the water at these Chukchi Sea stations results from a northerly flow at all depths from the Bering Sea.

The marked change in the T-S relationship at stations

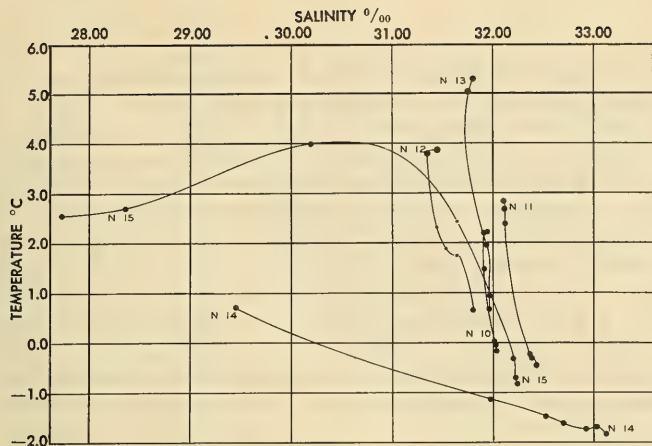


Figure 36. Temperature-salinity diagrams from stations in the central Chukchi Sea (see fig. 1 for location of stations).

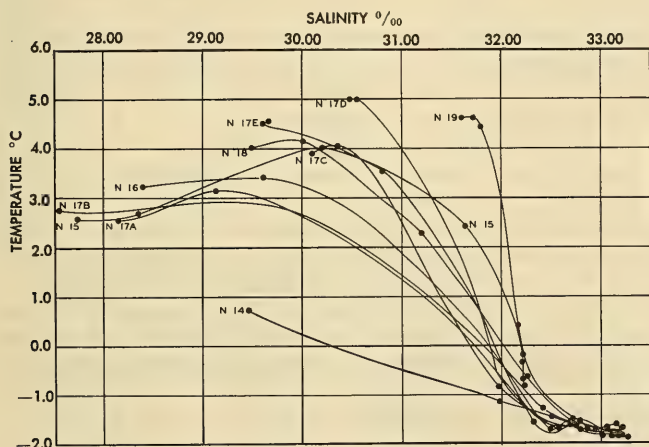


Figure 37. Temperature-salinity diagrams from stations in the northern Chukchi Sea near ice pack (see fig. 1 for location of stations).

N14 and N15 is indicative of a change from water whose recent origin is the Bering Sea to water resulting from the melting of the ice in the northern Chukchi Sea. The elongation of the T-S relation for stations N14 and N15 toward low salinity in the surface layers is indicative of melt water.

The T-S relationships for stations N16, N17 (A through E), N18, and N19 appear in figure 37 with a repetition of the

diagrams for stations N14 and N15. These stations show fairly similar T-S curves. The low-salinity surface water indicative of melting is present to a greater or less degree on all curves. The spread of the curves in the central portion of the diagram is related to the amount of mixing between the low-salinity melt water and higher-salinity water. The higher-salinity, relatively warm water found at mid-depths seems to have originated in the Bering Sea and in this locality appears as a wedge between the surface melt water and the uniform bottom water that is found on all these T-S plots. The cold, relatively high-salinity water (33 o/oo), found on the bottom at all these stations, is probably the result of winter freezing. Because the freezing point is lowered by the presence of salt, relatively fresh water freezes first, especially in slow freezing. The result is that the water just below the freezing layer becomes more concentrated, and, since it is also being cooled, it becomes heavier than the underlying water and sinks to the bottom. Since this bottom water is probably formed in winter throughout the Chukchi Sea (probably in the northern part of the Bering Sea also), the failure of this high-salinity bottom water to appear farther south than station N14 is indicative of a northward transport along the bottom at the stations in the southern and central Chukchi Sea.

Nearer the Alaskan coast the T-S plots show higher temperatures and lower salinities, as can be seen for stations N20, N21, and N22 (fig. 38). Also shown on figure 38 are the T-S relationships for stations N26 and N27, in the southeastern part of the Chukchi Sea, and for stations N33, N34, and N35, located along the Alaskan coast south of Bering Strait, and in Norton Sound. The similarity of the T-S plots between these latter stations in the northeastern Bering Sea and the stations in the southeastern section of the Chukchi Sea further confirms the pattern of flow discussed under Dynamic Topography and Currents.

The vertical thermal structure in both Kotzebue and Norton Sounds is characterized by large, sharp thermal gradients and by lower-salinity water. The surface layer temperatures in these areas were the highest encountered on this cruise. Examples of temperature-depth and salinity-depth curves from Kotzebue and Norton Sounds are shown in figure 39.

A more detailed presentation of the surface temperature conditions is obtained from a continuous temperature trace made aboard the submarine USS BOARFISH by means of a CXJC instrument during the run northward from the north Bering Sea through the central Chukchi Sea to the ice pack

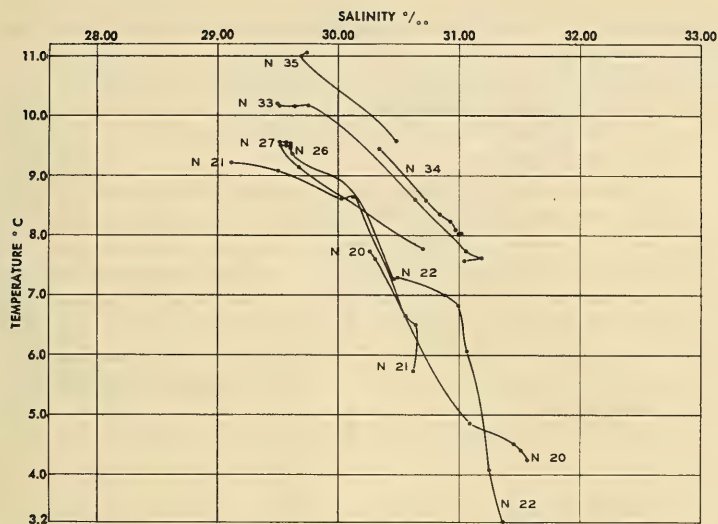


Figure 38. Temperature-salinity diagrams from stations in Kotzebue and Norton Sounds (see fig. 1 for location of stations).

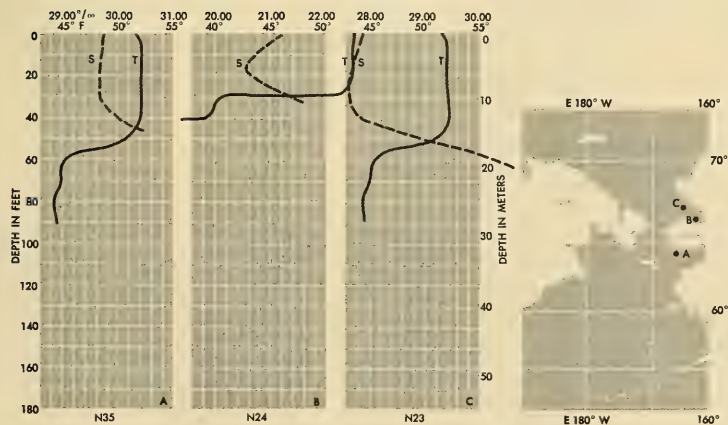


Figure 39. Bathythermograms (T) and salinity traces (S) taken in Kotzebue and Norton Sounds.

and back to Unimak Island. These surface-temperature profiles, together with charts indicating their location, are shown in figures 40 and 41. The general change in surface temperature shown in these figures is similar to that found from measurements taken from the USS NEREUS. The large local temperature variations, however, are brought out in detail by this presentation.

Of particular interest is the relation between certain marked temperature changes and the occurrence of fog. With marked decreases in sea surface temperature, fog was encountered, but with increasing sea surface temperature, the fog dissipated. In one 4-hour period, there were three sharp temperature minima (fig. 40), and in each case fog occurred. The sharp maxima in temperature between these minima were associated with a clearing of the fog conditions. Notations of fog conditions, as well as of ice conditions, are marked along the profile. The hydrographic data from all stations are presented in table VI.

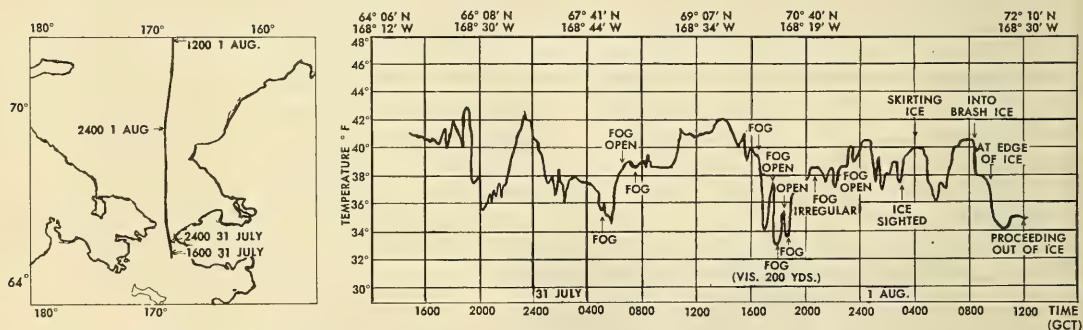


Figure 40. Continuous water temperature recorded near the sea surface from a recording bathythermograph on USS BOARFISH between Bering Strait and the ice pack. Note the relation between sharp breaks in the temperature profile and the occurrence of fog.

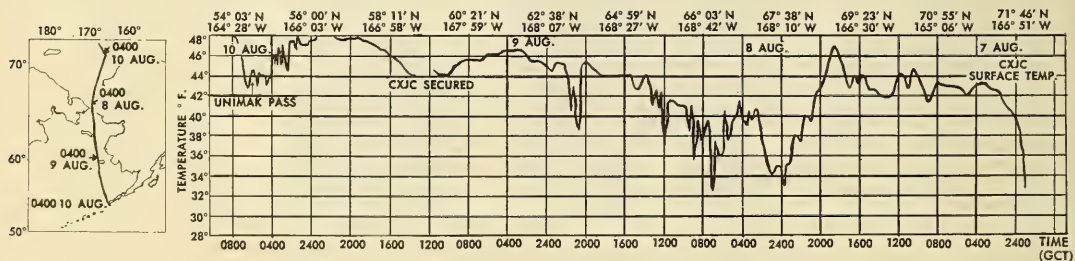


Figure 41. Continuous water temperature recorded near the sea surface from a recording bathythermograph on USS BOARFISH between the ice pack and Aleutian Islands.

TABLE VI
HYDROGRAPHIC DATA

STATION	OBSERVED VALUES			INTERPOLATED VALUES			σ_t
	Depth (meters)	Temperature (degrees C)	Salinity ($^{\circ}/_{\infty}$)	Depth (meters)	Temperature (degrees C)	Salinity ($^{\circ}/_{\infty}$)	
Station N1	0	7.06	32.05	0	7.06	32.05	25.11
27 July 1947	12	6.95	32.16	5	7.02	32.11	25.16
1815 GCT	27	6.62	32.10	10	6.97	32.15	25.20
56° 54' N 170° 36' W	42	4.74	32.12	15	6.91	32.15	25.21
	57	3.47	32.07	20	6.82	32.13	25.21
	72	3.25	32.18	25	6.70	32.11	25.21
	88	2.98*	32.32	30	6.41	32.10	25.24
				40	5.04	32.11	25.41
				50	3.88	32.09	25.51
				75	3.20	32.21	25.67
Station N2	0	7.78	32.14	0	7.78	32.14	25.08
29 July 1947	11	7.24*	32.12	5	7.52	32.13	25.11
0900 GCT	22	6.99	32.07	10	7.28	32.12	25.14
57° 21' N 170° 44' W	33	5.71	32.16	15	7.18	32.09	25.14
	45	4.50	32.21	20	7.08	32.08	25.14
	57	3.64	32.23	25	6.72	32.08	25.18
	69	3.67	32.23	30	6.10	32.13	25.30
				40	5.01	32.20	25.48
				50	4.04	32.23	25.60
Station N3	0	7.56	31.87	0	7.56	31.87	24.90
29 July 1947	11	7.38	32.10	5	7.49	32.03	25.05
1450 GCT	22	6.95	32.18	10	7.40	32.09	25.10
58° 23' N 170° 20' W	34	3.33	31.96	15	7.28	32.15	25.16
	46	0.46	31.94	20	7.12	32.17	25.20
	58	0.60	32.03	25	6.10	31.98	25.19
	70	0.49*	32.09	30	4.60	31.97	25.34
				40	1.48	31.95	25.59
				50	0.46	31.97	25.67
Station N4	0	6.33	31.44	0	6.33	31.44	24.73
29 July 1947	11	5.90	31.60	5	6.12	31.52	24.82
2037 GCT	21	5.48	31.62	10	5.93	31.59	24.89
59° 21' N 169° 53' W	32	1.39	31.62	15	5.73	31.62	24.94
	42	1.25	31.64	20	5.52	31.62	24.97
	54	1.28	31.65	25	4.43	31.63	25.09
	64	1.16*	31.65	30	2.00	31.64	25.31
				40	1.28	31.65	25.36
				50	1.27	31.65	25.36
Station N5	0	5.56	31.17	0	5.56	31.17	24.60
30 July 1947	6	5.49	31.17	5	5.50	31.17	24.61
0245 GCT	12	5.49	31.17	10	5.49	31.17	24.61
60° 32' N 169° 25' W	18	5.45	31.15	15	5.47	31.16	24.61
	24	5.40	31.18	20	5.43	31.14	24.60
	30	5.36	31.17	25	5.39	31.16	24.62
	37	5.00*	31.26	30	5.36	31.17	24.63
Station N6	0	6.06	30.84	0	6.06	30.84	24.29
30 July 1947	5	5.85	31.08	5	5.85	31.08	24.50
0807 GCT	10	5.84	31.06	10	5.83	31.06	24.49
61° 37' N 168° 54' W	14	5.80	31.06	15	5.78	31.06	24.49
	19	5.75	31.06	20	5.75	31.07	24.50
	25	5.73	31.15	25	5.72	31.15	24.57
	30	5.30*	31.18	30	5.27	31.18	24.65

* Temperatures thus marked were obtained from GM American-made thermometers and are thought to be correct only to $\pm 0.05^{\circ}$ C. Other temperatures were obtained with Richter and Weise German-made thermometers and are considered to be accurate to $\pm 0.02^{\circ}$ C.

TABLE VI (continued)
HYDROGRAPHIC DATA

STATION	OBSERVED VALUES			INTERPOLATED VALUES			σ_t
	Depth (meters)	Temperature (degrees C)	Salinity (‰)	Depth (meters)	Temperature (degrees C)	Salinity (‰)	
Station N7 30 July 1947 1436 GCT 62° 46' N 168° 15' W	0	6.28	31.08	0	6.28	31.08	24.45
	4	6.21	—	5	6.20	31.15	25.51
	9	6.20	31.24	10	6.19	31.24	24.59
	14	6.17	31.24	15	6.08	31.24	24.60
	19	4.70	31.27	20	4.69	31.27	24.78
	23	4.68	31.27	25	4.61	31.28	24.80
	28	4.53*	31.29				
Station N8 30 July 1947 2030 GCT 63° 57' N 168° 20' W	0	6.33	31.56	0	6.33	31.56	24.82
	5	6.23	31.56	5	6.23	31.56	24.83
	8	6.23	31.56	10	6.23	31.56	24.83
	12	6.23	31.56	15	6.21	31.57	24.84
	17	6.20	31.58	20	6.14	31.56	24.84
	21	6.03	31.56	25	4.89	31.71	25.11
	26	4.56*	31.71				
Station N9 31 July 1947 0227 GCT 65° 12' N 168° 31' W	0	5.50	31.65	0	5.50	31.65	24.99
	7	4.96	31.67	5	5.04	31.66	25.05
	15	4.86	31.80	10	4.95	31.70	25.09
	22	2.90	31.85	15	4.82	31.80	25.18
	30	1.82	31.87	20	3.25	31.81	25.34
	38	1.29	32.00	25	2.36	31.86	25.46
	45	1.15*	32.00	30	1.82	31.87	25.50
				40	1.23	32.00	25.65
Station N10 31 July 1947 0824 GCT 66° 24' N 169° 03' W	0	2.24	31.94	0	2.24	31.94	25.53
	8	2.22	31.92	5	2.22	31.93	25.52
	16	1.47	31.91	10	2.11	31.91	25.52
	24	0.01	32.00	15	1.56	31.91	25.55
	33	-0.02	32.01	20	0.66	31.94	25.63
	42	0.02	32.01	25	-0.02	32.00	25.71
	50	-0.15*	32.03	30	-0.02	32.01	25.72
				40	0.02	32.01	25.72
				50	-0.14	32.03	25.74
Station N11 31 July 1947 1450 GCT 67° 35' N 169° 03' W	0	2.83	32.10	0	2.83	32.10	25.61
	8	2.71	32.11	5	2.73	32.11	25.63
	15	2.40	32.11	10	2.61	32.11	25.64
	23	-0.33	32.37	15	2.42	32.11	25.65
	31	-0.27	32.36	20	0.70	32.20	25.84
	39	-0.30	32.39	25	-0.34	32.30	25.97
	47	-0.43*	32.43	30	-0.28	32.35	26.00
				40	-0.32	32.39	26.04
Station N12 31 July 1947 2027 GCT 68° 41' N 169° 03' W	0	3.88	31.44	0	3.88	31.44	24.99
	7	3.81	31.35	5	3.81	31.37	24.95
	15	2.33	31.44	10	3.13	31.37	25.00
	23	1.89	31.53	15	2.24	31.44	25.13
	31	1.75	31.62	20	2.00	31.50	25.20
	39	1.78	31.64	25	1.82	31.55	25.25
	46	0.66*	31.80	30	1.76	31.61	25.30
				40	1.61	31.66	25.35

*Temperatures thus marked were obtained from GM American-made thermometers and are thought to be correct only to $\pm 0.05^\circ \text{C}$. Other temperatures were obtained with Richter and Weise German-made thermometers and are considered to be accurate to $\pm 0.02^\circ \text{C}$.

TABLE VI (continued)
HYDROGRAPHIC DATA

STATION	OBSERVED VALUES			INTERPOLATED VALUES			σ_t
	Depth (meters)	Temperature (degrees C)	Salinity ($^{\circ}/_{\text{oo}}$)	Depth (meters)	Temperature (degrees C)	Salinity ($^{\circ}/_{\text{oo}}$)	
Station N13 1 August 1947 0136 GCT 69° 55' N 168° 51' W	0 6 12 19 26 32 39	5.30 5.05 5.05 5.02 1.96 0.93 0.65*	31.80 31.78 31.76 31.76 31.94 31.96 31.96	0 5 10 15 20 25 30 40	5.30 5.05 5.05 5.02 4.89 2.16 1.16 0.63	31.80 31.78 31.77 31.76 31.76 31.94 31.95 31.96	25.13 25.14 25.14 25.13 25.15 25.54 25.61 25.65
Station N14 1 August 1947 0840 GCT 70° 27' N 168° 48' W	0 5 10 16 22 28 34	0.72 —1.13 —1.45 —1.60 —1.72 —1.68 —1.84*	29.45 31.98 32.52 32.70 32.94 33.04 33.12	0 5 10 15 20 25 30	0.72 —1.13 —1.45 —1.57 —1.69 —1.71 —1.68	29.45 31.98 32.52 32.68 32.85 33.01 33.06	23.63 25.73 26.18 26.31 26.45 26.58 26.62
Station N15 1 August 1947 1430 GCT 71° 02' N 168° 51' W	0 6 12 18 24 30 36	2.56 2.69* 4.00* 2.42* —0.68 —0.30 —0.80*	27.72 28.35 30.19 31.64 32.21 32.21 32.23	0 5 10 15 20 25 30	2.56 2.65 3.60 3.07 1.97 —0.64 —0.30	27.72 29.24 29.54 31.00 31.90 32.21 32.21	22.14 23.36 23.51 24.71 25.52 25.90 25.90
Station N16 1 August 1947 2132 GCT 72° 07' N 169° 00' W	0 8 15 23 31 39 48	3.22 3.40* —1.70* —1.50* —1.76 —1.71 —1.86*	28.39 29.60 32.48 32.72 33.08 33.21 33.21	0 5 10 15 20 25 30 40 (50)	3.22 3.37 3.28 —1.70 —1.57 —1.54 —1.74 —1.70 (—1.90)	28.39 29.14 30.04 31.11 32.19 32.87 33.05 33.21 (33.21)	22.62 23.21 23.94 25.04 25.92 26.47 26.62 26.74 (26.75)
Station N17A 2 August 1947 0019 GCT 72° 05' N 168° 58' W	0 7 15 23 31 38 46	2.56 3.15* —1.57* —1.63* —1.75 —1.70 —1.82*	28.15 29.13 32.32 32.68 32.77 33.21 33.21	0 5 10 15 20 25 30 40	2.56 3.07 2.92 —1.57 —1.65 —1.65 —1.74 —1.71	28.15 28.80 30.58 32.32 32.61 32.70 32.76 33.21	22.49 22.97 24.39 26.02 26.26 26.33 26.38 26.74
Station N17B 2 August 1947 0712 GCT 72° 02' N 168° 53' W	0 7 15 23 31 38 46	2.78 2.82* —1.28* —1.61* —1.76 —1.71 —1.88*	27.54 29.76 32.41 32.84 33.19 33.22 33.26	0 5 10 15 20 25 30 40	2.78 2.81 2.73 —1.28 —1.50 —1.67 —1.75 —1.70	27.54 29.01 30.90 32.41 32.73 32.92 33.15 33.23	21.98 23.15 24.66 26.09 26.35 26.51 26.70 26.76

*Temperatures thus marked were obtained from GM American-made thermometers and are thought to be correct only to $\pm 0.05^{\circ}$ C. Other temperatures were obtained with Richter and Weise German-made thermometers and are considered to be accurate to $\pm 0.02^{\circ}$ C.

TABLE VI (continued)
HYDROGRAPHIC DATA

STATION	OBSERVED VALUES			INTERPOLATED VALUES			σ_t
	Depth (meters)	Temperature (degrees C)	Salinity ($^0/_{\infty}$)	Depth (meters)	Temperature (degrees C)	Salinity ($^0/_{\infty}$)	
Station N17C	0	3.89	30.10	0	3.89	30.10	23.93
2 August 1947	7	4.06*	30.37	5	4.04	30.24	24.03
1226 GCT	15	-0.82*	31.96	10	4.00	30.93	24.58
71° 59' N 168° 48' W	23	-1.64*	32.75	15	-0.82	31.96	25.71
	31	-1.75	33.03	20	-1.44	32.52	26.18
	38	-1.71	33.19	25	-1.70	32.84	26.44
	46	-1.86*	33.19	30	-1.75	33.00	26.57
				40	-1.71	33.19	26.73
Station N17D	0	4.99	30.55	0	4.99	30.55	24.17
2 August 1947	7	4.99*	30.48	5	4.98	30.49	24.13
1842 GCT	15	5.05*	30.48	10	5.01	30.48	24.12
71° 56' N 168° 44' W	23	-0.57	31.94	15	5.05	30.48	24.12
	31	-1.71	32.56	20	4.96	31.42	24.87
	38	-1.69*	33.15	25	-1.11	32.11	25.84
	46	-1.84*	33.17	30	-1.66	32.48	26.15
				40	-1.71	33.16	26.70
Station N17E	0	4.52	29.65	0	4.52	29.65	23.51
2 August 1947	7	4.50*	29.61	5	4.50	29.62	23.50
2355 GCT	15	3.55*	30.81	10	4.33	30.00	23.81
71° 54' N 168° 40' W	23	-1.53*	32.41	15	3.55	30.81	24.52
	31	-1.77	33.03	20	-0.96	31.88	25.65
	38	-1.62	33.15	25	-1.65	32.63	26.27
	46	-1.84*	33.17	30	-1.77	32.98	26.56
				40	-1.66	33.15	26.70
Station N18	0	4.00	29.49	0	4.00	29.49	23.44
3 August 1947	7	4.14*	30.01	5	4.12	29.88	23.74
0829 GCT	15	2.30*	31.20	10	3.55	30.41	24.21
71° 41' N 168° 20' W	22	-0.62*	32.25	15	3.67	31.28	24.89
	30	-0.77	32.29	20	0.49	32.05	25.73
	38	-1.59	32.77	25	-0.70	32.27	25.96
	46	-1.82*	33.12	30	-0.76	32.28	25.97
				40	-1.67	32.90	26.49
Station N19	0	4.61	31.60	0	4.61	31.60	25.05
3 August 1947	7	4.62*	31.73	5	4.62	31.70	25.13
1430 GCT	15	4.44*	31.80	10	4.60	31.77	25.18
70° 39' N 167° 39' W	23	0.41*	32.16	15	4.44	31.80	25.22
	31	-0.18	32.21	20	3.63	31.98	25.44
	39	-1.54	32.79	25	0.27	32.20	25.86
	47	-1.66*	32.86	30	-0.07	32.22	25.89
				40	-1.57	32.82	26.41
Station N20	0	7.72	30.26	0	7.72	30.26	23.62
3 August 1947	7	7.62*	30.30	5	7.67	30.28	23.64
2050 GCT	14	4.85*	31.09	10	7.12	30.55	23.93
69° 37' N 166° 53' W	22	4.52*	31.46	15	4.79	31.19	24.71
	29	4.40	31.51	20	4.57	31.42	24.91
				25	4.47	31.49	24.98
	36	4.25*	31.56	30	4.38	31.52	25.01
				40	4.15	31.57	25.07

* Temperatures thus marked were obtained from GM American-made thermometers and are thought to be correct only to $\pm 0.05^\circ \text{C}$. Other temperatures were obtained with Richter and Weise German-made thermometers and are considered to be accurate to $\pm 0.02^\circ \text{C}$.

TABLE VI (continued)
HYDROGRAPHIC DATA

STATION	OBSERVED VALUES			INTERPOLATED VALUES			σ_t
	Depth (meters)	Temperature (degrees C)	Salinity ($^{\circ}/_{\text{oo}}$)	Depth (meters)	Temperature (degrees C)	Salinity ($^{\circ}/_{\text{oo}}$)	
Station N21 4 August 1947 0225 GCT 68° 39' N 167° 25' W	0	9.22	29.11	0	9.22	29.11	22.50
	6	9.09*	29.49	5	9.12	29.58	22.89
	13	8.62*	30.03	10	8.84	29.85	23.14
	20	8.66*	30.12	15	8.63	30.10	23.37
	27	6.61	30.55	20	8.66	30.13	23.39
	34	6.50	30.64	25	7.13	30.42	23.83
	41	5.72*	30.61	30	6.57	30.65	24.08
				40	5.80	30.62	24.15
Station N22 4 August 1947 0850 GCT 67° 50' N 166° 32' W	0	7.28	30.48	0	7.28	30.48	23.85
	8	7.00	30.88	5	7.11	30.77	24.10
	15	6.82	31.00	10	6.95	30.93	24.25
	23	6.07	31.06	15	6.83	30.99	24.31
	31	4.08	31.24	20	6.41	31.03	24.40
	38	3.20*	31.36	30	4.36	31.21	24.77
				40	3.10	31.37	25.01
Station N23 4 August 1947 1430 GCT 67° 27' N 164° 40' W	0	11.22	27.12	0	11.22	27.12	20.65
	3	11.22	26.76	5	11.19	26.71	20.33
	7	11.19	26.71	10	11.26	26.63	20.26
	11	11.29	26.62	15	11.21	27.05	20.59
	14	11.28	26.80	20	9.11	29.68	22.96
	18	10.11	29.67				
	22	7.64*	29.87				
Station N24 4 August 1947 2353 GCT 66° 21' N 162° 43' W	0	11.05	22.30	0	11.05	22.30	16.95
				5	11.08	21.58	16.39
				10	11.45	22.60	17.11
	2.5	11.10	21.58*				
	5	11.08	21.58				
	7	11.17	21.58*				
	10	11.43	22.54*				
Station N25 5 August 1947 0330 GCT 66° 43' N 163° 35' W	0	11.25	28.64	0	11.25	28.64	21.03
	3	11.21	25.44	5	11.17	25.43	19.36
	6	11.18	25.43*	10	11.35	25.88	19.67
	9	11.23	25.43	15	11.39	28.90	22.01
	12	11.54	27.45*				
	16	11.30	29.60*				
Station N26 5 August 1947 0825 GCT 67° 03' N 165° 40' W	0	9.50	29.60	0	9.50	29.60	22.85
	3	9.50	29.60	5	9.50	29.60	22.85
	7	9.50	29.60*	10	9.52	29.60	22.84
	11	9.53	29.60	15	9.47	29.60	22.85
	15	9.47	29.60	20	8.95	29.65	22.97
	19	9.38	29.61*				
	23	7.24	30.46*				
Station N27 5 August 1947 1430 GCT 66° 40' N 168° 03' W	0	9.56	29.56	0	9.56	29.56	22.81
	3	9.56	29.51	5	9.53	29.51	22.76
	7	9.52	29.52	10	9.53	29.55	22.80
	11	9.55*	29.56	15	9.52	29.57	22.82
	15	9.54	29.56	20	9.24	29.96	23.17
	19	9.14*	29.67				
	23	7.78*	30.70				

* Temperatures thus marked were obtained from GM American-made thermometers and are thought to be correct only to $\pm 0.05^{\circ}$ C. Other temperatures were obtained with Richter and Weise German-made thermometers and are considered to be accurate to $\pm 0.02^{\circ}$ C.

TABLE VI (continued)
HYDROGRAPHIC DATA

STATION	OBSERVED VALUES			INTERPOLATED VALUES			σ_t
	Depth (meters)	Temperature (degrees C)	Salinity ($^{\circ}/_{\text{oo}}$)	Depth (meters)	Temperature (degrees C)	Salinity ($^{\circ}/_{\text{oo}}$)	
Station N28	0	4.44	31.71	0	4.44	31.71	25.15
5 August 1947	9	4.37	31.65	5	4.42	31.67	25.12
1859 GCT	18	4.39	31.67	10	4.38	31.65	25.11
65° 52.2' N 168° 54' W	26	4.36*	31.71	15	4.40	31.67	25.13
	35	3.83	31.74	20	4.40	31.70	25.15
	44	1.98*	31.87	25	4.37	31.72	25.17
	53	1.65*	31.89	30	4.16	31.73	25.20
				40	2.86	31.80	25.37
				50	1.75	31.89	25.52
Station N29	0	4.80	31.76	0	4.80	31.76	25.15
5 August 1947	7	4.74	31.65	5	4.69	31.67	25.10
2107 GCT	15	4.71	31.67	10	4.73	31.66	25.08
65° 50' N 168° 44' W	23	4.60*	31.71	15	4.71	31.67	25.09
	31	2.97	31.80	20	4.66	31.68	25.11
	38	2.34*	31.89	25	4.42	31.73	25.17
	46	1.84*	31.89	30	3.08	31.79	25.34
				40	2.21	31.89	25.49
Station N30	0	6.11	31.65	0	6.11	31.65	24.92
5 August 1947	6	5.92	31.65	5	5.93	31.65	24.94
2117 GCT	15	5.86	31.62	10	5.97	31.65	24.94
65° 46.5' N 168° 33' W	25	5.26*	31.71	15	5.89	31.62	24.92
	32	2.96	31.80	20	5.57	31.66	24.99
	38	2.96*	31.82	25	5.20	31.71	25.07
	46	2.71*	31.80	30	3.52	31.78	25.30
				40	2.92	31.82	25.38
Station N31	0	6.67	31.42	0	6.67	31.42	24.67
5 August 1947	6	5.97	31.47	5	6.06	31.47	24.78
2235 GCT	14	5.96	31.51	10	5.96	31.49	24.81
65° 45.2' N 168° 20' W	23	5.94*	31.56	15	5.96	31.52	24.84
	31	5.84	31.55	20	5.95	31.55	24.86
	41	5.73*	31.55	25	5.90	31.56	24.87
	50	5.64*	31.55	30	5.85	31.56	24.88
				40	5.74	31.55	24.88
				50	5.64	31.55	24.90
Station N32	0	10.50	29.42	0	10.50	29.42	22.54
5 August 1947	6	10.25	29.38	5	10.27	29.38	22.55
2345 GCT	13	10.23	29.38	10	10.25	29.38	22.55
65° 43' N 168° 15' W	19	9.92*	29.40	15	10.15	29.38	22.57
	26	8.06	30.64	20	9.80	29.45	22.68
	33	7.51*	30.93	25	8.37	30.44	23.67
	40	7.44*	31.04	30	7.55	30.87	24.12
				40	7.44	31.06	24.28
Station N33	0	10.18	29.76	0	10.18	29.76	22.86
6 August 1947	6	10.18	29.51	5	10.16	29.54	22.69
0230 GCT	12	10.20	29.49	10	10.26	29.46	22.62
65° 23' N 167° 59' W	17	8.60	30.64*	15	9.27	30.17	23.33
	23	7.72	31.06	20	8.07	30.89	24.07
	29	7.58	31.04*	25	7.66	31.05	24.25
	35	7.62	31.08*	30	7.60	31.04	24.25

* Temperatures thus marked were obtained from GM American-made thermometers and are thought to be correct only to $\pm 0.05^{\circ}$ C. Other temperatures were obtained with Richter and Weise German-made thermometers and are considered to be accurate to $\pm 0.02^{\circ}$ C.

TABLE VI (continued)
HYDROGRAPHIC DATA

STATION	OBSERVED VALUES			INTERPOLATED VALUES			σ_t
	Depth (meters)	Temperature (degrees C)	Salinity ($^{\circ}/_{\text{oo}}$)	Depth (meters)	Temperature (degrees C)	Salinity ($^{\circ}/_{\text{oo}}$)	
Station N34	0	9.44	30.32	0	9.44	30.32	23.42
8 August 1947	4	8.59	30.72	5	8.51	30.77	23.91
0835 GCT	9	8.36	30.84	10	8.32	30.88	24.02
64° 58' N 167° 28' W	13	8.24	30.93*	15	8.18	30.95	24.10
	18	8.10	30.97	20	8.06	30.98	24.14
	23	8.04	30.99*	25	8.04	31.00	24.16
	27	8.05	31.00*				
Station N35	0	11.05	29.74	0	11.05	29.74	22.70
8 August 1947	5	11.00	29.69	5	11.00	29.69	22.67
1430 GCT	10	11.00	29.69*	10	10.98	29.70	22.69
64° 17' N 165° 19' W	15	9.58	30.48*				
Station N45	0	9.89	30.46	0	9.89	30.46	23.46
11 August 1947	5	8.13	30.86	5	8.13	30.86	24.03
2235 GCT	11	7.60*	31.46	10	7.67	31.38	24.51
54° 36.8' N 163° 59.6' W	17	7.14*	31.53	15	7.27	31.52	24.67
Station N46	0	8.61	31.18	0	8.61	31.18	24.21
12 August 1947	5	8.22	31.42	5	8.22	31.42	24.45
0435 GCT	10	7.44	31.53	10	7.44	31.53	24.65
54° 23.7' N 164° 33' W	15	6.83	31.62*	15	6.83	31.62	24.80
	20	6.78	31.64	20	6.78	31.64	24.82
	25	6.68	31.64*	25	6.68	31.64	24.84
	30	6.66	31.64*	30	6.66	31.64	24.84

*Temperatures thus marked were obtained from GM American-made thermometers and are thought to be correct only to $\pm 0.05^{\circ}$ C. Other temperatures were obtained with Richter and Weise German-made thermometers and are considered to be accurate to $\pm 0.02^{\circ}$ C.

INTERNAL WAVES

An attempt was made in and near the ice area to determine whether any vertical oscillations in temperature, commonly known as internal waves, existed. At station N17 repeated bathythermograph observations were obtained every 30 minutes for about 24 hours and, in addition, at shorter intervals for 2 hours and 50 minutes.

The plots of isotherms for the 24-hour series (fig. 42) show the vertical temperature structure as a function of time, resulting in an extremely complicated pattern. The analysis of these data to determine internal waves is difficult for several reasons. First, the drift of the ship into water of different character produced an apparent vertical displacement of isotherms when plotted against a time scale. Second, a differential movement of the water at various depths distorts the vertical column originally under the vessel and produces apparent vertical fluctuation of the isotherms. In the analysis of similar data from the open ocean these factors are small compared to the effect of the large physical changes associated with internal waves. However, in the Chukchi Sea the amplitudes of internal waves are so small that the changes in temperature structure due to advection predominate. The customary semi-diurnal internal tidal fluctuation in temperature is small in the Chukchi Sea as compared to that observed in the open ocean. A definite analysis of the diurnal and semi-diurnal internal waves cannot be conclusive since it is believed that halfway through the series the ship drifted into water of markedly different character. About 12 hours after the start of the repeated bathythermograph observations, the USS NEREUS drifted out of the ice and into a water mass where the thermocline was deeper. Thus, this particular lowering of the thermocline (fig. 42) should be attributed to the drift of the ship and not to internal waves. Other small irregular vertical displacements, apparent throughout the series, may be rapidly damped-out internal waves caused by variations in wind velocity. The most striking feature of the thermal condition in the arctic, however, is the occurrence of pockets of warm and cold water just above the main thermocline. This series of observations shows one pocket of warm water about 25 feet thick. This pocket of warmer water (2 degrees F higher than the surrounding water) lasted for 4-1/2 hours. Assuming a relative drift of about 1/2 knot, the length of the pocket would be about 2 miles long. Such pockets are further evidence that the changes in temperature are advective rather than due to internal waves.

Smaller thermal pockets were noted when observations were taken every 3 minutes (fig. 43). Thermal pockets 2 degrees F warmer than adjacent water were found to be as small as 5 feet thick and less than 150 feet long. In all cases the pockets were just above the main thermocline.

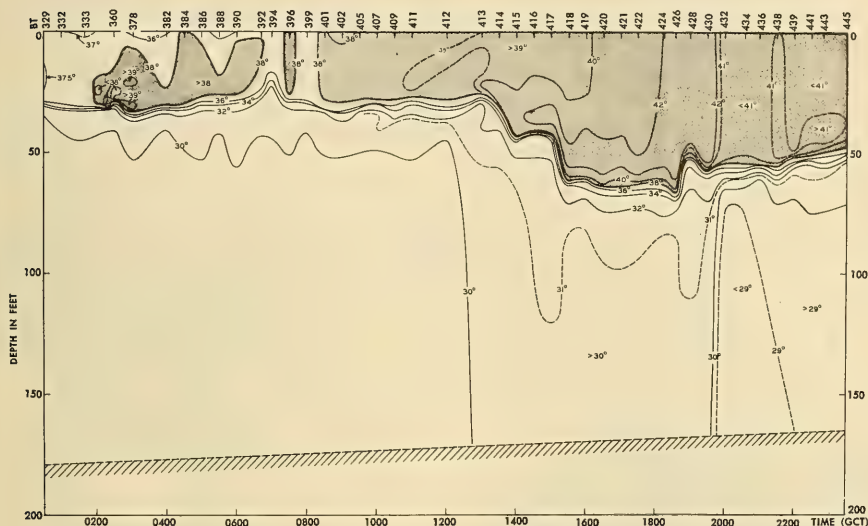


Figure 42. Fluctuations in vertical temperature structure (degrees F) from repeated bathythermograph observations for 24 hours at station N17 in the brash ice region ($72^{\circ} 07' N$ to $71^{\circ} 54' N$, $67^{\circ} 57' W$ to $167^{\circ} 40' W$).

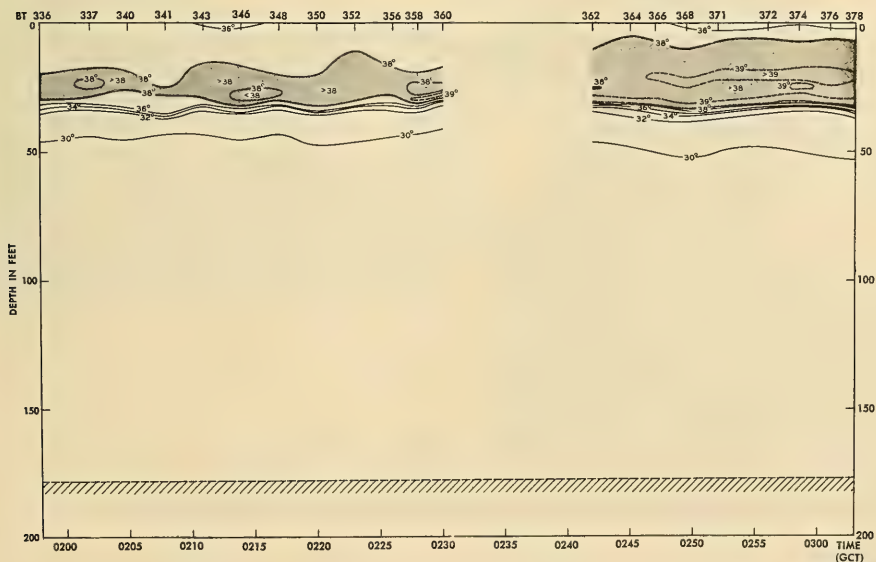


Figure 43. Fluctuations in vertical temperature structure (degrees F) from rapidly repeated bathythermograph observations for one hour at station N17 in the brash ice region ($72^{\circ} 04' N$, $167^{\circ} 56' W$).

The best example of the development of thermal pockets was obtained from bathythermograms taken from the USS BOARFISH. Observations made for 14 hours in one locality well within the pack ice region show that a vertical series of pockets can exist (fig. 44). For example, at station B26 a cold tongue was observed at 10 feet, below which a warm pocket occurred. Still deeper a cold tongue was found overlying the continuous warm layer just above the main thermocline. The temperature range in these thermal pockets was found to vary as much as 4 degrees F.

Thermal pockets are undoubtedly due to the melting of ice cakes coupled with the advection of warm, higher-salinity water through the Bering Strait. This warmer water, being of higher salinity, sinks below the colder but lower-salinity melt water. The size and depth of the pocket is determined by the size of the ice cake, the rate of mixing, the rate of advection, the rate of melting, and the salinity of the water masses. The salinity of the ice is lower than the salinity of the surrounding water. The lower-temperature melt water of low salinity may be less dense than warmer high-salinity water and so may remain on top of the warmer layers without producing instability.

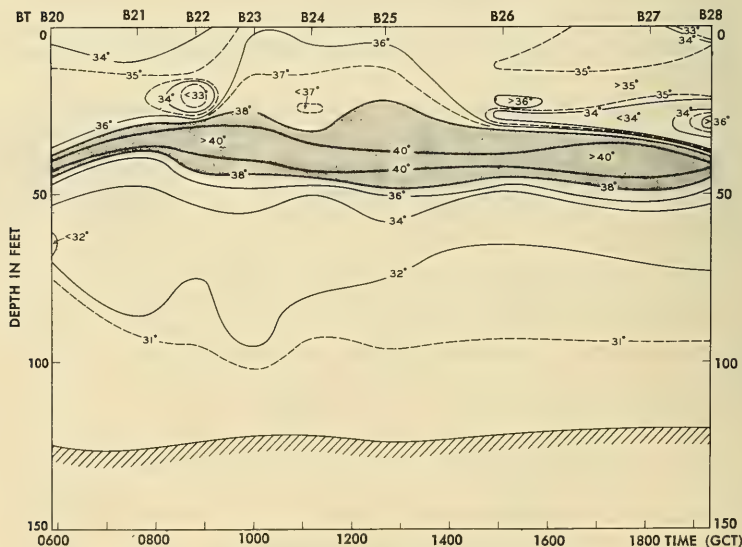


Figure 44. Fluctuations in vertical temperature structure (degrees F) from repeated bathythermograph observations for 13 hours on 6 August 1947 in the ice pack region (72° 02' N, 164° 50' W).

DENSITY

Because of the close relationship between the isopleths of temperature and salinity, the isolines of density ρ , here expressed as σ_t [$\sigma_t = 10^3(\rho - 1)$], are very similar to the isotherms and isohalines. Charts giving the horizontal distribution of σ_t at the surface, at 25 meters, and at 40 meters are shown in figures 45, 46, and 47. The general parallel character of the isopleths of these physical variables indicates that, in general, the conditions are stationary and that the current will flow parallel to the isolines of temperature, salinity, and density.

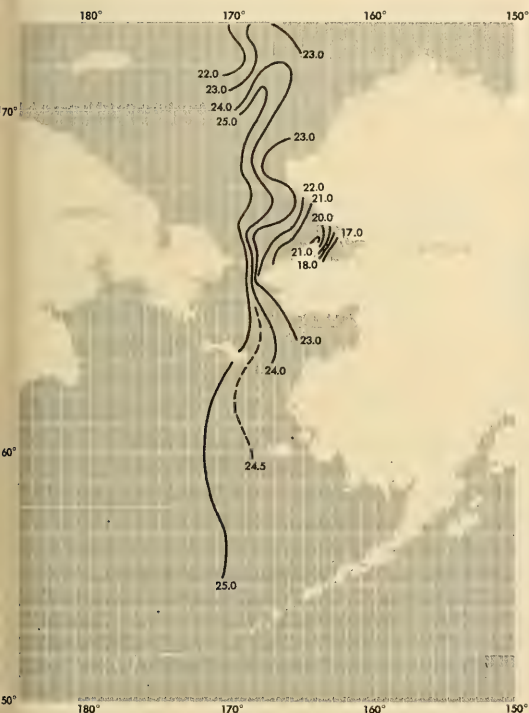


Figure 45. Horizontal distribution of σ_t in Bering and Chukchi Seas, at the surface.

Figure 46. Horizontal distribution of σ_t in Bering and Chukchi Seas, at a depth of 25 meters.





Figure 47. Horizontal distribution of σ_t in Bering and Chukchi Seas, at a depth of 40 meters.

South of Point Hope the isopycnals run approximately parallel to the depth contours. The lower-density water is found at all depths along the Alaskan coast; very low-density water ($\sigma_t = 16.8$) is found in Kotzebue Sound. In the northern Chukchi Sea, regions of low density occur in the surface layer to the west of the line of stations (away from the Alaskan coast). This area of low surface density is related to melt water of low salinity. At greater depths (25 and 40 meters) in the northern Chukchi Sea, the isopycnals again decrease toward the Alaskan coast.

Vertical cross sections C, D, and E of σ_t are shown in figures 48, 49, and 50, respectively. The general characteristics of the distribution of lighter water (warmer and less saline) and the heavier water (cooler and more saline), as discussed above in Temperature and Salinity Structure, are further emphasized in these sections. They show, however, that the greatest variation of density with depth occurs in the northern and eastern part of all sections.

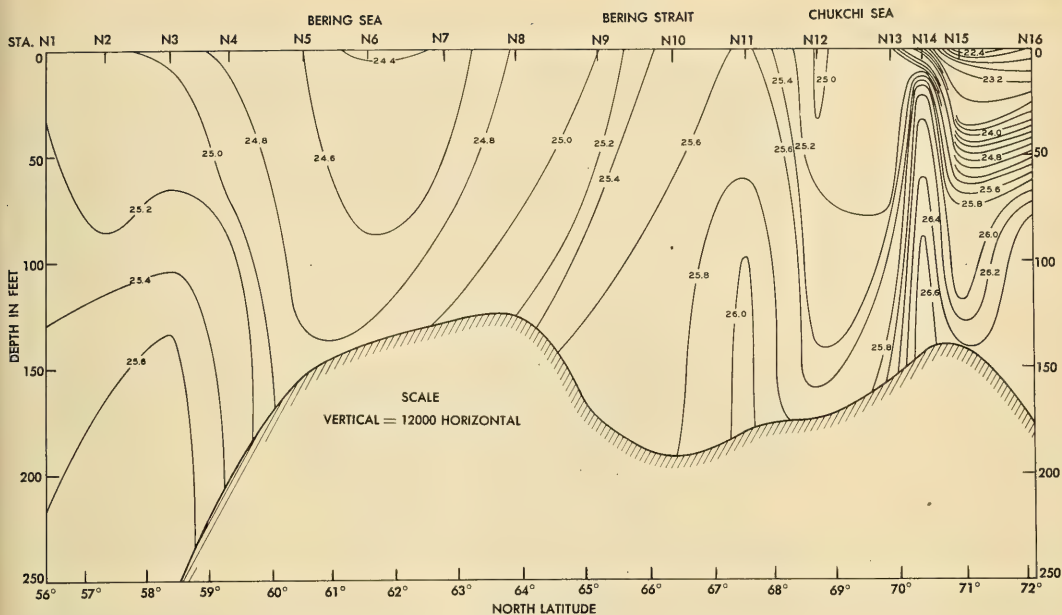


Figure 48. Vertical section C of σ_t from Pribilof Islands through Bering Strait to 72° N latitude (see fig. 13 for location of section).

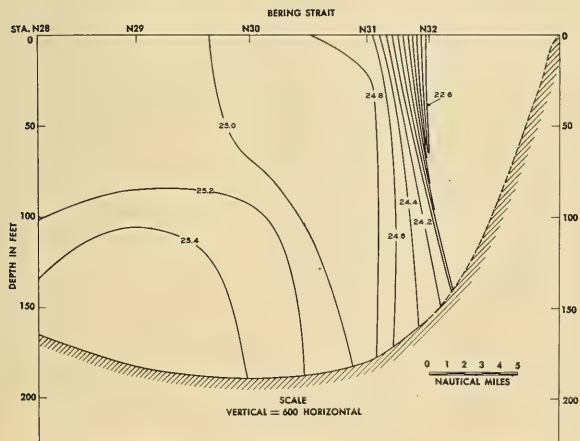


Figure 49. Vertical section D of σ_t across eastern side of Bering Strait (see fig. 13 for location of section).

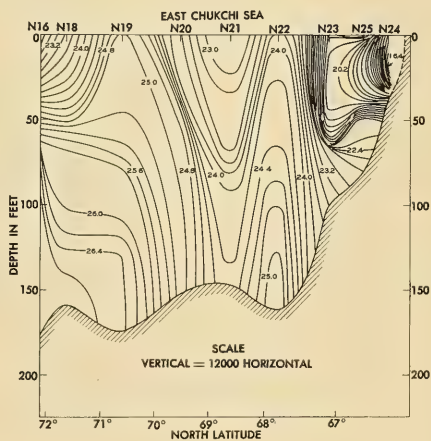


Figure 50. Vertical section E of σ_t from 72° N latitude to Kotzebue Sound (see fig. 13 for location of section).

DYNAMIC TOPOGRAPHY AND CURRENTS

Since the distribution of temperature and salinity is strongly indicative of the existence of generally stationary conditions throughout much of the area studied, it would be expected that quite satisfactory current determinations could be made from dynamic computation, providing a suitable level reference surface were found. This latter requirement cannot be met, however, for the area in general is less than 50 meters deep and the pressure surfaces are apparently inclined relative to the level surfaces at all depths. Dynamic computations suffice only in indicating the flow of the surface relative to some deeper level, here taken at 45 meters. The results indicate, however, that the dynamic topography gives the direction and relative magnitude of the surface flow quite well, though the absolute magnitudes of the currents as obtained from the dynamic computations are lower than the magnitudes of the observed currents.

The dynamic topography, based on the dynamic height anomaly of the surface over 45 decibars, is shown in figure 51. In order to use 45 decibars as a reference level, it was necessary to extrapolate the data for several stations, using several reference stations as guides. It was found that the final value for the dynamic anomaly was not greatly affected by the manner in which this extrapolation was performed.

The solid arrows on figure 51 show the direction of drift of the USS NEREUS during several periods when the ship was allowed to drift with the current and the wind. Because the vessel has a high freeboard, it is likely that the drift is greatly affected by the wind. This is seen most clearly at the drift stations taken at the edge of the ice pack, where the dynamic topography indicates a northerly flow. The USS NEREUS drifted southeastward, however, at a speed of about $1/2$ knot. This drift was largely related to the observed northwest wind of about 7 knots, for the drift was observed to be southward relative to the pieces of floating ice which surrounded the ship at the beginning of the drift.

The observed velocities of drift at stations N8, N9, and the five stations in Bering Strait gave directions which were very close to the direction of flow indicated by the dynamic topography. However, the computed velocities were in every case much smaller than the observed velocities (approximately $1/10$ as large). This is to be expected since the bottom waters also are apparently in motion to the north. Some of the difference between observed and computed currents in Bering Strait can be related to wind drift of the ship, for the

wind was blowing at an average speed of 17 knots from the south during the period of observations.

For the southern Bering Sea region the current stream lines, as deduced from the distribution of temperature alone, are shown on figure 51 as dashed lines. Previous investigators⁷ have reported the existence of eddies similar to the one depicted here in this region of the Bering Sea.



Figure 51. Dynamic height contours (0/45 dynamic meters) in dynamic centimeters observed in the Bering and Chukchi Seas with direction of calculated current flow indicated by arrowheads along the contours of dynamic height. Observed drift of ship is indicated by short heavy arrows.

ICE

The types and the extent of ice in the Chukchi Sea were determined by means of observations made from the USS NEREUS (AS17), the USS BOARFISH (SS327), the USS CHUB (SS329), the USS CABEZON (SS334), and the USS CAIMAN (SS323). The southern limit of floating ice was plotted from observations made by each ship. A composite of these plots is presented in figure 52.

The USS NEREUS reached the southern limits of the floating ice (latitude $72^{\circ}02'N$, longitude $168^{\circ}53'W$) at 0930 LCT on 1 August. Brash and block ice were encountered, but since the ice covered less than 10 per cent of the sea surface, there remained sufficiently large spaces of water for navigation. Proceeding in a northerly direction, the USS NEREUS reached a point about 2 miles beyond the southern ice limits at 1000 LCT of the same day. The scattered ice

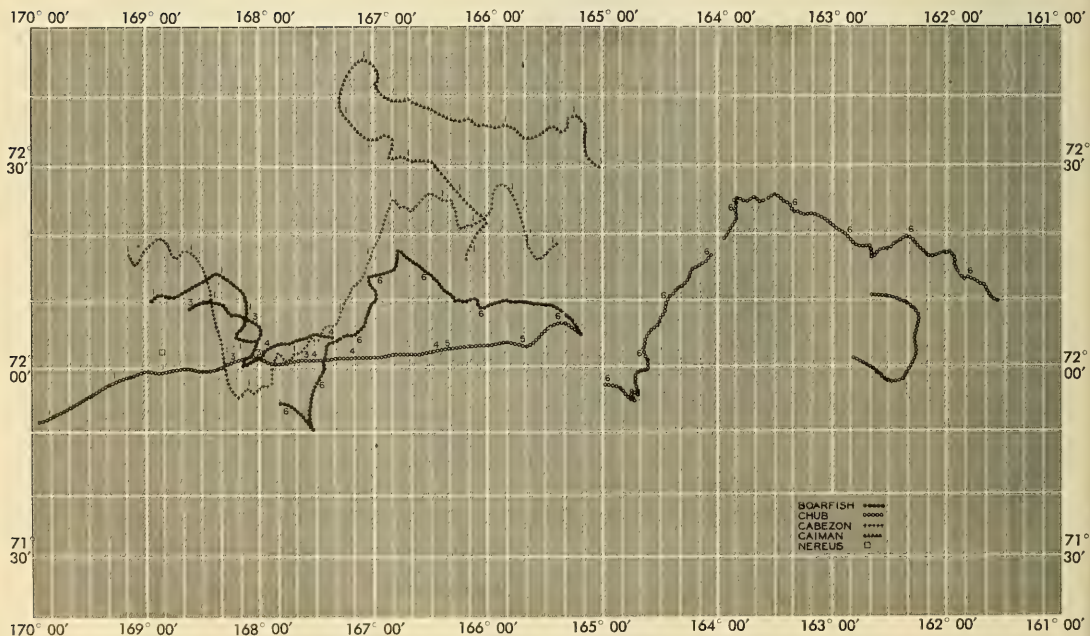


Figure 52. Composite chart of southern limit of arctic ice pack as observed by the four submarines and tender, 1 to 6 August 1947. Small numbers indicate day of month.

encountered at this point was thicker and included both blocks and small floes, some of which ranged as high as 6 feet above the surface of the water. Many of the floes were hummocked, and occasionally their surfaces bore evidence of rotten ice. (See figs. 53A through 53H.)

On 2 August, the day on which the USS NEREUS left the ice area, air reconnaissance dispatches reported the southern limits of the arctic pack ice to be at about $72^{\circ}44'N$ latitude in this longitude. On the same day, a party left the USS NEREUS,



Figure 53A. The brash and blocks making up the southern limit of drift ice ($72^{\circ}02'N$, $168^{\circ}53'W$) was easily navigable.

Figure 53B. Blocks and small floes found a few miles north of southern ice boundary. Hummocky blocks in left foreground.





Figure 53C. Greater ice cover with increasing latitude. Dark patches on ice in foreground consist of sediment.



Figure 53D. Floe ice extending about 6 feet above water. At $72^{\circ} 14' N$ navigation difficult.

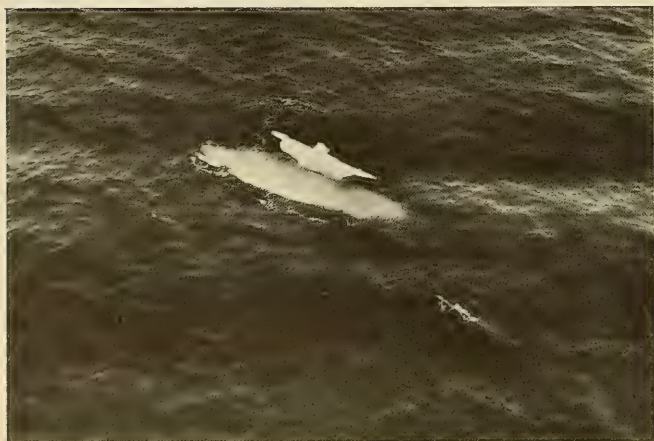


Figure 53E. Glaçon showing relative amounts of ice submerged and above water. Note also the melting which has occurred at water surface.

Figure 53F. Glaçon composed of rotten ice (right foreground).



Figure 53G. Flat glaçon about 50 feet in diameter (center right).



Figure 53H. Glaçon which appears to have tilted about 90 degrees recently so the sediment is in a vertical plane. The exposed honeycombed side shows evidence of melting while exposed to the water.



then at 72°06' N, 168°42' W, and travelled northward by motor launch. The northernmost point reached was about 72°14' N latitude. Small floes with occasional hummocking were encountered in this region. This ice extended 6 to 9 feet above the water and covered from 10 to 25 per cent of the total surface area. Some of the floes were as much as 200 feet in length. These ice conditions extended north to the horizon.

By reference to the composite ice chart (fig. 52) it will be noted not only that the USS CAIMAN traversed the southern ice limits on 1 August, but also that she made more northerly observations than any of the other ships. A study of the USS CAIMAN's ice plot indicates that after entering a lead, her most northerly latitude was 72°45' N. This point was almost identical with the southern limit of the arctic pack ice (72°44' N) as reported to the USS NEREUS by aircraft.

The USS CABEZON traversed the ice limit on 1 August only. The ice plot of the USS CABEZON shows that in the western part of the area investigated the ice limits varied from 71°55' N to 72°27' N between 169°21' W and 165°24' W.

The ice chart of the USS CHUB shows that this ship was travelling continuously in or near the ice from 1 August through 6 August. The USS CHUB was the only ship to report on the ice condition in the eastern region extending between longitudes 165°00' W and 161°35' W. The detailed ice plot of the USS CHUB for 6 August, the day on which the ship traversed this section, shows that the most northerly point attained was 72°26.5' N latitude. The ice observed was classified as one or another of the various sizes from brash to floe ice. While the USS CHUB was leaving the ice area on 7 August, a large ice concentration was observed and later described as a "floating island"

The USS BOARFISH also traversed the ice from 1 August through 6 August. However, her most easterly travel took her only as far as 165°W. Ice plots show the most northerly point to be latitude 72°18' N, longitude 166°48' W. The USS BOARFISH reported a polynya (a sizeable sea water area encompassed by ice), three miles in diameter, at latitude 72°17.2' N, longitude 166°49.9' W. In the same region, many glacons that rose as high as 15 to 20 feet above the water were observed. Ice observations for 1, 3, 4, and 6 August indicate that brash and floe ice were encountered.

Variations in the limits of the ice as indicated in the composite ice chart (fig. 52) by the four ships may be attributed not only to navigational difficulties, but also to a difference in interpretation of the ice limits. In some cases a single piece of ice may have been used to define the ice

limit, while in other cases a definite ice concentration may have defined it. Ice plots made on successive days by the USS BOARFISH in the region around 72°N and 168°W would indicate that the ice limits were not fixed and that the ice was moving in a southeasterly direction.

From these ice observations, it can be stated that during the period 1 to 6 August 1947 the southern limits of the ice lay near 72°N latitude in the range included between longitudes 161°W and 169°W. The extreme southern limits of the drift ice at that time were found at 71°50'N latitude, as reported by the USS BOARFISH. The southern limits of ice found in this particular year were much farther north than those given in the H. O. Ice Atlas.¹⁶

TRANSPARENCY MEASUREMENTS

Transparency measurements of the surface layer were obtained at each hydrographic station in the Bering and Chukchi Seas by a visual method. A standard Secchi disc (a white disc 30 centimeters in diameter) was lowered from the main deck, 25 feet above sea level, and a measurement was taken of the depth at which the disc disappeared from sight. It was lowered further and then raised so that a second measurement could be taken of the depth at which the disc reappeared.

Since the readings were taken well above sea surface, the measured depths are shallower than those taken from a ship with a low freeboard. The depths, furthermore, are somewhat less in rough sea than in smooth sea, and less during dim light than during bright light. These factors are believed to be secondary, however, and amount to corrections not exceeding 20 to 25 per cent.

The measurements shown in figure 54 show that an opaque (low-transparency) region was observed to extend through Norton Sound, to the eastern edge of Bering Strait. This opaque region may be the effect of sediment-laden water supplied by the Yukon and other Alaskan rivers. Another low-transparency region occurs just north of Bering Strait and is probably caused by sediment-laden water from the north Siberian shelf.

There are two main regions of relatively high transparency: one in the northcentral portion of the Bering Sea, the other in the Chukchi Sea, north of latitude 69°N. The boundary between the opaque and the highly transparent water in Bering Strait is remarkably sharp and coincides with the region of maximum horizontal temperature gradient.



Figure 54. Transparency measurements made near the surface in the Bering and Chukchi Seas. Values indicate depth in feet to which a Secchi disc is visible from ship.

The transparency is relatively high at stations north of Cape Hope, as compared to stations in the Bering Sea, Kotzebue Sound, or Norton Sound. A Secchi disc can be seen to an average depth of 36 feet at these Chukchi Sea stations. A visibility of 36 feet corresponds to poor transparency for open sea conditions, but is much better than the visibility found under average coastal conditions.

AMBIENT NOISE

During the cruise, ambient noise measurements were made at the hydrographic stations in the Bering and Chukchi Seas in order to obtain some information about the magnitude and characteristics of ambient noise in arctic waters. To avoid maintenance and operational difficulties aboard ship, only a single unit of simple listening equipment was used. This consisted of a Brush Manufacturing Company type C-23 hydrophone, an amplifier with attenuator and meter, and a set of earphones. The response of the system was reasonably

flat from 400 cps to 15 kc. The system was capable of measuring over-all sound pressures as low as 0.1 dyne per square centimeter, corresponding in the wide band covered to an average spectrum level of approximately 0.001 dyne per square centimeter. This level was found to be inadequate for the extremely low noise levels encountered.

For many of the measurements, it was impractical to get far enough away from the ships to record water noises. At other locations, surf noises predominated. In a few locations, however, measurements were possible where ships and surf noises did not interfere and, in most of these cases, characteristic sounds could be recognized and described. Near the ice pack the noises were too low to be read on the meter, but they could be heard in the earphones. These noises were in the medium or low audio-frequency range and were compared to the sounds of rushing water with an occasional splash, as if from large chunks of ice sinking beneath the surface. Although exact levels could not be established, it can be concluded that a very low noise level occurs in this area, with no evidence of noises of a biological origin.

IV. biological observations

DEEP SCATTERING LAYER

In recent years, since the development of the more powerful echo sounders which make a continuous tape recording of depth versus time, layers which scatter sound have been frequently noted in the ocean at depths of from 100 to 450 fathoms. The trace on the fathogram caused by scattering layers has the appearance of a false bottom. Typically developed only during the day, these deep scattering layers descend from the surface in the morning and rise in the evening. The scatterers are presumably certain types, or perhaps many types, of marine zooplankton which exhibit a marked negative phototropism dominating a negative geotropism. These organisms swim to the surface at night to feed in the diatom-rich surface water and descend during the day to regions of darkness in order to avoid destruction by their predators. Although probably zooplankton, the scatterers may possibly be nekton (e.g., fish or squid), which follow and feed upon the migrating zooplankton. Although comparatively few in number, nekton are generally much larger than zooplankton forms and therefore more efficient scatterers of sound.

The deep scattering layer was recorded on the fathogram of the USS NEREUS during the passage from Hawaii to Adak, but this particular layer has been reported on separately by Dietz.¹ Within the limits of the Bering and Chukchi Seas the deep scattering layer was noted only on 26 July when the USS NEREUS, during her passage from Adak to the Pribilof Islands, crossed the deep oceanic basin which comprises the southern portion of the Bering Sea.

This record of the layer can be seen in figure 3A. As is usually the case, the layer is absent during the night and is developed only during the day. It can first be seen at 75 fathoms as a distinct layer resolved from the outgoing ping at 0700 LCT (1800 Z). Echo extension of the outgoing signal for about two hours prior to this time suggests that, although the record of the layer is partially masked by the outgoing ping, it actually began to form and descend at about sunrise (0500 LCT on this date).

The scattering layer is continuously developed all during the morning and early afternoon hours at a depth of from 75 to 100 fathoms. This is an unusually shoal depth for the development of the layer which, in other parts of the Pacific, is more commonly at a depth of from 175 to 250 fathoms and occasionally at a depth as great as 450 fathoms. Since the

deep scattering layer is presumably caused by light sensitive organisms, this shoal depth of the layer may be correlated with the overcast sky condition on this date, with the low angle of the sun at this latitude, and with the high opacity of the water related to high organic production. All of these factors would decrease the depth of light penetration in the ocean. In the late afternoon, the layer descended to a greater depth of from 125 to 175 fathoms and became more strongly developed. Shortly prior to sunset at 2051 LCT, the USS NEREUS reached the shallow water of the Bering Sea shelf; observations showed that the deep scattering layer ends where it abuts against the continental slope.

During the remainder of the arctic passage, the USS NEREUS was in the shoal shelf waters of the Bering and Chukchi Seas. These shoal waters (always less than 75 fathoms and generally less than 30 fathoms) precluded the development of a deep scattering layer. Although shoal scattering layers are occasionally observed in shallow water, none were present on the fathogram of the USS NEREUS. This may be due to the absence of shallow scatterers or, more likely, to the low gain setting used in obtaining bottom echoes in shoal water, a setting usually insufficient to bring in echoes from scatterers.

ZOOPLANKTON

During the arctic cruise, the USS NEREUS occupied a series of stations for taking net hauls: seven stations along a line between the Hawaiian and the Aleutian Islands; twenty-one stations on a line extending northward from the Pribilof Islands, through the Bering Strait to 72°N latitude in the Chukchi Sea, and back to Kotzebue Sound; and one station just south of Unimak Island. Only the samples from this last station and the stations north of the Aleutian Islands will be considered here in some detail (see fig. 55). The samples were all collected within the period, 27 July to 12 August; hence they are representative of summer conditions only.

These collections form a valuable supplement to the series collected by the U. S. Coast Guard Cutter CHELAN in 1934⁸ and contribute in no small way to our slowly accumulating knowledge of the plankton biology of these remote areas. In a later report it is planned to integrate more fully the findings of these two surveys.



Figure 55. Plankton stations of the USS NEREUS.

The samples were collected with a Nansen net, 1.5 meters long, constructed of No. 0 and No. 8 bolting silk, and with a 40-centimeter mouth. In operation the net was lowered by means of a weight and hauled in vertically while the ship was hove to. South of the Aleutian Islands, most of the samples were taken in vertical hauls from a depth of 200 meters to the surface. In the Bering Sea and northward, the hauls were made from the bottom, usually at 40 to 60 meters, to the surface.

Figure 56 gives the relative volumes (measured by displacement) of total plankton, adjusted for comparison to 60-meter hauls. Both zooplankton and phytoplankton are included, hence the numbers represent total particulate organic material screened from the water by means of this type net. Usually the bulk, which in no case was large, was made up of zooplankton, but at stations N11, N14, and N16 the bulk was primarily made up of diatoms. At stations N11 and N14, *Thalassiosira rotula*, *Thalassiosira nordenskiöldii*, *Fragillaria striatula*, and *Nitzschia seriata* were dominant; at station N16 *Fragillaria* was overwhelmingly dominant.

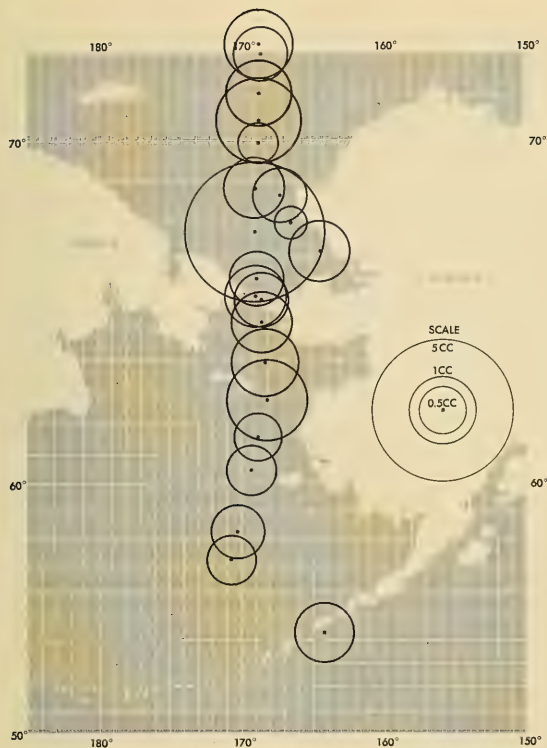


Figure 56. Displacement volumes of total plankton (adjusted to 60-meter vertical hauls expressed in cubic centimeters).

While there was considerable variation in volume, no area was barren; the Chukchi Sea showed a good population with some flares of diatoms. The correlation of plankton concentration (fig. 56) with transparency (fig. 54) is generally not good, but it can be seen that relatively large plankton concentrations occurred off Norton Sound where transparency was low and that, at station N11 where the lowest transparency occurred, the greatest concentration of plankton (mainly diatoms) was found. In the Chukchi Sea, this correlation is poor.

The only two stations occupied for plankton in Kotzebue Sound showed a small to moderate plankton concentration, hence the low transparency there may be due to suspended sediment. No plankton samples are available from Norton Sound. In the narrows of Bering Strait the low transparency would appear to result from causes other than plankton. At station N28 more detritus than usual was included with the plankton.

From these studies it appears that transparency is affected by plankton only when it is present in relatively great concentrations. In all cases the volumes are certainly minimal, since much of the finest material passes through the meshes of the net and the larger, fast-swimming forms escape it.

Table VII gives the numbers, adjusted to 60-meter hauls, of the important species of plankton taken at each station. Station 32 is omitted from the table since the sample was not complete. From this table it can be seen that copepods are the major constituent of the plankton. The most abundant copepods numerically were the small species Oithona similis (O. helgolandica in the CHELAN report⁸) and Pseudocalanus minutus, both of which occurred at every station, usually in appreciable numbers, and probably constitute a staple element in the diet of larval fishes and other plankton feeders. Important also among the microcalanids was Acartia longiremis, with centers of abundance off Cape Romanzof and in Kotzebue Sound.

Calanus finmarchicus was the most abundant and widespread of the larger copepods, occurring at all but two stations (N5 and N23). This is in keeping with its well-known extensive distribution in other northern waters, where it is often the major food for many fish and baleen whales. Other large copepods important in the Bering and Chukchi Seas are Calanus tonsus, Calanus cristatus, and Eucalanus bungii bungii. The number of these large species was minimal, since for best results larger coarser nets should have been used.

Certain other copepods, while not always abundant, are of special interest because of their characteristic distribution (fig. 57). For example, Epilabidocera amphitrites, Centropages mcmurrici, and Tortanus discaudatus occurred only in the warmer (39 degrees F or above) waters with some neritic influence, suggesting a close affinity to the Alaskan coast; whereas, Metridia lucens was characteristic of the more open cold waters to the west and north where this species entered the plankton community together with the larger calanoids mentioned above.

In the study of the CHELAN samples⁸ it was brought out that only the northern variety of Eucalanus bungii occurred in the Bering Sea area. The present series of samples verify this finding. The extensive area covered by the USS NEREUS makes possible a further comparison of that interesting species. In the series of stations occupied south of the Aleutians it was found that only the northern variety, Eucalanus bungii bungii, was present at the station at 43°29'N latitude

and at all stations north, whereas at the next station south ($38^{\circ}49'$ N latitude) it was almost completely replaced by the southern variety, *Eucalanus bungii californicus*. In the sample taken at this latter station only two adult specimens of the northern variety were found among forty specimens of the southern variant. The USS NEREUS bathythermograms show an 8-degree F difference in surface temperature between these stations. On the west coast of North America the two varieties overlap along the Oregon coast and southward to Cape Mendocino, California.

A study of the copepod larvae and juveniles indicates that active restocking was taking place over much of the area. The nauplii were especially abundant at Bering Sea stations and at station N23 in Kotzebue Sound, where *Acartia* was actively reproducing. The presence of the cladocerans, *Podon* and *Evadne*, at stations N21 and N23 is also correlated with the warmer coastal water. *Sagitta* sp. was most abundant at stations in the Bering Sea but was distributed all the way to the northernmost station in the Arctic, where both young and adults were taken.



Figure 57. Locality records of certain copepods.

TABLE VII
NUMBERS OF PRINCIPAL PLANKTON ORGANISMS TAKEN BY THE USS NEREUS
IN THE BERING AND CHUKCHI SEAS, 1947. (Adjusted to 60 meters vertical haul.)

STATION	N2	N3	N5	N6	N7	N8	N9	N10	N11	N12	N13	N14	N15	N16	N17 E	N21	N22	N23	N28	N30	N46
Acartia longiremis	297	113	4115	5584	2671	170	70			5	152	1			1	6	296	3530	1	68	2605
Acartia nauplius				1088	1972	85	140			1								974		135	1146
Calanus cristatus	5																				
C. finmarchicus	30	341		26	175	55	257	25	39	74	8	7	44	6	8	29	213		104	60	9
C. tonsus	1	1					4	64	4	5			1		1	3		111			7
Centropages mcmurricchi																					
Epilabidocera amphitrites																					
Eucalanus bungii bungii	21	6		1			3														
Eucalanus nauplius	88	57					140	172		116						8	9				19
Metridia lucens	41							7	6					1	2		1		1	1	
Microsetella																					
Oithona similis	12,233	1644	1397	798	2076	8436	5180	3272	98	580	236	457	1485	522	484	2831	9065	2313	2381	2774	11,983
Oncaea borealis					1																
Pseudocalanus minutus	438	3062	1	4786	4785	937	1820	2153	684	754	76	1523	4137	1043	761	2359	2463	1947	1012	677	2709
Tortanus discaudatus			2	3						1						1					
Calanoid nauplius							511	1750	1033	755	696	114	1980	2334	730	691	2463	1582	92	609	938
Euphausiid	1	2	2					1		2						2					11
Euphausiid larva			155				596	70					1								
Euphausiid egg			1																		
Amphipod	10	1		1	13	8	19	39	14	1	2	1		1	1		3		6	3	6
Evadne																189		365			
Podon																189		486			
Appendicularia	284		1			3420	1260	258	389	464	558	2129	849	107	78	1038	986	1826	92	1962	729
Barnacle nauplius	172				4	8		173	367	1		726	2334	4	484	755		1	92		729
Barnacle cypris	44							1	98	1	10	7	1803	1	277	189	1	111		1	
Crab larva	16	1	4	1	4		6	4	1					1	1	1	1	4	2		10
Annelid larva				1	6		2		3												
Cham larva	132	113	155	73	7059	1960	1820		679	464	1	152	212	1	1	189	1	988	184	203	1876
Veliger larva	658	1701					70			1						3397	3744	2434	1421	1421	3960
Chaetognath 0.8mm	19	11	78	334	364	47	1	8	31	27	2	5	49	6	9	44	93	19	13	19	
Chaetognath 0.15mm	160	6			4		2	2	2	6	5	7	1		1		4	12	14	19	
Chaetognath > 15mm	13			1	26		85	4	2			1		10	1		15		3		
Bipinnarian	44		7													189		1			521
Echinopluteus			1	163,739		170	2030			290						2170	3252	609		11,164	
Ophiopluteus	219				623	257	420			174	1					1321	197	1		118	7502

Among the pelagic larvae of bottom living animals, none were so conspicuous as certain echinoderm larvae. Echinoplutei were taken from station N5 northward to station N12 (fig. 58), the greatest numbers occurring at station N6 off Cape Romanzof. It is interesting to note that station N6 is in the area in which the water temperature was found to be uniformly warm, 43 to 40 degrees F from surface to bottom, (see figs. 17, 18, 19, and 23). These larvae were perhaps the result of recent spawning in or near the area, since the larvae were mostly in the 4-arm stage, which at 13 to 14 degrees C is reached about 46 hours after the eggs are spawned, according to studies in Puget Sound. Other successful hauls were made in water with greater temperature stratification, in the band of relatively warm surface water extending out from the Alaskan Coast. No echinoplutei were taken immediately north of Bering Strait (stations N10, N27, and N11) where the surface isotherms are bent towards the east by cold water flowing along the western portion of the strait;

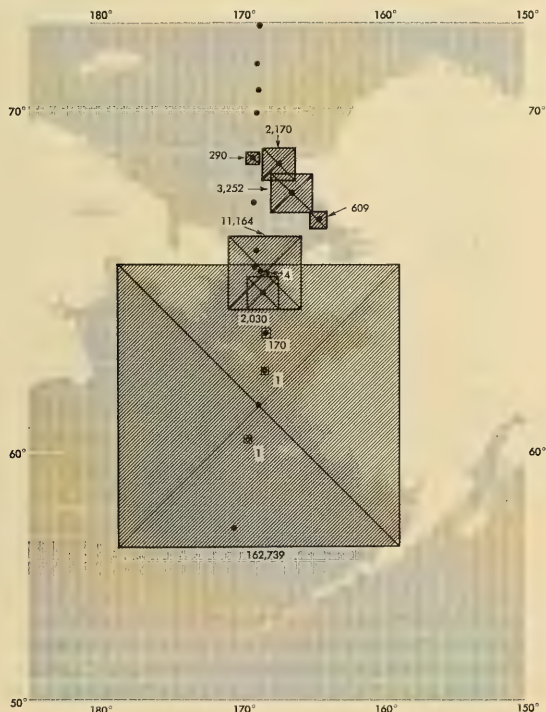


Figure 58. Locality records of Echinopluteus, giving the number of individuals per haul, adjusted to 60-meter vertical hauls (size of shaded area proportional to number of individuals caught at that point).

however, at stations N12, N21, and N22, where the warm water from Cape Lisburne and Kotzebue Sound is again felt, the larvae again appear, apparently having drifted out with the surface water from areas having a warmer bottom.

Specific identification of the echinoplutei was not made, but in most samples the larval skeleton was preserved sufficiently to indicate the larval type. Examination of numerous specimens revealed only larvae with fenestrated bars in the postoral and postero-dorsal arms and with the body and recurrent rods forming a calcareous basket similar to the clypeasteroid, Dendraster excentricus. The basket, however, appeared to be somewhat more open than in the species from Puget Sound, and the lower ventral transverse rods were not seen. These rods apparently do not always develop until late in the larval life.

From this survey of echinoplutei found among the plankton, it is evident that either the shallow waters of the Bering Sea and Alaskan coast abound in adults of these animals or the spawning season is especially abrupt and intense during this time of year.

The ophiopluteus larvae of the brittle stars were more widely distributed, but less abundant than the echinoplutei. Like the latter they were also characteristic of the warmer water (fig. 59). Bipinnarian larvae of sea stars were found only at stations off the Pribilof Islands, Kotzebue Sound and Unimak Island (N2, N3, N21, and N46). It is of special interest to note that the chief plankton constituent at station N15 was barnacle larvae, mainly in the nauplius stage but including some in the cyprid stage (fig. 60). Other stations in the Chukchi Sea yielded many barnacle larvae. Polychaete worm larvae were scattered throughout the area and were especially abundant at stations N14 and N15 in the Arctic Ocean. Clam larvae occurred throughout the area clear up to the northernmost station, but the greatest concentrations were at station N46 off Unimak Island and at station N7 near St. Lawrence Island.

Crab larvae were nowhere abundant, but occurred consistently at nearly all stations northward to station N15 in the Chukchi Sea. In view of the abundant crabs forming new fisheries in part of the Bering Sea area, it might be expected that pelagic larval stages would be abundant in the plankton, but apparently the season of shedding larvae was past. This observation might be of great economic importance since the fishery operations for these crabs, if made during the summer, would then cause less interference with the restocking.



Figure 59. Locality records of *Ophiopluteus*, giving the number of individuals per haul, adjusted to 60-meter vertical hauls (size of shaded area proportional to number of individuals caught at that point).


Fish eggs and larvae were surprisingly scarce. A few eggs were taken at stations N5 and N22, and some larvae taken at station N2. The cyphonautes larvae of Bryozoa, which are so characteristic of shallow neritic waters farther south, were totally absent from the catches. The occurrence of many planktonic larvae of bottom-living animals at the northern stations is of interest since, elsewhere in the world, larvae of these temporary plankton are often noticeably scarce.



Figure 60. Locality records of Barnacle Nauplius and Cyprid Larva, giving the number of individuals per haul, adjusted to 60-meter hauls (size of shaded area proportional to number of individuals caught at that point).

list of references

1. Dietz, R. S., "Deep Scattering Layer in the Pacific and Antarctic Oceans," *Journal of Marine Research*, vol. 7, No. 3, 15 November 1948, pp. 430-442.
2. Dietz, R. S., *Some Oceanographic Observations on Operation HIGHJUMP*, USNEL Report No. 55, 7 July 1948, p. 61.
3. Emery, K. O., and R. S. Dietz, "Gravity Coring Instrument and Mechanics of Sediment Coring," *Bulletin of the Geological Society of America*, vol. 52, October 1941, pp. 1685-1714.
4. Emery, K. O., and H. Gould, "A Code for Expressing Grain Size Distribution," *Journal of Sedimentary Petrology*, vol. 18, No. 1, April 1948, pp. 14-23.
5. Fleming, R. H., and R. Revelle, "Physical Processes in the Ocean, Recent Marine Sediments," *Bulletin of the American Association of Petroleum Geologists*, vol. 23, 1939, pp. 134-136.
6. Flint, R. F., *Glacial Geology and the Pleistocene Epoch*, John Wiley and Sons, New York, 1947.
7. Goodman, J. R., J. H. Lincoln, and others, "Physical and Chemical Investigations: Bering Sea, Bering Strait, Chukchi Sea, during the Summers of 1937 and 1938," *University of Washington Publications in Oceanography*, vol. 3, No. 4, March 1942, pp. 107-169.
8. Johnson, M. W., "The Production and Distribution of Zooplankton in the Surface Waters of Bering Sea and Bering Strait," *U. S. Coast Guard Report of Oceanographic Cruise, U. S. Coast Guard Cutter CHELAN, Part II (B)*, 1934, pp. 45-82.
9. LaFond, E. C., and R. S. Dietz, "New Snapper-Type Sea Floor Sediment Sampler," *Journal of Sedimentary Petrology*, vol. 18, No. 1, April 1948, pp. 34-37.
10. Phifer, L. D., "The Occurrence and Distribution of Plankton Diatoms in the Bering Sea and Bering Strait," *U. S. Coast Guard Report of Oceanographic Cruise, U. S. Coast Guard Cutter CHELAN, Part II (A)*, 1934, pp. 1-44.
11. Stetson, H. C., "The Sediments of the Continental Shelf off the Eastern Coast of the United States," *Papers in Physical Oceanography and Meteorology*, Massachusetts Institute of Technology and Woods Hole Oceanographic Institution, vol. 5, No. 4, July 1938, p. 40.
12. Sverdrup, H. U., "The Waters on the North-Siberian Shelf: The Norwegian North Polar Expedition with the MAUD, 1918-1925," *Scientific Results*, vol. 4, No. 2, 1929, pp. 34-40.
13. Sverdrup, H. U., M. W. Johnson, and R. H. Fleming, *The Oceans*, Prentice-Hall, Inc., New York, 1946.
14. Trask, P. D., *Origin and Environment of Source Sediments of Petroleum*, Gulf Publishing Company, 1932, pp. 134-135.
15. *U. S. Coast Guard Report of Oceanographic Cruise, U. S. Coast Guard Cutter, CHELAN, Bering Sea and Bering Strait, 1934, and Other Related Data, Part I*, 1936.
16. U. S. Hydrographic Office, *Ice Atlas of the Northern Hemisphere*, Publication No. 550, Washington, D. C., 1946.



NEL San Diego (6-49) 215



Navy electronics laboratory
Oceanographic measurements from the USS NEREUS
on a cruise to the Bering and Chukchi Seas, 1947;
interim report, by E.C. LaFond, R.S. Dietz, and
D.W. Pritchard.
25 February 1949 96p. illus. RESTRICTED

Abstract: Measurements of thermal conditions, salinity, depth, transparency of water, ambient noise, scattering layers, and biological population discussed. Explanations of distribution of physical, chemical, biological, and geological variables are proposed.

1. Oceanography - Arctic
I. LaFond, E. II. Dietz, R. III. Pritchard, D
2. USS NEREUS

Navy electronics laboratory
Oceanographic measurements from the USS NEREUS
on a cruise to the Bering and Chukchi Seas, 1947;
interim report, by E.C. LaFond, R.S. Dietz, and
D.W. Pritchard.
25 February 1949 96p. illus. RESTRICTED

Abstract: Measurements of thermal conditions, salinity, depth, transparency of water, ambient noise, scattering layers, and biological population discussed. Explanations of distribution of physical, chemical, biological, and geological variables are proposed.

1. Oceanography - Arctic
I. LaFond, E. II. Dietz, R. III. Pritchard, D
2. USS NEREUS

Navy electronics laboratory
Oceanographic measurements from the USS NEREUS
on a cruise to the Bering and Chukchi Seas, 1947;
interim report, by E.C. LaFond, R.S. Dietz, and
D.W. Pritchard.
25 February 1949 96p. illus. RESTRICTED

Abstract: Measurements of thermal conditions, salinity, depth, transparency of water, ambient noise, scattering layers, and biological population discussed. Explanations of distribution of physical, chemical, biological, and geological variables are proposed.

1. Oceanography - Arctic
I. LaFond, E. II. Dietz, R. III. Pritchard, D
2. USS NEREUS

Navy electronics laboratory
Oceanographic measurements from the USS NEREUS
on a cruise to the Bering and Chukchi Seas, 1947;
interim report, by E.C. LaFond, R.S. Dietz, and
D.W. Pritchard.
25 February 1949 96p. illus. RESTRICTED

Abstract: Measurements of thermal conditions, salinity, depth, transparency of water, ambient noise, scattering layers, and biological population discussed. Explanations of distribution of physical, chemical, biological, and geological variables are proposed.

1. Oceanography - Arctic
I. LaFond, E. II. Dietz, R. III. Pritchard, D
2. USS NEREUS

Navy electronics Laboratory

Report no. 91

Oceanographic measurements from the USS NEREUS on a cruise to the Bering and Chukchi Seas, 1947; interim report, by E.C. LaFond, R.S. Dietz, and D.W. Pritchard.

25 February 1949 96p.

111us.

RESTRICTED

Abstract: Measurements of thermal conditions, salinity, depth, transparency of water, ambient noise, scattering layers, and biological population discussed. Explanations of distribution of physical, chemical, biological, and geological variables are proposed.

1. Oceanography - Arctic I. LaFond, E
- II. Dietz, R
2. USS NEREUS III. Pritchard, D

Navy electronics Laboratory

Report no. 91

Oceanographic measurements from the USS NEREUS on a cruise to the Bering and Chukchi Seas, 1947; interim report, by E.C. LaFond, R.S. Dietz, and D.W. Pritchard.

25 February 1949 96p.

111us.

RESTRICTED

Abstract: Measurements of thermal conditions, salinity, depth, transparency of water, ambient noise, scattering layers, and biological population discussed. Explanations of distribution of physical, chemical, biological, and geological variables are proposed.

1. Oceanography - Arctic I. LaFond, E
- II. Dietz, R
2. USS NEREUS III. Pritchard, D

Navy electronics Laboratory

Report no. 91

Oceanographic measurements from the USS NEREUS on a cruise to the Bering and Chukchi Seas, 1947; interim report, by E.C. LaFond, R.S. Dietz, and D.W. Pritchard.

25 February 1949 96p.

111us.

RESTRICTED

Abstract: Measurements of thermal conditions, salinity, depth, transparency of water, ambient noise, scattering layers, and biological population discussed. Explanations of distribution of physical, chemical, biological, and geological variables are proposed.

1. Oceanography - Arctic I. LaFond, E
- II. Dietz, R
2. USS NEREUS III. Pritchard, D

